Ministry of Higher Education and Scientific Research

University of Monastir

A Dissertation

by

Inés BELKACEM

In partial fulfillment of the requirements for the degree of

DOCTOR OF PHILOSOPHY

Major Subject: **Energy Engineering**

Host laboratories:
1. Laboratory of Thermal and Energy Systems Studies (LESTE), Tunisia
2. Environment, Planning, Safety and Eco-design Laboratory (EASE). Department of Mobility, Planning and the Environment (AME). Gustave Eiffel University (UGE). Lyon Campus. Lyon, France

---

Investigation of Vehicle Exhaust and Non-Exhaust Particle Emissions in Urban, Suburban and Rural Road Traffic Areas

---

June 29, 2021 at the National Engineering School of Monastir

Examining Board:

Mr. Rachid SAID, Professor, IPEIM, **Chairman**

Mr. Ali TRIKI, Associate Professor, ISSAT GABÈS, **Thesis Reviewer**

Mr. Walid HASSEN, Associate Professor, ENIM, **Thesis Reviewer**

Mr. Khalifa SLIMI, Professor, ISTLS, **Thesis Supervisor**

Mr. Salah KHARDI, Research Director, INSA de Lyon, (France), **Thesis Supervisor**

Mr. Mohamed Mahjoub DHIAF, Professor, Emirates College of Technology, (UAE), **Thesis Examiner**

Abstract

Road traffic is the major source of pollution and contributes remarkably to air pollution despite improvements in pollution control engines and technologies. Human effects and environment impacts associated with nanoparticles generated from road traffic have recently induced significant intensive research activities. To measure and assess knowledge of particle pollutants from road traffic, several methods are available, with their advantages and limitations. Such as the example of real-world measurements that make the evaluation of vehicle emissions (exhaust and non-exhaust emissions) according to real driver behavior and traffic conditions is a good reproducibility of test conditions. However, this approach remains insufficient and limited, particularly in the distinction between the sources of non-exhaust emissions. To solve the requirements on air pollution quality and sustainable mobility and morbidity, pronounced focus should be granted on nanoparticles produced from road traffic. In the first time, this dissertation starts to classify and analyze the existing knowledge of nanoparticles inroad traffic atmosphere, highlights recent progress and emphasizes research emerging and priorities aspects of this problem. It analyzes the actual state of research related to nanoparticles and highlights where future research activities on this topic should be addressed. In the second time, it measures the PNCs within the 5.6 and $560\ nm$ rangeusing a Fast Mobility Particle Sizer ^{TM} ($FMPS^{TM}$) Spectrometer ($Model\ 3091$). It investigates the effect of traffic volume, wind speed and direction, height above the road surface and distance from the source on both particle number concentration (PNC) and particle number distribution (PND). In addition, it estimates continuous real-world measurements of exhaust and non-exhaust particle emissions within the $0.35 - 22.5\ \mu m$ diameter size range over different road traffic areas, using the GRIMM series 1.108 Aerosol Spectrometer. Finally, this thesis predicts vehicle exhaust and non-exhaust particle number concentration using ANN models and multiple linear regressions, based on real-world measurements over urban road traffic. Equally, it compares the predicted with the measured $PNCs$ using the GRIMM.

Keywords: Exhaust particle; non-exhaust particle, brake wear, tire wear, road surface wear, resuspension, ANN, prediction, real-world measurements, unregulated pollutants.

Résumé

Le trafic routier est la source majeure de pollution malgré l'évolution technologique de motorisations et de contrôle de la pollution. Les effets sur l'homme et l'environnement des nanoparticules générées par le trafic routier ont récemment donné lieu à des activités de recherche intenses. Pour mesurer et évaluer les connaissances sur les polluants particulaires issus du trafic routier, plusieurs méthodes sont disponibles dans la littérature. Des mesures en conditions réelles ont été effectuées afin d'évaluer les émissions des véhicules (émissions à l'échappement et hors échappement), en tenant compte du comportement des conducteurs et des conditions de circulation réelles, est une approche efficiente. Cependant, elle reste insuffisante et limitée, notamment dans la distinction entre les différentes sources des émissions hors-échappement. Cette thèse commence par classer et analyser les connaissances existantes sur les nanoparticules engendrées par le trafic routier, met en évidence les progrès récents et souligne les aspects émergents et prioritaires de la recherche sur ce problème. Elle analyse l'état actuel de la recherche sur les nanoparticules et met en évidence les points sur lesquels devraient être menées les futures activités de recherche sur ce sujet. Ensuite, elle mesure la concentration en nombre des particules (PNC) avec une taille allant de $5{,}6$ jusqu'à $560\ nm$. Elle étudie l'effet du volume du trafic, de la vitesse et de la direction du vent, de la hauteur au-dessus de la surface de la route et de la distance sur la PNC et la distribution en nombre de particules (PND). Elle estime avec des mesures continues et en temps réel les émissions de particules d'échappement et hors échappement avec des diamètres allant de $0{,}35$ jusqu'à $22{,}5\ \mu m$ sur différentes zones du trafic routier. Elle évalue l'effet des vitesses et les manœuvres d'accélération et de décélération sur la concentration des particules en nombre et en masse. Finalement, elle prédit la concentration en nombre des particules (PNC) à l''échappement et hors échappement des véhicules à l'aide des modèles de réseaux de neurone et de régressions linéaires multiples, sur la base de mesures réelles dans une route urbaine. De même, elle compare les PNC prédits avec les PNC mesurés en temps réel.

Mots clés : Mesures en temps réels ; polluants non-réglementés ; usure des freins, usure des pneus, usure de la surface de la route, remise en suspension de la poussière ; ANN

ACKNOWLEDGEMENTS

The research work presented in this thesis was carried out jointly between the Laboratory of Thermal and Energy Systems Studies (LESTE), (ENIM- Tunisia) and Environment, Planning, Safety and Eco-design Laboratory, Department of Mobility, Planning and the Environment, (EASE), (UGE- France).

My sincere thanks go to Mr. **Rachid SAID,** Professor of Physics at the *Preparatory Institute for Engineering Studies of Monastir* (Tunisia) for accepting to chair the Examination Jury of this PhD thesis.

My thankfulness goes also to Dr. **Ali TRIKI**, Associate Professor of Mechanical Engineering at the *Higher Institute of Applied Sciences and Technology of Gabès* (Tunisia), and to Dr. **Walid HASSEN**, Associate Professor of Energy Engineering at the *Engineering High School of Monastir* (Tunisia) for accepting to review the present PhD thesis dissertation. Your review reports were insightful and allowed us to enhance in both form and content of the manuscript.

I make a point of thanking Mr. **Mohamed Mahjoub DHIAF**, Professor of Transportation and Logistics Sciences at the *Emirates College of Technology* (United Arab Emirates) for accepting to judge this thesis and to be part of this jury despite his multiple tasks as Dean of Business Faculty (UAE).

This dissertation would not have been possible without the guidance and the help of several individuals who in one way or another contributed and extended their valuable assistance in the preparation and completion of this study. I owe my gratitude to all those people who have made this dissertation possible and because of whom my graduate experience has been one that I will cherish forever. First and foremost, my utmost and deepest gratitude is to my advisors, **Pr. Khalifa SLIMI** (Full-time Faculty Member at the *Higher Institute of Transportation and Logistics*, ISTLS, University of Sousse, Researcher at the Thermal and Energy Systems Studies Laboratory, LESTE (LR99ES31), *Engineering High School of Monastir*, ENIM, Tunisia), **Dr. Salah KHARDI (**Research Director at *INSA de Lyon*; Contact and Structure Mechanics Laboratory LaMCoS (CNRS-INSA de Lyon UMR5259). MECALIPS "Mechanics, Lipidomic and Engineering for Health". Lyon - France), you were excellent directors whom I respect and look up to as my mentor. I would

like to express my deepest appreciation for your scientific comments, your kindness and your support. I will not forget how much you stood beside me, simplifying the difficulties that we encountered along the way, and helping me to overcome everything. It was a great pleasure meeting you and working with you.

Prof. Khalifa SLIMI, I have been amazingly fortunate to have an advisor like you during my PhD thesis preparation, who gave me the freedom to explore on my own and at the same time the guidance to recover when my steps faltered. I would like to thank you for your patience, guidance, encouragement and support that helped me overcome many crisis situations and finish this dissertation. I hope words are sincere enough to show how grateful I am.

Dr. Salah KHARDI, I would like to express my sincere gratitude. I would like to thank you for your help, understanding, wisdom and for pushing me farther that I thought I could go. Thank you for always listening and giving me words of encouragement. You were always available whenever I needed you, and I cannot thank you enough for it.

Dr. Ali HELALI, Assistant Professor of Mechanical Engineering and Director of the *Higher Institute of Transportation and Logistics of Sousse* (Tunisia), I would like to express my sincere gratitude for your encouragement, your insightful comments and constructive criticisms. Thank you for your help, your continuous guidance and support.

Dr. Amani CHROUDA, Assistant Professor of Analytical Chemistry at the *College of Sciences*, Al-Majmaah University (Kingdom of Saudi Arabia), I would like to address my gratitude for your help and comments.

I would like to thank all my friends at the Thermal and Energy Systems Studies Laboratory (LESTE).

Most importantly, none of this would have been possible without the love, concern, support, unceasing encouragement and patience of my family, to whom this dissertation is dedicated. I owe all my achievements to my father Bannour BELKACEM, my mother Monjia NOUIRA, my brothers Mohamed Amine & Nasr-Eddine, my sisters Chiraz & Imen and my partner Mehdi MEHREZ. I would like also to address my sincere gratitude to my uncle Prof. Lotfi BELKACEM for his encouragement.

Table of contents

List of Figures

List of Tables

Nomenclature

Symbol	Description
APS	Aerodynamic particle sizer
ANN	Artificial neural network
CPC	Condensation particle counters
DPF	Diesel particulate filter
DLPI	Dekati low pressure impactor
DMS	Differential mobility spectrometer
ELPI	Electrical low-pressure impactor
ELM	Extreme learning machine
FMPS	Fast Mobility Particle Sizer
GRNN	General Regression Neural Networks
GDI	Gasoline-Direct-Injection
GPS	Global positioning system
HDV	Heavy duty vehicle
LDV	Light Duty Vehicle
MAPE	Mean absolute percentage error
MLP	Multilayer perceptron
MAD	Mean absolute deviation
NEP	Non-exhaust particle
NEDC	New European driving cycle
OPC	Optical particle counter
PNC	Particle number concentration
PM	Particle Matter
PM2.5	Particle Matter with diameter 2.5 μm
PM1	Particle Matter with a diameter less than 1 μm
PM10	Particle Matter with a diameter less than 10 μm
PEMS	portable emissions measurement systems
PNDs	Particle Number Distribution
PMC	Particle mass concentration
QCM	Quartz crystal microbalance
R.H	Relative Humidity
R^2	Coefficient of determination
RMSE	Root mean squared error
RAM	Respirable aerosol monitor
RBFN	Radial basis function networks
SPN	Solid particles number
SMPS	scanning mobility particle sizer
TRW	Tire road wear
TEM	Transmission electron microscopy
TRWP	Tire road wear particle
UFPs	Ultrafine particles
WLTC	Worldwide harmonized light vehicles test cycles
WLTP	Worldwide Harmonized light vehicle test procedure

Introduction

Particle exhaust and non-exhaust emissions are two essential aspects to be considered for mitigating the ambient air pollution and ensure a sustainable mobility and environment. The four non-exhaust emissions sources are; resuspension, tire, road surface and brake wear. These particles have negative impacts not only on human health but also on visibility, air quality, the environment and both direct and indirect climate forcing. Measurements and modeling of particle number concentrations for both exhaust and non-exhaust emissions are the focus of this research.

Air pollution has become a critical issue (Silva et al., 2020a) worldwide. Road traffic has pronounced negative impacts on air quality (Silva et al., 2020b).The participation of road traffic can reach up to 90 % of total particle number concentrations PNCs in polluted urban areas(Kumar et al., 2014). Traffic particle emissions were the major contributor for air quality deterioration for many years. Atmospheric Particulate Matter PM has been recognized as causing around 430,000 premature deaths per year in Europe (European Environment Agency, 2015). Kheirbek et al., 2016 outlined that buses and trucks within New York City participated by about 53% of the $PM2.5$ attributable deaths and presented for the largest share of on-road mobile attributable ambient $PM2.5$. Harrison et al., 2012a conducted sampling measurements near a major road in London and demonstrated that $PM10$ non-exhaust emissions (brake wear) participated by up to 55%in wt.

Available studies indicating that PNCs are critical metric to define (Ibald-Mulli et al., 2002) and toxicological (Murr and Garza, 2009), the other studies relate exposure to ultrafine particles with adverse toxic effects.

Problem statement

Nanoparticle emissions from road traffic take place at the regions that are typically occupied by people. Diesel-powered vehicles constitute the major source of road vehicle pollution in the European Union (EU). Urban areas generate considerable human activity and a large proportion of pollution that induces significant adverse environmental impacts, not to mention health effects by virtue of penetrating into the deep lung (Stone et al., 2017).

In Europe, the contribution of road transport varied by around 32 % of the total nanoparticles in Greece to about 97% in Luxemburg. For the other European countries (Spain, France, Germany, UK, Italy, Poland) are the most PM emitters, where the road traffic contributes by about 72 % of the total traffic-engendered PM emissions in EU(Kumar et al., 2014).In addition, a wide PM concentration mass reaching up to 78 and 113 $\mu g\,.m^{-3}$of $PM2.5$ and $PM10$ respectively during a Brazilian city (Pereira et al., 2017). Suddenly increase of $PM2.5$ air mass concentration was observed during Beijing by Zhang et al. (2017), reaching up 150 to 250 $\mu g\,m^{-3}$.

Road traffic PM ($PM1, PM2.5, PM10$) emissions include both exhaust and non-exhaust particulate emissions. The exhaust PM particle emission is produced from tailpipe as a consequence of incomplete combustion of carburant inside the engine chamber; (2) primary and secondary particles produced from tire, brake and road wear; (3) primary particles engendered from resuspension due to vehicle-wheel turbulence (Schauer et al., 2006; Thorpe and Harrison, 2008; Mehel and Murzyn, 2015; Trejos et al., 2021). PM adversely affects human health in two ways, namely a diminished capacity of the respiratory tract to remove such deposits and a PM deposition mechanism acting in therespiratory tract, both of which are highly correlated with PM size (Mainka and Zajusz-Zubek, 2019). Smaller particles($< 1\mu m$) exerts a larger negative effect on human health, targeting asthma and the respiratory system (Mei et al., 2018). Despite these negative externalities, until now $PM1$ has not been frequently quantified since it lies outside the focus of air quality standards.In addition, environmental impacts have emerged from the ambient road traffic particles. In fact, visibility impairment is caused by build-up of the atmospheric particles that scatter or absorb light from the sun (Horvath, 2008). It decreases with wind speed and temperature and increases with atmospheric pressure and relative humidity (RH) (Tsai, 2005).
Resuspension and wear part can be considered as non-exhaust emissions (i. e. road dust, brake wear, tire wear and road surface)are shown to strongly influence urban air quality (Silva et al., 2020c; Trejos et al., 2021; Beji et al., (2020,2021)).

Research objectives

The main objective of this dissertation is to measure particle number concentration PNC under real traffic conditions in different road segment areas. It starts to measure the ambient air nanoparticles (exhaust and non-exhaust PNCs) in urban road with different traffic

conditions using the Fast Mobility Particle Sizer™ (FMPS™) Spectrometer (Model 3091). These measurements were taken at two different heights, as well as at different distances between source and sampling sites, ranging from 6.60 m to 330 m. Second, continuous real-world measurements of particle exhaust emissions were recorded over four road segment types (urban, rural, motorway and national (ring) road RN6)in the city of Bron, Lyon France). Third, continuous real-world measurements of particle non-exhaust emissions were recorded over four road segment types (urban, rural and motorway areas). In addition, it tends to assess the effect of vehicle speed and acceleration/deceleration maneuvers on vehicle exhaust particle emissions. The final objective is to predict both exhaust and non-exhaust PNCs based on the real PNCs measured by the GRIMM analyzer, series 1.108 Portable Aerosol Spectrometer, using the artificial neural networks models. These measurements were taken in order to ensure a sustainable environment and mobility.

Research contribution

This dissertation develops continuous measurements of PNCs taking into account real road traffic conditions. In fact, it contributes to the air quality in Lyon (France) by means of roadside monitoring of PNCs and PNDs. The effect of several parameters, like the distance from traffic, height above ground, traffic volume, wind speed and wind direction, was also taken into account during measurement campaigns. In addition, it tends to assess the effect of vehicle speed and vehicle acceleration/deceleration maneuvers on non-exhaust particle (NEP).

Dissertation Layout

The dissertation documents classified as follows:

- Chapter 1classifies and analyzes the existing knowledge of nanoparticles emissions from road traffic, highlights recent progress and emphasizes research emerging and priorities aspects of this environmental and health problem. This chapter describes of the main reasons behind the actual and progressive interest of the ongoing research in this field. This is followed by a brief discussion of the atmosphere nanoparticles major sources. The subsequent section focuses on the nanoparticles influencing parameters including climate conditions, height above the road surface and distance between source (road traffic) and sampling site. The next section provides a comprehensive summary on sampling measurement methodologies and instrumental techniques. Further section reviews health and environment implications associated with particle exposure. Finally, this chapter analyzes the actual state

of research related to nanoparticles and highlights where future research activities on this topic should be addressed.

Chapter 2 describes the methodology for measuring continuous ambient air nanoparticles in urban road traffic. The method allows to measure PNCs, which were resolved within the 5.6- and 560-nm range. Series of variables were taken into consideration during sampling measurement days; distances from the source, heights from ground, traffic volumes and atmospheric conditions (wind speed, wind direction, humidity and temperature). In addition, this chapter analyzes the effect of each variable on ambient PNC and particle number distribution PND.

Chapter 3 includes two sections:

Section 1 estimates, investigates and compares real-world, micro-scale *continuous exhaust* particle mass concentrations and number by optical size, from roughly *0.35 to 22.5*μm, under actual measurement conditions for diesel light-duty vehicles in order to improve road mobility within the framework of environmental sustainability. Furthermore, this section specifies the effect of vehicle speed/acceleration on the evolution of nanoparticles in the size range of *0.35 - 22.5* μm.

Section 2 estimates, investigates and compares real-world, micro-scale *continuous non-exhaust* particle mass concentrations and number by optical size, from roughly *0.35 to 22.5*μm, under actual measurement conditions for diesel light-duty vehicles. In addition, the current section evaluates the effect of vehicle speed and vehicle acceleration/deceleration maneuvers on NEP.

Chapter 4 also includes two sections:

Section1 predicts the exhaust PNCs under urban road traffic area based on continuous real PNCs measured by the GRIMM analyzer, series 1.108 Portable Aerosol Spectrometer. The artificial neural network ANN models (GRNN and MLP) have been chosen to predict PNCs. In addition, this section tends to compare the GRIMM output Vs ANNs output. Then, the test was ended when the error reached its minimum.

Section 2 predicts the non-exhaust PNCs under urban road traffic area based on continuous real PNCs measured by the GRIMM analyzer, series 1.108 Portable Aerosol Spectrometer. The artificial neural network ANN model (GRNN) and MLR have been chosen to predict

PNCs. Furthermore, this section compares the GRIMM output Vs GRNN and MLR outputs. The performance of the trained networks was evaluated, using several statistical parameters which are; RMSE, R^2, and MAPE.

Lastly a summary of the findings, the conclusions of the research effort and some recommendations for further research have been established.

Chapter 1. Literature review

1.1. Introduction

The designation of nanoparticle (NP) is mentioned to consult a wide range of particles, and delimitations change considerably between different research studies, depending on the technique/protocol of measurement and the context of the research. The most specific used size is particles smaller than 100 nm, using the term $PM0.1$ or ultrafine particles ($UFPs$). The $PM0.1$ (PM is designed to the subscripts and particulate matter show cut-off sizes in μm) have been strictly related with adverse health effects and act by mechanisms not shared with larger particles (WHO, 2013). It is worthy to note that $UFPs$ contribute by the major rate (~80 %) of the total number concentration of ambient nanoparticles with negligible mass concentration (Kittelson, 1998). Furthermore, it is powered by the close vicinity of vehicle traffic emissions with residential census. More precisely, $UFPs$ with a diameter smaller than 300 nm present over 99% of total particulate emissions (Kumar et al., 2009).

Nanoparticle emissions from road traffic take place at regions typically occupied by people. The induced nanoparticles can enter and assembled in car cabins (Joodatnia et al., 2013), due to poor ventilation, which is a very dangerous phenomenon for human health.

Nanoparticle emissions from road traffic can be classified into three-different classes: (1) primary (carbon monoxide (CO), nitrogen oxide (NOx) and sulfur oxide (SOx)) and secondary particles (ammonia ($NH3$), volatile organic compounds ($VOCs$), secondary organic aerosols (SOA) and secondary inorganic aerosols (SIA)) induced from vehicle exhaust.

Atmospheric nanoparticles have several terminologies. Regulatory agencies often use terms $PM10$, $PM2.5$ and $PM1$. On the other hand, toxicologists apply terms like coarse particles ($> 1000\ nm$), fine ($< 1000\ nm$) and ultrafine particles ($< 100\ nm$) (Araujo et al., 2008; Martinello et al., 2021).

In aerosol science, particles are examined in terms of modes including nucleation, Aitken, accumulation and coarse. Each mode has specific size range, chemical composition, sources, formation mechanisms and deposition pathways (Hinds, 1999). Historically, at the beginning of the $1990's$, the PM emissions were controlled for light duty vehicles ($LDVs$), by weighing the mass placed on filters. Since early 2000, the gravimetric analysis was not sufficient to accurately control the vehicle PM emissions equipped with Diesel Particulate Filter (DPF). Consequently, there was a serious need to be heading towards an accurate and sensitive

methodology that would complement the regulated gravimetric procedure with low investment costs. The latter specified method was focused upon counting solid particles number larger than $23\,nm$ ($SPN23$) (GRPE, 2003). In the other hand, vehicle with modern gasoline-direct-injection (GDI) presents the highest pollution sources (Xing et al., 2020). The size, elemental composition and morphology of the particles and their ageing in a smog chamber have been analyzed by the authors using the same method adopted by Xing et al. (2017, 2019).The particles were assessed using Tecnai$G2\ F30$ field emission high-resolution transmission electron microscope ($FE-HRTEM$), which is equipped with a scanning transmission electron microscopy ($STEM$) and an Oxford EDX (Fig. 2.1)

EU vehicle emissions legislation is the first one that regulates $SPN23$ emissions and recently was established China 5 and 6 limits. EU emission standards applied the first regulation of solid particle number (SPN) limit targeting the light vehicle diesel engines in 2011 ($Euro\ 5b$) with $6.0 \times 10^{11}(\#/km)$.

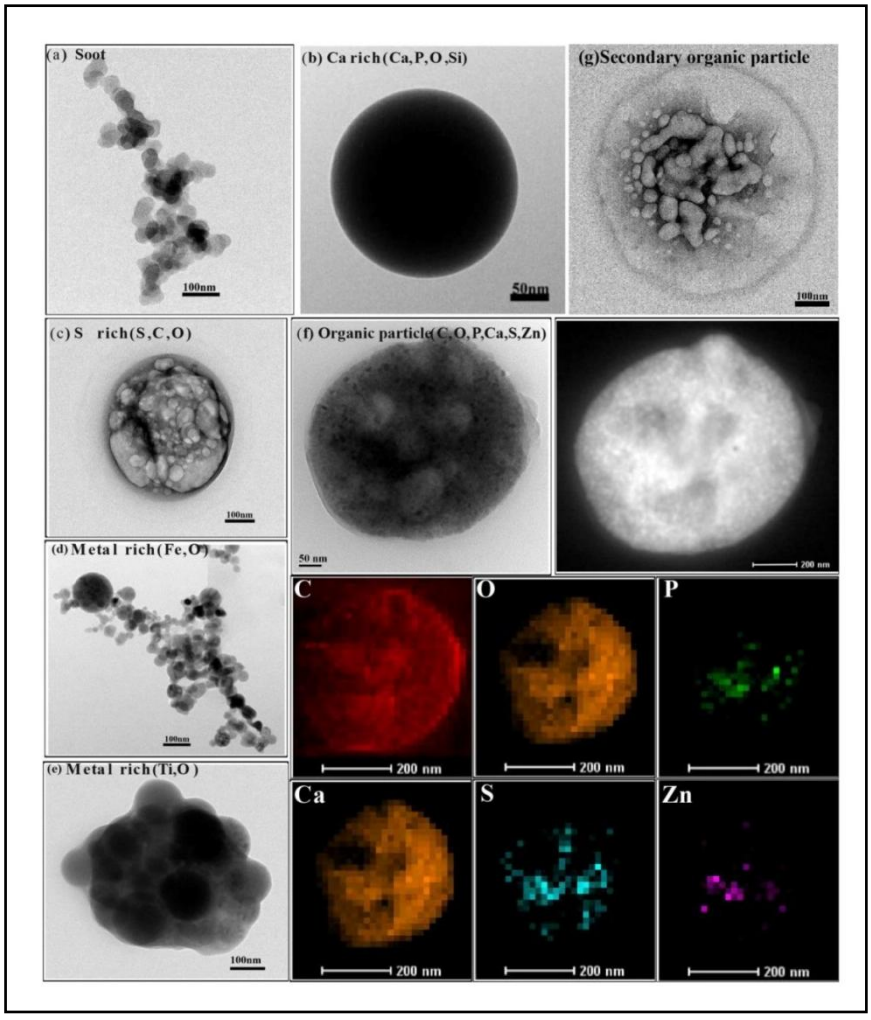

Figure 1. 1: TEM images of the individual primary particles emitted from the GDI-engine

Vehicle and the secondary organic particle in the chamber after exposure to ambient sunlight for 3.5 h. (a) Soot particle. (b) Ca-rich particle. (c) S-rich particles. (d) Metal-rich particles (Fe). (e) Metal-rich particles (Ti). (f) Bright-field-TEM and dark-field-TEM image of organic particles, and others are the mapping of the $C, O, P, Ca, S, and\ Zn$ in the organic particle. (g) Secondary organic particle in the chamber (Xing et al., 2020).

For light vehicle gasoil engines, the first $SPN\ 23$ limit appeared in 2014 ($Euro\ 6$). Table 1.1 summarizes the European and Chinese regulations concerning $SPN\ 23$ for both light-duty and heavy-duty vehicles. The most available studies in the open literature have only summarized the recent regulations of the European Union (Giechaskiel et al., 2012; Giechaskiel et al., 2014a; Bischof, 2015; Giechaskiel et al., 2018).

However, this current chapter has briefly updated the recent limitations of the European and Chinese standards, since the improvement of the vehicles$SPN23$ in one country of the world will result in a general improvement of the quality of air on our planet. As far as the authors knowledge is of concern, there are no regulations for solid particles smaller than $23nm$ (sub-$23\ nm$), that we find a critical size to be assessed. Solid particles sub-$23\ nm$ should be assessed for human health prevention reasons. In fact, they have different and complicated chemical composition (i.e. significant rate of metal oxides) and have considerable deposition efficiency in human respiratory system (Mayer et al., 2012; Giechaskiel et al., 2014b).

In this context, until now there are no specified information about the exact biological mechanisms involved about epidemiological health effects. Except, available studies indicating that PNCs are critical metric to define (Ibald-Mulli et al., 2002) and toxicological (Murr and Garza, 2009), the other studies relate exposure to ultrafine particles with adverse toxic effects.

As a matter of fact, ultrafine particles have (1) larger deposition in cardiovascular or respiratory systems and larger likelihood of penetration (Donaldson et al., 2005; Jonathan et al., 2012), (2) longer residence time and higher level of suspension in the atmosphere, (3) higher surface area per unit volume than particles with large size increasing the aptitude to absorb carcinogenic organic compounds and have largest potentially to penetrate the cell membrane (US Environmental Protection Agency, 2002; Donaldson et al., 2005).

Table 1. 1: European and Chinese regulations of SPN 23 for both light duty and heavy-duty

	Regulation	Cycle	SPN23[P/km or P/Kwh]
EU- For light duty vehicle (Euro 6)			
Type approval	2017/1151 2017/1154	WLTC On road (RDE[1])	6×10^{11} P/km CF[2]=1.5
In-Service Conformity(ISC)	2018/1832	WLTC On road (RDE)	6×10^{11} P/km CF=1.5
For heavy duty vehicle (Euro 6)			
Type approval	582/2011	WHTC[3] WHSC[4]	6×10^{11} P/km 8×10^{11} P/km
ISC	-	On road (RDE)	CF= 1.63
China For light duty vehicle (Euro 6): Vehicle with Spark Ignition (Gasoline)			
PI: positive ignition, (gasoline and natural gas)	2016/18352.6	WLTP[5]	6×10^{11} P/km
Vehicle with Compression Ignition (Diesel)			
CI: compression ignition (Diesel)	2016/18352.6	WLTP	6×10^{11} P/km
China For heavy duty vehicle (Euro 6):			
CI: compression ignition (Diesel)	2018/ 17691	WHSC WHTC WNTE[6]	8×10^{11} kWh^{-1} 6×10^{11} kWh^{-1} – CF=2

[1] RDE= real driving emissions
[2] CF=Correction factor,
[3] WHTC=World Harmonized Transient Cycle
[4] WHSC=World Harmonized Stationary Cycle
[5] WLTP= World Harmonized Light-Duty Vehicles Test Procedure
[6] World-harmonized Not-to-Exceed

Besides human effects, PNCs have pronounced and hazardous impact on global climate (Strawa et al., 2010). Particulate matter with size interval $[100 - 1000\,nm]$ is responsible for the limited visibility in urban area (Kim et al., 2006; Hujia et al., 2013). Furthermore, PM emissions vary with local ambient temperature and may be favorable to catastrophic phenomenon like acid rains, for example. PMs may be transported through wind over a long distance then deposited on water or ground. Due to their dangerous implications that threaten the environment and the humanity, a strict control of PMs is therefore necessary to put in place as rapid as possible.

In order to take complete and real information about particle measurements, laboratory control methods become insufficient measurement tools. For this reason, laboratory measurements have been enhanced through on-road-real driving emissions (RDE), using for example the portable emissions measurement systems ($PEMS$) (Giechaskiel et al., 2019a). Other analyzer tools like Fast Mobility Particle Sizer ($FMPS$), Scanning Mobility Particle Sizer ($SMPS$), Condensation Particle Counters (CPC) and Electrical Low-Pressure Impactor ($ELPI$) have also been used (Garg et al., 2000; Simon et al., 2017; Belkacem et al., 2020; Béjiet al., 2020). Studies have proved that solid particles with size lower than $23\,nm$ could largely exceed as many as $SPN23$ for gasoline vehicles (Giechaskiel et al., 2019b).

Detailed characterization of nanoparticles in the ambient atmosphere is essential for generating a regulatory framework. Several available instruments have recently appeared to measure particle concentrations and distribution were limited by a lack of standard protocols, methodologies and application guidelines. This chapter review seeks to highlight the strengths and weaknesses of the most important commercially particles instrumentation tools. It aims to delimit the different parameters that influence on nanoparticles emissions, including weather conditions (ambient temperature, precipitation, wind speed, and direction), distance from the source (traffic) and height above the ground. In addition, it tends to understand the impact of aerosols on climate change, environment and human health. Finally, it proposes some recommendations to increase sustainability in vehicular traffic by focusing on three important factors, namely vehicle technologies, road users and infrastructure.

It can be concluded that ambient traffic nanoparticle concentrations and characteristics are complex including simultaneously the driving style effects, the vehicle technologies (brake system, aspiration particles system, Brake Disks and Pads wear, etc.), and the meteorological

conditions. Furthermore, several dynamic phenomena may affect particle formation and nanoparticle emissions, transportation and transformation after emissions.

1.2. Sampling measurement methodologies and instrumental techniques

1.2.1. Sampling measurement methodologies

Three different sampling measurement methodologies are available for measuring particle number and mass concentrations; in-situ, laboratory and real-world emissions measurements. Particle number concentrations are not always comparable due to dissimilarity in instruments, sampling and traffic conditions. This present chapter presents the difference, weaknesses and strength of each methodology. Therefore, the objective of this paragraph is to help researchers choosing the most appropriate equipment to estimate particles.

Environmental road traffic particles are divided into exhaust emissions and non-exhaust emissions. Particle exhaust emissions extending much with size diameter less than $23\,nm$ (Kittelson, 1998). In real-time emissions, the mobile source is followed by a mobile laboratory either related by a trailer or placed inside the vehicle (Vogt et al., 2003; Jezek et al., 2015) to measure the exhaust plume of the vehicle providing a large range of operating conditions. Real-world measurements make it possible to examine a typical sample of vehicles for fleet characterization. The obtained results indicated qualitative good accordance for particles in the nucleation mode ($< 30\,nm$) (Rönkkö et al., 2006; Casati et al., 2007) and a good accordance for particles in the soot mode or accumulation mode ($100 - 300\,nm$) (Casati et al., 2007). However, the diluted vehicle exhaust of low emitting vehicles (i.e.diesel particulate filter (DPF)) will be close to the level of ambient particle background (Bergmann et al., 2009). Therefore, the obtained results will have a high level of variability and uncertainty. In-situ measurements allow us to determine a variety of variables under a wide range of conditions. They provide continuous time-series data at the unit time scale for some devices (i.e. The Fast Mobility Particle Sizer ($FMPS$)). Particulates are not measured on a sampling filter and analyzed after collection. This makes it very appropriate for the measurement of particle properties like sizes, number concentrations and size distributions. Some in-situ instruments are efficient to measure hot exhaust and undiluted at the tailpipe. However, some distinct disadvantages must be revealed when compared to real-time measurements. The source of particle concentrations measured in-situ (i. e. in the vicinity of

the road traffic) cannot be exactly specified (i. e. exhaust, tire wear, tire road wear (TRW), brake wear, road wear and resuspension). In addition, some important kinds of measurements are inadequate to be elaborate in the field. Table 1.2 (Annex 1) illustrates the most important studies available in literature that are divided into laboratory, in-situ and real-world measurements. It this table, we provide also the used particles instruments, size range, advantages and disadvantages that will be described in details in the next section.

1.2.2. Instrumental techniques

Ambient nanoparticles present a variety of shapes (irregular, tabular, aggregated) that are not perfectly spherical. This causes serious difficulty in their measurements. Electrical mobility equivalent (D_p) diameters, Stocks (D_s) and Aerodynamic equivalent (D_a) are used to categorize particles when the center of attention is on the behavior of particles in moving air. Different particulate instruments have been elaborated for PM measurements and particles number concentrations over the past decades. Some of them focused on surface area, particle number or chemical compositions. These instruments include a variety of condensation particle counter battery. The particle size magnifier and electrical mobility spectrometers have been characterized in laboratory experiments applying carefully designed calibration aerosols. They are generally executed in combination or alone, to investigate the gas-to-particle transition in experiments inducing particles with a wide range of composition (Kangasluoma et al., 2020). An overview of weakness and strength of the most advanced commercially instruments that are currently used for nanoparticles monitoring are provided below. The PMs concentration can be in number (N), mass (m) and surface area (S). These previous mentioned instruments can be divided into four measuring principles including optical, gravimetric, electrical and microbalance charge.

1.2.2.1. Concentration measurement methods

1.2.2.1.1. Optical Methods

According to Giechaskiel et al. (2014c), the optical detection methods, aerosol particles are lit by a light beam and distribute this light in all directions by means of scattering process. Fraction of this light is synchronously transformed into other energy forms by absorption. Moreover, the authors revealed that the extinction of light can be estimated by the addition of absorption and scattering.

Optical instruments used for measuring particle concentration, in real-time, are based on scattering and light extinction modes. This review starts by instruments based on light scattering including Respirable Aerosol Monitor (RAM), University of California Berkeley-Particle and Temperature Sensors ($UCB-PATS$), Optical Particle Counter (OPC) and Condensation Particle Counters (CPCs). Instruments based on absorption include Spotmeters/reflectometers and Photoacoustic Soot Sensor ($PASS$).

- Respirable Aerosol Monitor (RAM)

The RAM is the most commercial light scattering photometers instrument. It allows measuring angles of $90°$, $45°$ and $< 30°$ and visible light ($\sim 600\ nm$) (Vincent, 2007).
The aerosol was aspirated through a pump, and then progressed by a cyclone that separated the respirable aerosol fraction. The aerosol passes into the optical sensor zone, by scattering the infrared light in an angle of $45°$ to $90°$, and then the aerosol was observed by a photodiode (Amaral et al., 2015). The recent digital version is DataRam4, having the potential to measure continuously real-world median particle size and concentration of airborne dust, mist, fumes and smoke. Furthermore, relative humidity and temperature are displayed in the screen. The measure of maximum response of particle size (i. e. concentration measurements) ranges between 0.08 to $10\ \mu m$. In addition, the DataRam4 monitors mass concentrations of fine and coarse particulate ($PM1$, $PM2.5$ and $PM10$). In this context, Costa et al. (2012) used the DataRam4 in both field experiments and laboratory to sample $PM2.5$. A satisfactory correlation was demonstrated using DataRam4 with other instruments to measure particle and size concentration (Amaral et al., 2015).

- University of California Berkeley-Particle and Temperature Sensors (UCB-PATS)

The UCB-PATS operates the sensing chamber from a commercial home smoke detector influenced by natural airflow and diffusion to transfer particles into its sensing chamber. An infrared LED shines every 2 seconds; a photodiode receives the response at $30°$ forward scattering. The user-set interval in minutes was averaged the resulting amplitudes (Pillarisetti et al., 2017). The signal-to-noise report for particles range $150 - 500\ nm$ in volume mean diameter was ranging from $25 - 500\ nm$ and for mass concentrations between $0.50 - 16\ mg/m^3$(Edwards et al., 2006).

- Optical Particle Counter (OPC)

The OPC is among the most used instrument, which implements a light source, commonly a diode laser, to light a sample of particles in a designed angle. A photodetector estimates the light that scattered from the particles. Based on the intensity of the flash, particles can be measured and counted simultaneously. The scattered light is identified by a photodetector as an electric pulse. The particle size is defined from the height of the electric pulse, applying a calibration curve (Amaral et al., 2015). It makes sense to count and size particles within the $50 - 800\ nm$ diameter size range, and make a very high-resolution size distribution stretch up to 100 size bins. It is also able to operate at 10 applied the Hz, so it is efficient for measuring particle flux. In this context, Jiang and Bell (2008) applied a model of the OPC, known as Side Park Personal Aerosol Monitor model $AM510$ (TSI, Shoreview, MN, USA) to estimate $PM2.5$ concentration. They demonstrated that the aerosol sample is continuously penetrated inside the collection chamber.

- Condensation Particle Counters (CPCs)

The CPCs belong to the family of light scattering counters, which are used to measure the concentration with small-sized particles. In addition, it is able to detect airborne particles with size diameter less than $10\ nm$, over a concentration range between 0 to $1 \times 10^4 \#/cc$, and at an aerosol flow rate of $1.0\ l/min$, depending on the applied model. This instrument is perfectly appropriated for applications without high-concentration measurements, like filter, air cleaner testing, environmental monitoring, particle counter calibration and climate and atmospheric studies (www.arm.gov). When the particles are increased in size diameter by condensation, the CPC acts similarly like optical particle counters.

- Spotmeters

These instruments are also known as smoke filter meters or reflectometers owing to the light absorption estimating principal based on light reflection over filter.

Particle concentrations are measured by filtering the exhaust gas in a filter paper, and saving of the ratio between the light reflected by this unexposed spot and exposed spot (Giechaskiel et al., 2014c).

- Photoacoustic Soot Sensor (PASS)

Light absorbing particles comprised in the aerosol samples are frequently heated by modulated light–absorption of amplitude. The recorded signal is proportional to the

concentration in volume of light-absorbing particles with diameter size$< 300\,nm$, and it is proportional to the surface of particles with diameter size$> 300\,nm$ (Giechaskiel et al., 2014c). Lack et al. (2006) built up a very sensitive method to estimate aerosol absorption at $532\,nm$ particle diameter size, with efficient response time by applying photoacoustic absorption spectroscopy. It tested the variation of particle under different ambient temperature, pressure and relative humidity. Moreover, it has been selected to measure a condensation nuclei counter (CNC) and PM number, and considered as the most suitable technique.

1.2.2.1.2. Gravimetric Method

According to the gravimetric method, the particle mass concentration (PMC) is obtained by weighing the filters both before and after sampling time. The filter gathers PM in different granulometric fractions (nucleation, soot and coarse modes), unless there is an impactor or cyclone to eliminate larger particles (Giechaskiel et al., 2014c). Determination of PM mass can be modified depending on the conditioning conditions of the filter. Accordingly, Giechaskiel et al. (2014c) and Nussbaumer et al. (2008) depicted out that the filters are commonly packed under controlled conditions of relative humidity and temperature. Gravimetric method can collect particles and assess their concentration. For completed analysis, other techniques are required like Transmission Electron Microscopy (TEM) and Scanning Electron Microscopy (SEM). The highest resolution obtained in SEM depends on several factors, such as the interaction of the sample with the volume of the electron beam and the electron spot size. While it is unable to provide atomic resolution, some $SEMs$ can reach resolution below $1\,nm$. Actually, full sized $SEMs$ contribute resolution size range $1-20\,nm$ whereas desktop systems can produce a resolution of $20\,nm$ or more.

The TEM is considered to be the most used technique in characterizing nanomaterials in electron microscopy. The image and the chemical information of nanomaterials at a spatial resolution similar to the level of atomic dimension are produced using TEM. More details were provided in Kumar et al. (2019).

The cascade impactor is among the most popular gravimetric instruments for measuring particle size distribution in mass. This instrument activates based on the inertial classification of particles. Vincent (2007) revealed that the aerosol sample moves through a succession of stages. In each stage, an air jet including the aerosol attains the impacting plate and particle size larger than the cutoff diameter for the phase are collected. Particles with small size

diameter pursue the gas flow surrounding the collection plate and are received in the next phase. This phenomenon continues until particles with small size diameter are eliminated in the after-filter. The weakness of the conventional Cascade Impactors is that it is unable to select particles smaller than $0.4\ \mu m$. Another family of Cascade Impactors is based on Micro-Orifice Uniform Deposit Impactor ($MOUDI$). It collects particles with size diameter smaller than $0.056\ \mu m$ and considered as an efficient and accurate Cascade Impactors (Venkataraman and Rao, 2001).

1.2.2.1.3. Microbalance Methods

Giechaskiel et al. (2014c) outlined that when the particles are gathered, over the surface of an oscillatory microbalance, this latter use the transformation of the resonance frequency to measure the PM. There are two-principal measurement instruments applying the microbalance method: The Quartz Crystal Microbalance (QCM) and the Tapered Element Oscillation Microbalance ($TEOM$).

- Quartz Crystal Microbalance (QCM)

Quartz Crystal Microbalance (QCM) is a highly sensitive mass balance that estimates in the order of nanogram to microgram of changes in mass per unit area. In QCM, the quartz crystal has a piezoelectric property of changing its resonance frequency when there is a small addition of mass in its surface (Giechaskiel et al., 2014c). In addition, it is able to allow the user to evaluate small mass changes on the surface of covered quartz crystal.

- Tapered Element Oscillation Microbalance (TEOM)

Particulate matter assessing systems that use $TEOM$ technology are gravimetric instruments defining ambient air by continuously weighing the filter at a constant flow rate and calculating near real-world mass particulate mass concentration. It takes continuous real-time mass measurements of particulates with the Thermo Scientific ™ 1405 $TEOM$™. This instrument measures $PM1$, $PM2.5$ and $PM10$ airborne particulates with accurate short-term precision.

A pump draws a sample inside the instrument at $16.7\ l.min^{-1}$ by an inlet in order to allow only particles of the intended size range to exceed through. This air stream is shared so that $3\ l/min$ of sample is conducted to the tapered component and the remainder will be sanded to exhaust. In this context, Giechaskiel et al. (2014c) affirmed that placement of $TEOM$ in

aerosol measurement in mobile source (i.e. the vehicle) was a failed method that is related to problems with pressure changes, humidity and overload. On the contrary, Nussbaumer et al. (2008) outlined that the $TEOM$ is an efficient instrument for real-time measurements of $PM2.5$ and $PM10$ during biomass combustion. Other published studies have used the $TEOM$ for continuous $PM2.5$ and $PM10$ sampling (see for instance, Jiang and Bell., 2008; Elsässeret al., 2012).

1.2.2.2. Size distribution measurements methods

Size distribution measurement methods evaluate the aerosol size, that can be illustrated by diameter (aerodynamic, mobility) and the aerosol concentration.
Amaral et al. (2015) showed that the measurement of particle size distribution is terminated from a conjunction of several measuring instruments.

- Dekati Low Pressure Impactor ($DLPI$)

The $DLPI$ is consisted of 14-stage cascade impactor that is selected to measure airborne particle mass size distribution. It classifies and measures particles into 14 size fractions in the range of $16\,nm$-$10\,\mu m$at a flow rate of $10\,l/min$. In each size fraction, the particles are assembled on $25\,mm$ collection substrates that are weighed before and after the sampling to acquire size distribution of the particles gravimetrically. This instrument can be applied in several particle measurement applications and the high temperature version can be warmed up to $180\,°C$ for high temperature aerosols and direct sampling (www.ecotech.com). Rovelli et al. (2017) collected particle with size- segregated range $0.028-10\,\mu m$. Results revealed high level of agreement between co-located Harvard type $PM2.5$ Impactor and $DLPI$, allowing them to be selected as characterized and comparable by a reciprocal predictability.

- Differential mobility spectrometers (DMS)

The differential mobility spectrometer (DMS) employs electrical mobility measurements to measure number spectra/particle size in the range of $5\,nm$-$2.5\,\mu m$. Considering the classification of particles in relation to their differing electrical mobility integrates in parallel, the DMS series is capable to provide the fastest available number/size spectral measurement. The user interface prepares the spectral data in real-world to output surface area or number, particle mass and basic spectral information. Available studies demonstrated that DMS is

among the most used spectrometers based on particle mobility (Hosseini et al., 2010; Hossain et al., 2012).

- Fast Mobility Particle Sizer ($FMPS$)

The fast mobility particle sizer ($FMPS$) is characterized by a wide dynamic concentration range and flexible data management capabilities, which makes it more suitable for a variety of applications than other instruments (i. e. environmental research, indoor air quality tests, urban canyon studies, inhalation toxicology studies, etc.). It quantifies particles in the range of $5.6 - 560\ nm$ with $1\ Hz$ time resolution. This instrument provides 32 resolution channels. It has the same electrical mobility measurement technique compared to the $SMPS$ spectrometer. However, alternately of a CPC, the $FMPS$ spectrometer employs multiple, low-noise electrometers for particle detection. It operates at relatively high flow rate ($10\ l/min$) to reduce diffusion losses of nanoparticles and ultrafine. In addition, it operates at ambient pressure to avoid evaporation of volatile particles, and needs no consumables. Several studies in different fields have used the $FMPS$ (i.e.Belkacem et al., 2020;Beji et al., 2020).

- Scanning Mobility Particle Sizer (SMPS)

The scanning mobility particle sizer ($TSI\ SMPS$) has contributed gain new observations in particle research and facilitated with calibrating reference material and other instruments related to aerosol. The US National Institute of Standards and Technology ($NIST$) and other reference laboratories applied the $TSI\ SMPS$ for submicrometer particle size distribution measurements. The $SMPS$ spectrometer is a nanoparticle sizer able to estimate the size distribution of airborne submicron particles with acceptable precision. It combines single particle counting with electrical mobility sizing to provide nanoparticles concentrations in discrete size channels. Users may select among three-differential mobility analyzers ($DMAs$), two-different neutralization techniques and seven $CPCs$, enabling measurement in the range of $1\ nm$ to $1\ \mu m$. When the $SMPS$ is coupled with an Aerodynamic Particle Sizer (APS) or an Optical Particle Sizer (OPS), the continuous sampling range can be extended up to $20\ \mu m$ or $10\ \mu m$, successively.

Nussbaumer et al. (2008) and Giechaskiel et al. (2014c) confirmed that the$SMPS$ is the most efficient and precise instrument for high-resolution size distribution and number of particles from vehicle exhaust. They added also that the $SMPS$ has many versions, where the size range extends from few nanometers to few micrometers.

- Electrical Low-Pressure Impactor (*ELPI*)

The Dekati high-resolution ELPI®$_+$ is a developed version of the widely used *ELPI* instrument. The high resolution of this instrument combines the data inversion algorithm with features of the *ELPI* ®+$_+$ that gives real-time size distribution and particle number up to 500 size classes in the range of $6\ nm - 10\ \mu m$. Other high resolution *ELPI*® + features that provide the possibility to characterize chemical composition of size categorized particles after the real-time sampling, robust structure and wide particle sample concentration range. In this context, Coudray et al. (2009) and Beji et al. (2020) demonstrated that particle size distribution is rapidly and easy attained using an *ELPI* for biomass combustion and tire and road wear particles (non-exhaust particle emissions), respectively. According to Vincent (2007), the particles are electrically charged as they are aspirated in the *ELPI*. For this, Giechaskiel et al. (2014c) clarified that charging is performed by a unipolar corona charger. Charged particles progress through a low-pressure Cascade Impactor constituted by gathering steps electrically isolated (Amaral et al., 2015).

- Aerodynamic Particle Sizers (APS)

Aerodynamic Particle Sizer (*APS*™) is used to measure aerodynamic sizes. As revealed by Hosseini et al. (2010), APS provides real-time aerodynamic measurements with high resolution of particles from size ranging from 0.5 to 20 μm. This particle sizer estimates equally light scattering intensity in the equivalent optical size range of 0.37 to 20 μm. This instrument employs a patented, double-crest optical system for unequaled sizing accuracy. Furthermore, it provides an improved signal processing and redesigned nozzle configuration. This results in an improved accuracy of mass-weighted distribution, bigger small-particle sizing efficiency, and virtual elimination of false background counts.

- Laser Aerosol Spectrometer (*LAS*)

The LAS (*model* 3340) employs patented intra cavity laser and a wide-angle optics to measure the number and size concentration of airborne particles. It characterizes a monotonic response that concerns to light scattering intensity in the Mie range for efficient and precise resolution.

This commercial instrument is unique in its capability to estimate both sub and super micron particles in wide range size, making it an effective workhorse in any laboratory. It can

measure concentrations up to $1.8 \times 10^4 \# \, cm^{-3}$ and particles in the range $0.09 - 7.5 \, \mu m$ at a sample flow rate $0.1 \, l.min^{-1}$. Particle size distributions can be measured at a sampling time of about $1 \, s$ (TSI Inc. www.tsi.com).

-Ultrafine particle (UFP)

The UFP Monitor (model 3031) were designed to estimate ultrafine particles long-term strongly recommended in air quality monitoring networks. It describes the PNC in six size classes in the size range between 20 and 500 nm and needs only little maintenance. With six size classes, the UFP lies between $SMPS$™ spectrometer, which provide > 100 size classes, and CPCs that describe total number concentration (i.e. without any information about sizing). It is able to change in aerosol concentration and detect nucleation events. The data can easily be inserted into presented data acquisition systems, are tamper-proof, and remotely accessible (TSI Inc. www.tsi.com).

- GRIMM nanoparticle measuring systems

There are several versions in $GRIMM$ Aerosol (i. e. $GRIMM$ 1.107, $GRIMM$ 1.108, $GRIMM$ 1.109) which are not able to detect particle with small size diameter. The newest version is the PSMPS combining GRIMM SMPS+C system with the Airmodus Particle Size Magnifier (PSM). It is able to measure the number size distributions starting at 1.1 nm.

The measurement of aerosol number size distributions started from the sub $2 \, nm$ size range for understanding the basic phenomenon of new particle formation (Kulmala et al., 2013). Measuring capacity and time-response of the recent GRIMM versions are summarized in Table 1.2.

Table 1. 2: Features of GRIMM aerosol instruments for measuring particle number distributions and concentrations.

Instruments	Size range (nm)	Sampling rate (s)	Detected diameter	Detectable (min-max) concentrations ($\#/cm^3$)
$GRIMM\ SMPS + C$	5-1110	1	Dp[7]	1-10^7
$GRIMM\ WRAS$	5-32.000	1(CPC) ; 110 (DMA) ; 6 (Aerosol Spectrometer)	Dp Dp and Da[8]	1-10^7
$GRIMM\ SMPS\ + E$	0.8-1110	0.2(T90)	Dp	100-10^7
$PSMPS$ ($SMPS + C\ system\ + PSM$)	1.1 -55	< 3 s (T_{10}-T_{90})	Dp	10^7

1.2.2.3. In use compliance/in service conformity

There are limited number of commercially $PM - PEMS$ equipment based on Diffusion Charger (DC), QCM with parallel filter, and $PASS$ with parallel filter. High correlation with

[7]Dp=Electrical mobility Equivalent diameters
[8] Da= Aerodynamic equivalentdiameters

low bias was found for the $PASS$ equipment (Johnson et al., 2011), even for emission rates at the regulatory limit (Khan et al., 2012). In other research, the $PASS$ has been applied successively for on-board testing (Durbin et al., 2007). The $PM-PEMS$ is very sensitive to use and many problems might be present including operational problems such as software bugs, in use conditions problems as mechanical and electrical connections.

Recent commercial $SPN-PEMS$ instrument is considered as "black box" where linearity and efficiency tests have to be controlled with thermally stable soot same as aerosol.

The efficiency of this instrument is controlled with monodisperse aerosol (Giechaskiel, 2018). According to the author, the simplest forward way is to control the efficiency of the complete $PM-PEMS$. However, controlling the particle detector and the thermal pre-conditioning of the $PN-PEMS$ independently is also acceptable. In the second case, the two-results have to be combined in one penetration efficiency. For the linearity control, generally polydisperse aerosol is employed in order to achieve high concentration levels. The main measurement for the efficiency instruments includes (Fig.1.2):

- Bipolar chargers to conditioning the aerosol for the Differential Mobility Analyzer (DMA) and also for the PN-PEMS particle detector;
- A DMA for obtaining particles of the regulated electrical mobility diameters;
- A reference instrument to estimate the absolute concentration of the induced monodisperse particles.

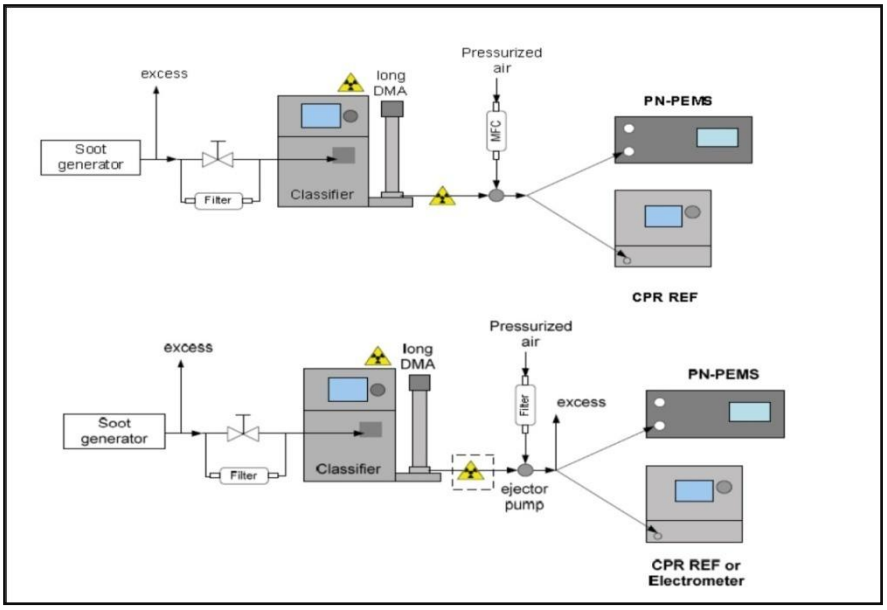

Figure 1. 2: Features of GRIMM aerosol instruments for measuring particle number distributions and concentrations.

Instead of PN-PEMS only, the particle detector or other parts of the PN-PEMS could be controlled. The second neutralizer is essential only when the PN-PEMS has a DC based particle detector. Instead of ejector pump, Mass Flow Controller (MFC) with a mixing orifice could be used (Giechaskiel, 2018).

1.2.2.4. Discussion of the capabilities of the equipment and future needs

As discussed above, there are several types of commercial instrument for measuring particle number distribution and concentrations. This current review summarized the characteristics of the major particles measuring instruments to guide the researchers in choosing the appropriate instrument to meet the objective of their study (Table 1.2, Annex1). Problems that need to be inspected in applying such equipment in any regulatory framework include time-response, portability, robustness for unattended operation over long sampling time, maintenance requirement, calibration, cost and size range (Giechaskiel et al., 2014c).

Real-time particle measurement is the favorite method sampling since it provides processes such as combustion to be observed. Moreover, instruments that quantify particle in real-time usually possess an automated system for recording data. Another feature that must be checked during the selection of the PM instrument is whether a dilution system is required. Dilution system can mitigate temperature and particle concentration of the combustion gas. Accordingly, the integration of a dilution system contributes to a representative sampling and more realistic of PM emissions (Amaral et al., 2015). Besides, this later mentioned system provides considerable durability for measuring equipment because of the requirements of the analyzers entry. Thus, the integration of a dilution system in such instruments becomes an absolute necessity like the example of $DLPI$.

The increase of noise level of a given equipment is mostly related to the increase in sampling rate. Accordingly, selection of a sampling frequency and suitable equipment depends essentially on the noise level of the instrument and the objectives of any individual study.

Methods applying filters are not precise, while the most important advantage of measuring particle employing filters and conventional Cascade Impactors is the capacity to perform a chemical analysis (Amaral et al., 2015). Sampling related to ultrafine particle is essential, notably in health-related studies. To this end, the most recommended instrument is to measure the particle number concentrations, as $FMPS, SMPS, OPC, ELPI$, and $PSMPS$ (Amaral et al., 2015).

It comes out the importance to choose the most suitable instrument for a specific case study. Thus, it is mostly important to set a standard protocol for measuring nanoparticles allowing therefore possible comparison between different available results.

1.3. Ambient environnemental conditions effects on nanoparticle concentrations

The contribution of road traffic on nanoparticles was strongly correlated to several parameters. This review gathers the most important and significant factors that have real impact on nanoparticles. For example, weather conditions (wind speed, wind direction and ambient temperature/relative humidity) (Charron and Harrison 2003; Virtanen et al. 2006; Casati et al. 2007; Belkacem et al. 2020), then, the distance from the road (Kittelson et al. 2004; Belkacem et al. 2020) have been taken into account in this review. Furthermore, height above the ground (Zhu and Hinds 2005; He and Dhaniyala 2012; Belkacem et al. 2020) has also been considered for a complete comprehensive analysis about factors having serious impact on nanoparticles as many people live in different apartment floors level with different height above the ground at urban area.

1.3.1. Weather conditions

Particle number size distribution and nanoparticle concentrations in traffic-influenced environments are strongly affected by weather conditions including wind speed and direction, ambient temperature, relative humidity (RH), and precipitation. Wind speed influences atmospheric resuspension, mixing and dispersion. Nanoparticle concentration reduces exponentially with wind speed. This is because high wind speed leads to better mixing and higher coagulation. Scavenging phenomenon and deposition are discovered at higher wind speed inducing a decrease in particles number (Arnold et al., 1999; Kumar et al., 2008).

High concentration level appears practically downwind rather than upwind directions from the road surface. Particles with size diameter greater than $100\,nm$ illustrates a "U-Shaped'' variation accompanied with wind speed in the range of $5-10\,m.s^{-1}$. PNCs with size range between $30-100\,nm$ reduce by 10^4 normalized counts per cubic centimeter as a result of wind speed increase (Arnold et al., 1999). Harrison et al. (2016) demonstrated no obvious relationship between the diameter and the meteorological conditions, with the exception of the first size diameter. Increasing wind speed leads to a reduction of the travelling time between the receptor and the source, causing therefore less time for evaporation. However, it

induces an increase of the dilution and turbulence leading in turn to a rapid dilution of the vapor component. Consequently, the concentration gradient between the particle surface and the ambient air is increased (Harrison et al., 2016). In addition, Silva et al. (2020a) demonstrated that particle mass concentrations PM ($PM2.5$ and $PM10$) rate is strongly influenced by wind speed.

The increase of solid particle number emissions is related to the decrease of the ambient temperature (Giechaskiel et al., 2015). In fact, during cold-start particles may be (1) semi-volatile material regenerating oxidation as the catalytic converters are not able to be evaporated in the SPN system and have not achieved the light-off temperature or (2) Blow-out of loose non-volatile solid particle deposits, since the filter exhibited to strongly transient operation compared to thermal and flow conditions (Giechaskiel et al., 2007). Giechaskiel et al. (2015) outlined that vehicle emissions with gasoline direct injection (GDI) increased by 160% when tested with the Worldwide Harmonized Light Vehicles Test Cycles ($WLTC$) at -$7°C$ as a replacement of $23°C$. The SPC emissions strongly decrease over time with a few exceptions like cold start cycles over low-temperatures. In the study developed by Harrison et al. (2016), it was found that, there is no relationship between diameter and ambient temperature/relative humidity with a small range in air temperature of $[12 - 18°C]$. In contrast, Rankko and Timonen (2018) affirmed that the volatility of "liquid" particles produced in the cooling dilution is higher than that of "solid" particles in the presence of high temperature. This means that particles induced during the cooling dilution of exhaust can disappear or evaporate when the particles are aged in the atmosphere (Harrison et al., 2012b). In addition, several studies demonstrated that higher nanoparticles concentrations are related to lower ambient temperatures, and relate this result with strengthen atmospheric nanoparticle formation from road traffic emitted gaseous compounds (Charron and Harrison, 2003; Kittelson et al., 2003; Pirjola et al., 2006). In the same context, Olivares et al. (2007) have proved that PNCs doubled with a sharp decrease in ambient temperature. Recently, for particle number concentration ($> 10\,nm$), it has been shown that particle size distribution was dominated by nanoparticles in both summer and winter seasons (Saha, et al., 2018). However, in summer-time, the concentration reaches its highest point close to $10\,nm$ particle size; while in winter-time the peak concentration was approximately $15 - 20\,nm$. In other hand, roadside particle study reported $1.8 - 3.4$ times lower PNCs in summer than in winter (Pirjola et al., 2006). Similarly, Schneider et al., (2020) confirmed notably higher levels of $PM1$ in winter-time than in summer-time.

Rönkkö et al. (2017) and Hietikko et al. (2018) have demonstrated a vast contribution of particles with size diameter lower than $10\,nm$ compared to the total particle number of road aerosol and pronounced contribution of particles with size diameter sub-3 nm.

In order to understand the effect of the relative humidity independently of ambient temperature, Vehkamaki et al. (2003) have tested the variation of PNCs with the same ambient temperature and four different relative humidity values. They demonstrated that particles with size diameter greater than $3\,nm$ were more influenced by high relative humidity than under high ambient temperature. Olivares et al. (2007) have also reported high nucleation particle concentrations (between 5 and $30\,nm$ ($N5-30$)) during very humid period. Similarly, Hussein et al. (2006) outlined that with nucleation and Aitken modes, particles increase three-times when the ambient temperature drops from $280\,K$ to $250\,K$.

Rainy weather conditions have been found to reduce the roadside ambient PNCs, although despite the fact that weather conditions may have adverse effects. In fact, rainy weather clean urban atmosphere by reducing the condensation sink induced by particles, resulting in turn to an increase of PNCs in road environment. Similarly, Easter and Peters (1994) and Charron and Harrison (2003) registered high nanoparticle concentrations immediately after several rainy days. However, an Indian study was found exactly the opposite precipitation effect, where particulate matter increased with the decrease of rainfall precipitation (Deshmukh et al., 2013). The highest particle number concentrations of the first hour after rain might be explained by the rapid drop in ambient temperature during precipitation. This temperature reduction induces high saturation ratio for semi-volatile species. Elevated saturation ratio along with limited surface area of particles allows formation of new particles. This results in a significant increase of PNCs.

1.3.2. Distance from the road effects

This section summarizes the most important results available in literature dealing with distance from the road effects on nanoparticle emissions. The spatial extent concept is known as the distance that separate the source of nanoparticle emissions (i.e. road traffic) and population and individuals' groups. An Austrian study measured the number of UFPs in two-different sites in the vicinity of major roads (Hitchins et al., 2000). The obtained results demonstrated that particles with size diameter smaller than $0.7\,\mu m$ decreased significantly with the increase of distance from the road. At a distance of $150\,m$, the concentration

decreases about 50 % of the maximum induced at 15 m from the source. In addition, the fraction of particles with various morphologies of 50 nm particles are intensified when the distance from the road is increased (Rönkkö and Timonen, 2019). More recently, Belkacem et al. (2020) have conducted an experimental study to analyze the effect of the distance between the sampling site and the urban road traffic. Three different positions from the emission source were selected ($d1 = 6.60\ m$, $d2 = 30\ m$ and $d3 = 330\ m$). The authors demonstrated that the relationship between PNCs and distance from the source could be explained by a negative linear polynomial model with 95 % confidence bounds and a high reliability coefficient of 96.69 %. It is worthy to note that similar results have been obtained by several previous published studies (see for instance, Zhu et al., 2002; Kittelson et al., 2004).

1.3.3. Height above the ground effects

As far as the authors knowledge is of concern, the effect of vertical and horizontal dispersion on the particle concentration profiles near roads is not sufficiently studied. However, this is a critical parameter to take into account, since, in urban areas, all population lives in apartments with different floors. The measurement of particle concentrations gives an overview of the level at which particles remain active.

A field measurement study conducted in Germany outlined that PNCs downwind of a motorway exponentially decreased with increasing height from 5 to 30 m above the ground (Imhof et al., 2005). Moreover, very restricted PNC information on heights less than 5 m above ground are found, despite the fact that this height encompasses a critical zone for pedestrian and cyclist exposure. Recently, Belkacem et al. (2020) have conducted measurements at heights above ground of less than 3 m due to this critical spatial interval for cyclists and pedestrians' health. The authors examined the effect of height on PNDs. Two-measurement days ($D2$ and $D3$) were considered with two-heights: $h1 = 2.03\ m$ (horizontal position), and $h2 = 2.82\ m$ (vertical position) above the road pavement. The obtained results demonstrated high nanoparticle number with channel size diameters in nucleation mode primarily in 10.75 nm, reaching up to $5.61 \times 10^3\ \#/cm^3$ at height $h1$, and $3.23 \times 10^4\ \#/cm^3$ at height $h2$. Similarly, Goel and Kumar (2016) have obtained the same results with four different heights less than 4.7 m above the ground. Quang et al. (2012) depicted out that particles with a diameter smaller than 30 nm are strongly influenced by height. The resultant increase occurred in the nucleation mode (diameter less than 30 nm), while decreasing above 30 nm due to new particle formation event tied to the amount of global

radiation. In fact, nucleation mode practically consisting of nitrogen, volatile organic and sulfur compounds; it may be extracted not only from traffic exhaust emissions or non-exhaust emissions but also from regional particle nucleation.

1.4. Nanoparticles effects on human health, environment and climate

1.4.1. Health impacts

This paragraph illustrates the available published results regarding the effect of nanoparticles on human health and

environment issues. It has been demonstrated that regularly exposure to nanoparticles may harmfully affect human health (Feng et al., 2020). The main process underlying the pathological consequences of particles in the cardiovascular system and lungs is inflammation, asthma, involved in at herothrombosis, chronic abstractive lung disease, cancer and pulmonary fibrosis (Donaldson and Tran, 2002; Silva et al., 2020b). Nel et al. (2006) explained that nanoparticles penetrate human body through the lung, skin and gastrointestinal tract. Their small size diameter permits them to be breathed profoundly into the lungs where they are able to enter the vascular space and pulmonary interstitium to be absorbed immediately into the blood stream, and penetrated the alveolar epithelium (Terzano et al., 2010). They may also be displaced within the body to the axial nerve system, the brain to organs and into the systemic circulation like the liver (Helland et al., 2007). Figure 1.3 summarizes the system health effects of nanoparticles as illustrated in Terzano et al. (2010).

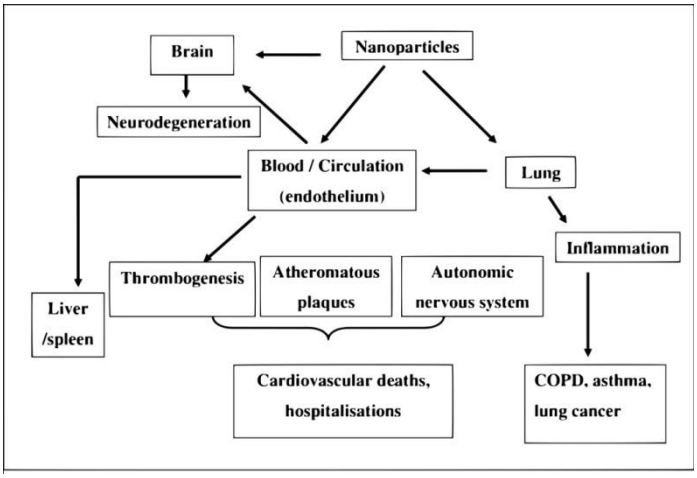

Figure 1. 3: Systemic health impacts of ambient nanoparticles (Terzano et al., 2010).

The potentially of particles to prolong, initiate or worsen inflammation can be considered as a key property. Several researchers have investigated the pro-inflammatory effects of NPs, owing to their capability to cause inflammation. The first dominant findings were that nanoparticles have a more pronounced effect on cell stimulation, cell damage and inflammation than an equal mass of particles of the same materials with bigger size (Donaldson et al., 2000).

Approximately $6\,\%$, $18\,\%$ and $58\,\%$ of these deaths were related with lung cancer, acute respiratory infections and chronic obstructive pulmonary disease, and stroke and ischemic heart disease (World Health Organization, 2018).

Solely, around $20\,\%$ of nanoparticles are eliminated once filed in alveolar regions in animals' subjects after $24\,h$ exposure. On the contrary, about $80\,\%$ of particles greater than $500\,nm$ could be eliminated (Oberdörster et al., 2005a). In the same context, Chalupa et al. (2004) discovered about 74% deposition of carbon ultrafine particles in asthmatic human subjects during 2 hours exposure.

Surface area is the metric inducing the pro-inflammatory effects. This is evident in both vivo Duffin et al. (2002) and vitro Donaldson and Tran (2002), particles with different sizes generating inflammatory effects that are strongly linked to the surface area dose. This surface area dose, linked to inflammatory response, is partially related to transition metals. However, it is also established with low toxicity materials and an ambiguity on cellular mechanism. Even with low toxicity, surface area has also the potentiality to produce oxidative stress and free radicals in cells that has nothing to do with transition metals. This is because there is no soluble toxic component that could mitigate the effect (Brown et al., (2000, 2001)). Toxicological studies have proved vehicular traffic associated organic ultra-fine particles and nanoparticles to be related with adverse human health like asthma exacerbation and pulmonary inflammation (Shao et al., 2017; Niu et al., 2020). In fact, internal combustion engines (ICEs) produce large quantity of PAHs that are divided between gas and particle phases. Moreover, gasoline exhaust includes lower proportions of volatile and semi-volatile PAHs than that of diesel vehicles (Zhu et al., 2017). Rapid evolution may participate to the often-puzzling survival of newly constituted particles in mega-cities. These particles are produced at proportions consistent with sulfuric-acid–base nucleation and tend to grow at typical proportions (about $10\,nm$) with extremely high condensation, sinks that evidently should scavenge all of the tiny nucleated particles (Wang et al., 2019).

The low toxicity surface free radical effect is obvious in their potentiality to produce oxidants in cell-free chemical systems (Brown et al., 2001; Wilson et al., 2002). In cells, high surface area doses manifest to initiate inflammation passing by a number of pathways accompanied with important oxidative stress-responsive gene transcription. Oxidative stress extended in cells exposed to activation of oxidative stress-responsive (Mroz et al., 2008) and some nanoparticles types (Donaldson and Stone, 2007).

Few studies supported particle surface area as an appropriate metric to evaluate human exposure whilst several others preferred particle number concentrations. In this framework, Maynard and Maynard (2002) revealed that higher surface area to mass ratio of ultrafine particles authorizes remarkable contact for adsorbed compounds to react with biological surfaces. Unlike to epidemiological studies that supported number concentration as a metric, Pekkanen et al. (1997) demonstrated incorporations between exposure to ultrafine particles and deficits in peak expiratory flow among asthmatic children. Moreover, other researches relate this exposition with cardiovascular diseases like cardiac-rhythm disturbance and heart attacks (Wichmann et al., 2000; Oberdörster et al., 2005b). Delfino et al. (2005) demonstrated indirect epidemiologic signs relating the adverse cardiovascular effects with ultrafine-dominated fraction of fossil-fuel combustion particles. Several studies outlined that with a short-term exposure to ambient nanoparticles intensify existing cardiovascular and pulmonary diseases. Whereas, the increased risk of death and cardiovascular disease are strongly related to long-term duplicated exposure (Brugge et al., 2007). Stölzel et al. (2007) demonstrated a significant correlation between cardio-respiratory mortality and increased nanoparticle number concentrations $(10 - 100\, nm)$ applying time-series epidemiological analysis. Toxicological studies have proved the toxicity of nanoparticles, while very restricted epidemiological evidence was noticed on health effects. For instance, there is a very limited quantitative review of concentration-response functions for nanoparticles that could be applied in health effect evaluation. Furthermore, for fine and coarse particles there are also practically restricted epidemiological studies on the health impacts of ambient nanoparticles. Exposure of nanoparticle number concentrations harmfully affects human health. Owing to scarcity of data and the exact biological and chemical mechanisms of such nanoparticles that causes death or disease are not yet fully described and specified. This is clearly a field of nanoparticles research that needs more toxicological and epidemiological evidence.

1.4.2. Environmental impacts

Visibility impairment is caused by build-up of the atmospheric particles that scatter or absorb light from the sun (Horvath, 2008). It decreases with wind speed and temperature and increases with atmospheric pressure and relative humidity (RH) (Tsai, 2005). At high RH ($\sim 90\%$), the light scattering cross-sectional areas of particles extend by uptake of water (Kumar et al., 2010).

Several local and global scale studies have proved high correlation between reduction visibility and mass concentration of both $PM10$ and $PM2.5$ (Cheng and Tsai, 2000; Mahowald et al., 2007; Che et al., 2009). Particle sizes contribute to a critical role for the interaction with light, where larger particles have a strong association between mass concentrations and visibility impairment (Strawa et al., 2010). Composition and shape of particles are suitable for visibility limitation; particles including nitrate species, organic carbon and sulphate may cause $60 - 95\ \%$ of reduction, whereas carbon particles may participate with $5 - 40\ \%$ of overall visibility (Kumar et al., 2010).

Despite the abundant number of carbonaceous and sulphate nanoparticles that are emitted by diesel vehicle notably in urban area, the role of nanoparticles in visibility is not sufficiently developed and established. Particles of these compositions limit visibility, implying that nanoparticles might be pertinent on visibility impairment. However, the most comprehensive of nanoparticles role invisibility impairment is fundamental (Slezakova et al., 2013) and requires further advanced research.

1.4.3. Climate impacts

Variables that can impact on climate are generally known as 'radiative forcing'. Direct impacts correspond to the climate effects of the aerosol particles (Yu et al., 2006). The latter can absorb and scatter solar radiation. In fact, a fraction of the scattered radiation will be reflected back into space, resulting in a cooling process of the atmosphere. Particles with size diameter from 0.1 to 2 μm are the most efficient at backscattering of solar radiation. The sized particles are the major factor governing the force of the direct effect.

Black carbon (BC) belongs to a class of environment pollutants known as particulate matter (PM). PM compounds of soot liquid droplets, wood smoke particles and small particles of dust suspended in air. It has been demonstrated that BC is the second largest contributor to

global warming. If BC particles are combined into cloud droplets, the cloud droplet may evaporate owing to the local heating, and then lens influence of the water intensifies the absorption. This is known as semi-direct effect (Verheggen and Weijers, 2010; Seo et al., 2020).

1.5. Alternatives to increase sustainability in vehicular traffic

Improving sustainable mobility is the major widespread objectives in transportation sector. In fact, the term of sustainable mobility was deduced from the concept of "sustainable development". According to the World Commission on environment and development, sustainable development is known as the "*development that meets the needs of the present without compromising the ability of future generations to meet their own needs*". Equally, environmental sustainability is the aptitude to protect global ecosystems and conserve natural resources to keep human health and environment of the current and future generation. In this direction, we will be interested in three complementary factors that we believe essential to have a sustainable environment and mobility, namely road users, vehicle and infrastructure. In addition, as a solution to these problems, specific mitigation, improvements, prevention and compensation measures must be implemented shortly.

- Vehicle technologies

In order to reduce nanoparticles formation, the new emerging technologies refer mostly to particle filter which is expected to be efficient in the reduction of particulate emissions produced by both diesel particulate and gasoline injection engines. Furthermore, it is recommended to focus on ICEs fueled by alternative sources of fuels, such as fuel cell cars (Mac Kinnon et al., 2016), biofuels and flex-fuel vehicles. At this look, some studies considered that electric vehicles may reduce pollution (Condurat et al., 2017), while, they are the main source of non-exhaust emissions owing to their relative high weight (Timmers and Achten, 2016). In fact, the same source found that there is a positive relationship between non-exhaust PM emissions and weight. Generally, enhancing the vehicle characteristics leads to significant mitigation in atmospheric pollutants mainly of nanoparticle concentrations. The development of new composite materials, new polymers and so-called 'memory metals', which are lighter and more resilient as compared with conventional materials should also conduct to pronounced mitigations in quantities of burned fuels (Condurat and Patterson, 2016).

- Infrastructure

As vehicle technologies, infrastructure is an important factor to improve air quality in order to ensure a sustainable transport and environment. In the past few years, among the most important issues for urban areas is the problem of air quality degradation. The intensive increase of particle emissions proves the causality of the degradation (European Environment Agency, 2019). Mostly, the term of "green infrastructure" widely used and analyzed (See for instance, Bealey et al., 2007; Hewitt et al., 2020), has a positive impact on environment and air quality (Nowak et al, 2006), focusing particularly on suspended particles. In this context, Nowak and Heisler (2010) revealed that the green infrastructure mitigates pollution with suspended particles by filtration and absorption of particles.

It is worth noting that very scarce number of studies were found focusing on the evaluation of the relationship between infrastructure and nanoparticles. More attention should be paid to the drainage system of roads particularly for the developing countries in order to favor the phenomenon of scavenging. In fact, during rainy season water is precipitated into the roadway, making cyclists and pedestrian exposed to nanoparticles for a long-time period.

- Road users

Road users is the most difficult and complex component as compared to the two-last mentioned factors (i. e. the infrastructure and the vehicle technologies). In fact, each driver has his own driving style including rational (or economic driving mode) and aggressive driving mode. Driving behavior is strictly correlated to acceleration and deceleration maneuvers. Accumulation and coarse modes formed directly by incomplete combustion with level mostly during sudden vehicle acceleration and deceleration maneuvers (Beji et al., 2020). Several policies have been imposed like the increase in fuel price. In fact, most drivers tend to save fuel by decreasing their vehicle speed by up to 5.5% (Levinson, 2010).

Many recommendations may be forced to be implemented for urging the driver to follow a rational driving mode like; learning Eco-Driving (Training and Education), automated device to support driver's behavior and simple advice.

Information as to how and when drivers should restyle their behaviors is very important to influence changes in their driving cycle (Jamson et al., 2015). Training and education in eco-driving by a set of rules such as helping the drivers on when and how to accelerate, and how

to use the brake (Caulfield et al., 2014). The recent technological evolutions in telecommunication have been made several innovations in traffic engineering (Orfila et al., 2015). In this context, automated devices are integrated in some new vehicles providing real-time information on the traffic state and thus, offering drivers the optimum operating speed (Keyvanfar et al., 2018).

1.6. Conclusion

The European vehicle exhaust regulation includes a solid particle number with size diameter greater than $23\,nm$ ($SPN\,23$) limited to non-road mobile machinery and heavy-duty and light-duty vehicles. In fact, the majority of particle exhaust emissions are equipped with size diameter smaller than $23\,nm$ requiring a thoroughly revision of this regulation. On the other hand, the regulation did not include non-exhaust emissions (i.e. road wear, tire wear, brake wear and resuspension), despite their contribution exceeding particle exhaust emissions. Furthermore, particles lower than $23\,nm$ are strictly related to adverse health. The lognormal distribution is an efficient fit to the size distribution over a vast particle size diameter range in the nucleation, Aitken, accumulation and coarse modes. Each particle mode presents specific sources and characteristics. The size ranges mentioned for these modes vary frequently, but practically the largest proportion of particle number concentrations is present in nucleation and Aitken modes.

Atmospheric nanoparticles may be induced from various sources. In this review chapter, we were only focusing on nanoparticles produced from road traffic as it contributes by the highest percentage. Human body exposure to vehicle nanoparticles depends on several variables including weather conditions (i.e. wind speed and direction, ambient temperature, relative humidity and precipitation), distance from the road traffic and height above the ground. The comparison of particle number and mass concentrations between different studies is an insufficient method due to the absence of standard protocol, methodologies and to dissimilarity in instruments. There are three different sampling measurement methodologies for measuring particle number and mass concentrations, namely laboratory, In-situ, and real-world emissions measurements. Each of these mentioned sampling measurements has strengths and weaknesses. Real-world measurements help in the determination of continuous time-series data under real conditions (i.e. traffic conditions, climate conditions, road surface geometry). This chapter illustrated practically the large majority of available commercial nanoparticles instruments in order to help researchers choosing the most suitable equipment

for nanoparticles measurement after having set the purpose of their research. In this review, all mentioned studies related to nanoparticles (i.e. characteristics, sources, sampling measurements, instrumentation) are analyzed in order to characterize the human health, environmental and climate impacts. In fact, ambient nanoparticles constitute an area of growing health concern. The magnitude of the effects of nanoparticles on environment and human health has still not been plainly understood. Limited answers from epidemiological researchers and exposure-response relationships in association to ambient nanoparticles make difficult to develop health guidelines. Aerosol instrument tool used in continuous real-world measurements is an efficient method as it could be reached in the short term. However, as a longer-term objective, equipment might be generated allowing also direct estimation of the toxic potential of the aerosol. This is a challenge to cooperate across the area of instrumentation design, toxicology and epidemiology.

Predicting ambient air pollutants and PNCs is a critical research area for mitigating road transport emissions on environment. Artificial neural networks (ANNs) were commonly being frequently used for the simulation of ambient air pollution and environment induced from road traffic.

Chapter 2. The influence of urban road traffic on nanoparticles: Roadside measurements

2. 1. Introduction

The presence of nanoparticles has been gradually increasing over the last few years, which has attracted increased interest from the relevant authorities in order to mitigate ambient air pollution. The total road traffic particles include both exhaust and non-exhaust particulate emissions. However, the focus is more oriented towards vehicle exhaust particle emissions, which lead to a continuous increase in total particulate emissions.

Nanoparticles can be defined as particles $< 300\ nm$ in diameter for two reasons: 1) this size range includes more than 99 % of all $PNCs$ in urban road environments (Kumar *et al.*, 2009a); and 2) this range also encompasses the ultrafine sizes ($< 100\ nm$), which cover up to 80% of all atmospheric $PNCs$ (Kumar *et al.*, 2008b). The first nanoparticle emissions management policy was applied with the European Union's (EU) $Euro\ 5 - Euro\ 6$ vehicle emission standards (EU, 2008), which proposed a measurement suitable to particle size distributions between 23 and $2{,}500\ nm$ applicable to all light-duty vehicle (LDV) categories (Kumar *et al.*, 2010). Vehicles generate submicrometer exhaust particles that affect both human exposure and the air quality in urban particulate pollution environments, due to the extreme smallness of their size, capable to reach few nanometers (Virtanen *et al.*, 2006). Diesel exhaust particles are known to be either solid carbonaceous agglomerate produced during an incomplete burning of combustible fuel, involving an "accumulation mode" or "soot mode" created by the condensation and nucleation of semi-volatile material during exhaust dilution in the atmosphere (nucleation mode) (Harris *et al.*, 2001; Seigneur *et al.*, 2009). On the other hand, non-exhaust sources, such as road surface particles, brake particles and tyre wear particles, induced from the interaction between road surface and tire have increased considerably. In this context, Kumar *et al.* (2013) categorized 11 vehicle non-exhaust sources (NES) as significant sources of nanoparticle emissions into the atmosphere. Moreover, the same authors revealed that the nanoparticles from each vehicle non-exhaust source had dissimilar characteristics, owing to their different formation mechanisms. The increase in particle number concentrations ($PNCs$) in urban environments, particularly along heavily-trafficked roads and streets, has generated increasing interest in determining the quantification and contributing factors. Such steps are required in both developed and

developing nations in order to meet national air quality standards and ensure therefore sustainable highway environment. In this aim, the guideline stipulates that $PM2.5$ must not surpass $25\ \mu g/\ m^3$ as a $24-hour$ mean or $10\ \mu g/\ m^3$as an annual mean; moreover, $PM10$ must not surpass $50\ \mu g/m^3$ as a $24\ hour$ mean or $20\ \mu g\ /m^3$ as an annual mean (WHO, 2005). Furthermore, EU emission standards implemented the first particle number limit values on diesel vehicles in $Euro\ 5$ on January 2011, (i.e. $6.10^{11}\#\ /km$). Subsequently, the particle number limit values from $Euro\ 6$ included both diesel and gasoline-powered vehicles, also at $6.\ 10^{11}(\#\ /km)$. Ultrafine particles (diameter $< 100\ nm$) account for approx. 80 % of total PNC(Heal *et al.*, 2012) and up to 90 % close to major roads (Choi *et al.*, 2014). Ruuskanen*et al.* (2001) asserted that particle concentrations in terms of number should be measured in order to help developing a comprehensive assessment of urban air quality. In addition, Barrios *et al.* (2012) pointed out that the environmental and health impacts induced by the nanometric particles are being neglected despite their high numbers. This chapter serves as a continuation of the efforts made to analyze nanoparticles and to explain their major characteristics (PNC and PND), by taking several variables into account: distance, height, traffic, wind speed, and wind direction. A study conducted by Morawska*et al.* (2008) revealed that nanoparticles are expressed and measured in terms of concentration number per unit volume of air. These particles could be produced directly from combustion (primary particles) or from gas-to-particle conversion (secondary particles). The authors confirmed that the particle size depends on the process as well as the sources that lead to their formation. Both the size distribution and number of nanoparticles modify rapidly in the vehicle near wake, assumed as being due to the influence of several physical and chemical transformation processes (turbulence, condensation and distribution) induced during rapid turbulent dilution and mixing (Kumar *et al.*, 2011). The vehicle wake contains of two-regions: 1) the near wake, which is characterized by a distance of about $10\ to\ 15$ times the vehicle height; and 2) the far wake, which is a region above the near wake (Hucho, 1987). Moreover, the impacts of meteorology, (i.e. temperature, wind speed and direction, and relative humidity), and road viewing installations and topography are all important factors in modeling the temporal and spatial variability of particle number and size distributions. The road structure plays an important role in particle dispersion. In fact, the initial dispersion of particles and pollutants from road traffic emissions may be affected by vehicle turbulence (Kalthoff*et al.*, 2005; Mehel and Murzyn, 2015). These barriers are common characteristics of high-volume traffic, especially on thoroughfares running through high-density urban areas. Such barriers may

actually stop dispersion, increase initial mixing and turbulence, and enhance the level of deposition (Tan and Lepp, 1977; Veerabhadra Swamy and Lokesh, 1993). In this context, Pasquier and Andre (2017) demonstrated that just behind the barrier, concentrations are smaller and then rise at greater distances, with background concentrations being more extensive than without any barrier in place. Urban areas typically engender high particle concentrations due to dispersion being restricted by barriers (buildings).

Kim *et al.* (2015) proved that wind direction constitutes a key parameter influencing particle dispersion. They in fact observed low pollutant concentrations on days with high wind speed, thus indicating a high dilution of air pollutants and dispersion from the line source. Several studies have estimated the dispersion of $PNCs$ and size distributions at various distances from the source (road traffic) (see, for instance, Gramotnev and Ristovski, 2004; Pirjola*et al.*, 2006; Zhu *et al.*, 2004). Most of these studies have measured $PNCs$ at a distance varying from $10\ to\ 300\ m$. The available studies have demonstrated that distance from the source is inversely proportional to PNC. The current study is focused on measuring $PNCs$ and $PNDs$ at distances between source and sampling site ranging from $6.60\ m$ to $330\ m$.

Imhof *et al.* (2005) showed that $PNCs$ downwind of a highway increased with the height above ground being lowered from $30\ m$ to $5\ m$. To the best of the authors' knowledge, PNC information on heights less than $5\ m$ above ground is lacking despite the fact that this height encompasses a critical zone for pedestrian and cyclist exposure. The current study has conducted measurements at heights above ground of less than $3\ m$ due to this critical spatial interval for cyclists' and pedestrians' health. Furthermore, this study has determined $PNCs$ at three distinct distances between source and sampling site, with a large margin ranging from $6.60\ m$ to $330\ m$. Several studies have nonetheless taken the distance effect into account with small margins of less than $100\ m$ (e.g. Goel and Kumar, 2016; He and Dhaniyala, 2012). Given the remarkable increase of nanoparticles in atmosphere from mobile sources, due to the increase in number of circulating vehicles and the intensive use of heavy-duty vehicles, the present study contributes to the air quality management program in the Bron area near Lyon (France) by means of roadside monitoring of $PNCs$ and $PNDs$. The effect of several parameters, namely the distance from traffic, the height above ground, the traffic volume, the wind speed and wind direction, was also investigated during this measurement campaign. The measurement periods were set for eight days during the summer season (June and July) covering different time durations depending on atmospheric conditions. Taking measurements on days with hot temperature or rainfall was avoided in order to preserve measurement

instrument safety. To the best of the authors' knowledge, this study represents the first initiative to comprehensively evaluate nanoparticles on major urban roads in the Bron-Lyon area. It also investigates continuous micro-scale particle distribution and numbers. The current study has highlighted the critical situation experienced in this area with regard to both short- and long-term effects.

2. 2. Materials and Methods

2.2.1. Study area

Bron is a municipality within the Lyon Metropolitan Area in eastern France's Auvergne-Rhône-Alpes region, with an average elevation of $696\ ft$. Its land area spans $10.3\ km^2$, and it contained a population of 41,589 in 2016 (Insee Agency, 2016).

The sampling site for this study was chosen to cover an array of distances from the source, heights from ground level, traffic volumes and atmospheric conditions (wind speed, wind direction, humidity and temperature) surrounding the selected study area. $PNCs$ were resolved within the $5.6-$ and $560-nm$ range along the road at three fixed distances: $d1 = 6.60\ m$, $d2 = 30\ m$, and $d3 = 660\ m$, sequentially at two above-ground heights: $h1 = 2.03\ m$, and $h2 = 2.82\ m$. The road segment is located in the Bron-Lyon area and connects the city center with a business activity zone (see Fig. 2.1).

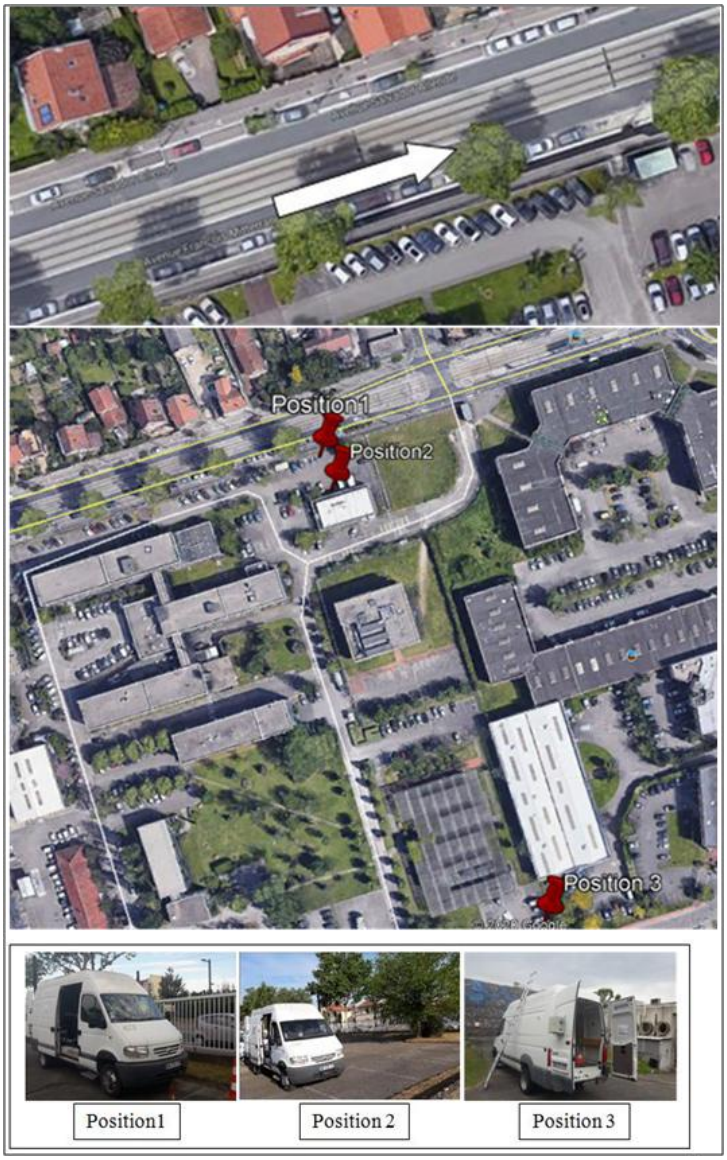

Figure 2. 1: Field study set-up

2.2.2. Instrumentation and sampling

Atmospheric nanoparticle number size concentrations and distributions were measured using a Fast Mobility Particle Sizer ™ ($FMPS$ ™) Spectrometer ($Model$ 3091), once a second with a 10 L/min aerosol inlet flow rate. All equipments have been calibrated before starting the sampling measurements. This equipment measures particles ranging from 5.6 nm to 560 nm distributed across 16 channels per decade (32 channels of resolution in all) with a $1-Hz$ time resolution. This set-up ensures users collect a full-size distribution of rapidly changing aerosols. The $FMPS$ is a powerful and useful tool for monitoring particle exposure in a quickly changing environment due to a 1 Hz particle size distribution frequency and the

integration of a two-decade size distribution. It uses an electrical mobility measurement technique and multiple, low-noise electrometers for particle detection. This enables particle-size-distribution measurements in real time, providing the unique ability to visualize particle events and dynamic changes in particle size distribution. The electric power of the instruments was generated with an electric power cable connected from the buildings of the center for studies expertise on risk, environment, mobility and development ($CEREMA$) and the French Institute of Science and Technology for Transport, Development and Networks ($IFSTTAR$) - Bron- Lyon according to the sampling position ($d1, d2, d3$). The required electrical power of the $FMPS$ is $50\ or\ 60\ Hz$, $100\ to\ 240 VAC$ and $170\ W$ maximum. This equipment was chosen because it captures particles with a very small diameter up to $5.6\ nm$, i.e. a size that can easily enter into the respiratory and cardiovascular systems. Particle number concentrations are calculated as the total number of particles per unit volume of air sampled, in $\#/cm^3 (number/cm^3)$.

Meteorological variables, such as wind direction, wind speed (km/h), relative humidity (%) and air temperature ($°C$), were extracted from the official French weather website: (https://www.meteociel.fr/temps-reel/obs_villes.php?code2=7480) for each measurement day (Table 2.1). In addition, all sampling measurement days were scheduled on weekdays.

A near-road field measurement was conducted in the Bron-Lyon vicinity (France's Rhone-Alps Region) on warm days in June and July 2019. The sampling period was mainly scheduled between $8:15\ am$ and $5:00\ pm$. Time change was allowed to account for adverse weather conditions, namely extreme temperature or rain events, in order to maintain equipment safety.

The $FMPS$ is indeed sensitive to high temperature and may yield false measurements, which might even lead to an unintentional stop. The measurements were performed at two-heights: $h1 = 2.03\ m$ (in the horizontal position) and $h2 = 2.82\ m$ (in the vertical position) above ground level in separate measurement days.

Table 2. 1: Data on climatic conditions during sampling days

Day	Starting time	Ending time	Wind direction	Mean temperature ($°C$)	Min wind speed (m/s)	Max wind speed (m/s)	Mean relative humidity (%)	Distance (m)
D1	3:08 pm	4:00 pm	North	26.8	1.1	4.4	41	6.6
D2	7:51 pm	5:00 pm	East, southeast, south	19.3	6.3	11	32	6.6
D3	8:02 am	12:00 pm	Southeast, south	21.05	7.2	15.2	40.2	6.6
D4	8:33 am	1:00 pm	West, northwest, north, northeast	13.52	1.4	3.9	85.83	6.6
D5	8:22 am	3:40 pm	South, southwest	16	3.1	7.1	57.4	6.6
D6	8:20 am	4:50 pm	South	20.85	1.7	8.6	42.9	6.6
D7	8:30 am	12:50 pm	North, northwest	19.48	1.7	7	39	30
D8	8:30 am	6:05 pm	East, north, northwest	29.65	0.5	9	36	330

Throughout the measurement period, the number of vehicles passing per minute or traffic volume was also considered (Table 2.2).

Table 2. 2: Traffic volume data

Time of day	15-min volume (veh/h)	30-min volume (veh/h)	45-min volume (veh/h)	60-min volume (veh/h)	Total volume (veh/h)
8:00 - 9:00 am	258	113	73	33	477
9:00 - 10:00 am	94	92	109	81	376

10:00 - 11:00 am	85	70	90	73	318
11:00 am - 12:00 pm	84	71	92	74	321
12:00 - 1:00 pm	80	84	90	91	345
1:00 - 2:00 pm	90	85	90	105	370
2:00 - 3:00 pm	120	90	92	74	376

Vehicles were continuously monitored manually at a $15\,min$ frequency only during the measurement period of just one day ($D2$) and for one lane of traffic, flowing towards the business activity zone, due to the unavailability of a traffic counting camera (Fig. 2.2). As such, one measurement day has been selected with normal traffic conditions. Indeed, Mondays and Fridays were avoided due to their unique traffic conditions (heavy outbound and inbound employee traffic). Heavy-duty vehicles ($HDVs$), light-duty vehicles ($LDVs$) and motorcycles were not counted separately since the traffic was considered to be homogenous. According to the official website of France's Ministry for the Ecological and Inclusive Transition (http://www.dir.centre-est.developpement-durable.gouv.fr/donnees-de-trafic-r87.html), the average daily traffic volume circulating in the Bron-Lyon area amounted to 13, 4810 vehicles per day, with 5 % composed of $HDVs$. The average traffic volumes for the lane directed into the activity area (i.e. lane 1) and into the city center (lane 2) were: 5,499 $veh/\ day$ and 4,949 $veh/\ day$, respectively. Furthermore, the maximum hourly traffic flows for lane 1 and lane 2 were: 559 $veh/\ h$ and 468 $veh/\ h$.

Particle measurements were conducted in close proximity to the avenue François Mitterrand in Bron-Lyon. This urban area was selected due to the high rates of pedestrians and cyclists, as well as large road traffic flows, given its role connecting the city center with the business activity area. In addition, pedestrians and cyclists are the category of the most users vulnerable to be affected by particle exposure. The measurement vehicle was first parked near the site of road traffic, and its distance to the road traffic was set at three different positions: $d1 = 6.60\,m$, $d2 = 30\,m$, and $d3 = 330\,m$. It was then parked on the eastern side facing the direction into the activity zone. The vehicle was equipped with a Fast Mobility Particle Sizer TM ($FMPS^{TM}$) Spectrometer and accompanying laptop. Also, three pipe lengths connected the $FMPS$ to the vehicle's outdoor environment, as shown in Figure 2. 2. The effect

of several parameters, namely the distance from the traffic, the height above ground, the traffic volume, the wind speed and wind direction, was also investigated during these measurements. The pipe outlet was exited outside the measurement vehicle at a height of $h1 = 2.03\,m$ (horizontal position) above ground and directed towards the road traffic. Simultaneously, continuous real-time data were recorded by the $FMPS$ software. As a next step, measurements were recorded under practically the same conditions as the first test (horizontal position), except that the pipe was changed to the vertical position at a height of $h2 = 2.82\,m$. Figure 2. 2 shows the equipment connection both inside and outside the measurement vehicle with the two different pipe positions and heights: $h1 = 2.03\,m$ (horizontal position) and $h2 = 2.82\,m$ (vertical position). The tube diameter of the first and second positions was identical, (i.e.$1\,cm$), while the tube lengths for the horizontal and vertical positions were: $1.56\,m$ and $2.27\,m$, respectively.

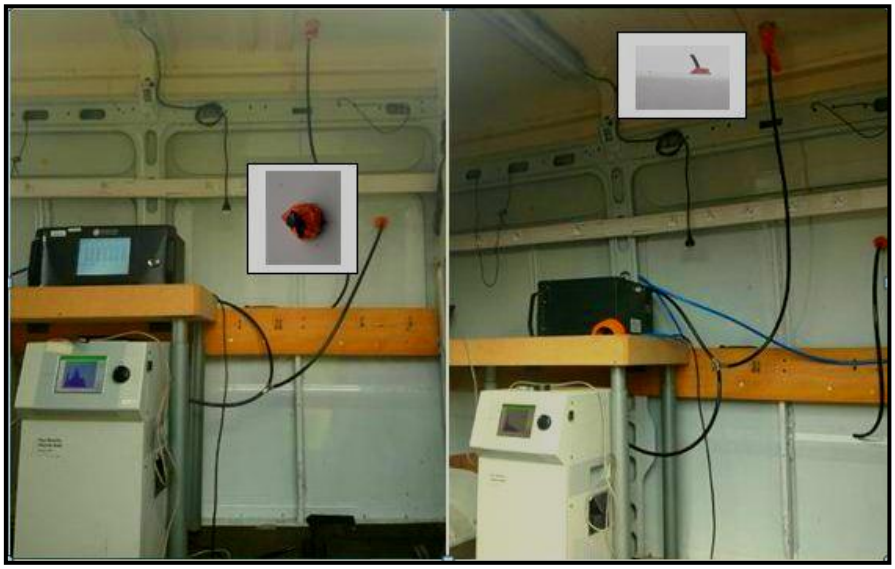

Figure 2. 2: Equipment assembly at two-different heights

2. 3. Results and Discussion

2.3.1. Effects of wind speed and direction on $PNCs$ and $PNDs$

This section is aimed at measuring the total particle number concentrations ($PNCs$). It is obvious that the dispersion of pollutants in an urban area is highly dependent on wind speed and direction. As such and in order to better evaluate the effects of wind speed and direction in an urban area, we have considered road traffic measurements in Bron-Lyon to represent a line pollution source. The measurements were recorded at two-heights: $h1 = 2.03\,m$, and $h2 = 2.82\,m$ above the road pavement. The obtained experimental results indicate that the

average PNC ranges between $1.04.10^4$ cm^{-3} and $2.70\ .10^4 cm^{-3}$ on measurement days (i.e.$D1$-$D6$), with the same fixed distance separating road traffic and the measurement vehicle, as noted in several published studies (see He and Dhaniyala, 2012; Schneider *et al.*, 2015). Figure 2.3 reveals a change in the mean particle number concentration across the various measurement days due to changing distance between source and sampling site.

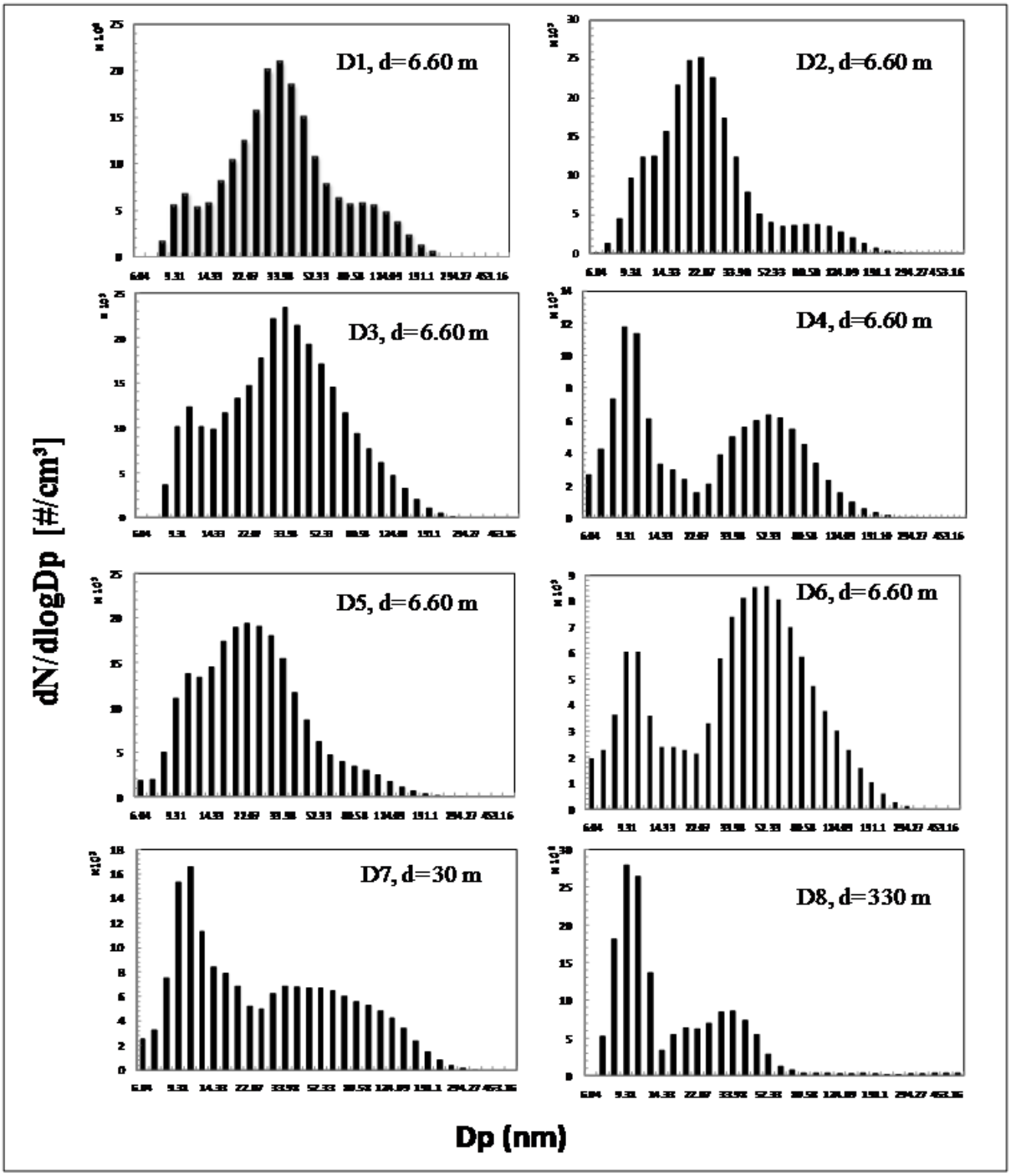

Figure 2. 3: Particle number distributions for all sampling days, D1-D8

Indeed, the distance was raised about five times and fifty times during $D7$ and $D8$ successively as compare to the first 6 days. By comparing days at the same distance (i.e.$D1$-$D3 - D4 - D5 - D6$) with those at different distances from road traffic ($D7$ and $D8$), a remarkable change in both size particle distribution and number appears. The nanoparticle size distribution decreases when the distance between source and sampling site increases, as validated in a peer-reviewed study developed by Rönkkö and Timonen (2019). The fourth measurement day, $D4$, was characterized by the highest concentration rate due to a wind direction blowing into the sampling site. In contrast, $D3$ gave rise to the lowest particle concentration rates as a result of the high wind speed, reaching $15.2\ m/s$ in a direction away from the sampling site (Table 2. 3).

At a distance from the source above $300\ m$ ($D8$), $PNDs$ ($>60\ nm$) tend to zero due to the high ambient temperature of $\sim 30°C$, as indicated in Table 2.1. In this context, Virtanen *et al.* (2006) reported higher $PNCs$ at a lower ambient temperature. $D2$ was found to contain the highest nucleation $PNCs$ compared to the five other days at the same distance ($D1 - D3 - D4 - D5 - D6$), due to the change in tube position (vertical position at $2.82\ m$) and the low relative humidity, promoting a high rate of road dust resuspension.

Table 2. 3: Spatial mean $\boldsymbol{PNCs}$, standard deviation and mean concentrations for the nucleation, Aitken and accumulation modes (expressed in $\boldsymbol{particles/cm^3}$)

Measurement day	PNC	S.D	Nucleation	Aitken	Accumulation	Pipe Position
D1	2.09×10^4	1.55×10^3	7.69×10^3	1.07×10^4	2.48×10^3	Horizontal
D2	2.04×10^4	1.83×10^3	1.40×10^4	5.33×10^3	1.06×10^3	Vertical
D3	1.04×10^4	7.20×10^2	4.97×10^3	4.96×10^3	5.06×10^2	Horizontal
D4	2.70×10^4	1.99×10^3	1.05×10^4	1.45×10^4	1.63×10^3	Horizontal
D5	2.01×10^4	3.5×10^3	1.29×10^4	6.59×10^3	5.67×10^2	Horizontal
D6	1.60×10^4	2.9×10^3	8.02×10^3	6.14×10^3	1.83×10^3	Horizontal
D7	1.16×10^4	3.3×10^3	3.47×10^3	6.89×10^3	1.25×10^3	Horizontal

D8	1.38×10^{3}	2.28×10^{2}	1.06×10^{3}	296.8	19.65	Horizontal

Figure 2.4 compares the effect of meteorological parameters (wind speed, temperature) on $PNCs$ at different measurement days. Results reveal that temperature between $\sim 16-25°C$ has no significant effect on $PNCs$ as found by Casati *et al.* (2007).

In contrast, wind speed has a significant effect on $PNCs$. Indeed, if the direction of the wind directed towards the sampling station, it was shown high $PNCs$ with high wind speed and vice versa.

To analyze nanoparticles behavior, the channel size was divided into four ranges: the first between 5 and $30\,nm$ $(N5-30)$ for the nucleation mode; the second between 30 and $100\,nm$ $(N30-100)$ for the Aitken mode; the third between 100 and $300\,nm$ $(N100-300)$ for the accumulation mode; and the last between 300 and $560\,nm$ $(N300-560)$ to denote the coarse mode, like in Al-Dabbous and Kumar (2014).

For all considered study days, it was observed that PND is dominated by the nucleation and Aitken modes due to traffic exhaust emissions (Fig. 2.3). In order to evaluate $PNDs$ close to the road traffic, all sampling days were included in the analysis. Irrespective of the included variables, $PNDs$ showed a bimodal distribution with modes in the nucleation and Aitken range. The first nucleation mode centered at $10.75\,nm$ and the second was between $22.07\,nm$ and $52.33\,nm$. A number of studies have validated the obtained results, e.g. Garg *et al.* (2000), who tested a brake dynamometer in different pads using the Electrical Low Pressure Impactor ($ELPI$).

The authors demonstrated that the highest particle number appeared in diameters smaller than $30\,nm$. In the same context, Mathissen*et al.* (2011) analyzed the potential generation of ultrafine particles under ($UFPs$) various actual driving conditions and conducted a road simulator study. They found a bimodal number size distribution with a first nucleation mode at $10\,nm$ and the second between 30 and $50\,nm$. Several studies have confirmed that the larger number mode was at $10\,nm$, which is consistent with fresh vehicle emissions (see Al-Dabbous and Kumar, 2014; Beji et al., 2020; Choiand Paulson, 2016; Kittelson*et al.*, 2004; Kozawa*et al.*, 2012; Zhu *et al*., 2002a, b).

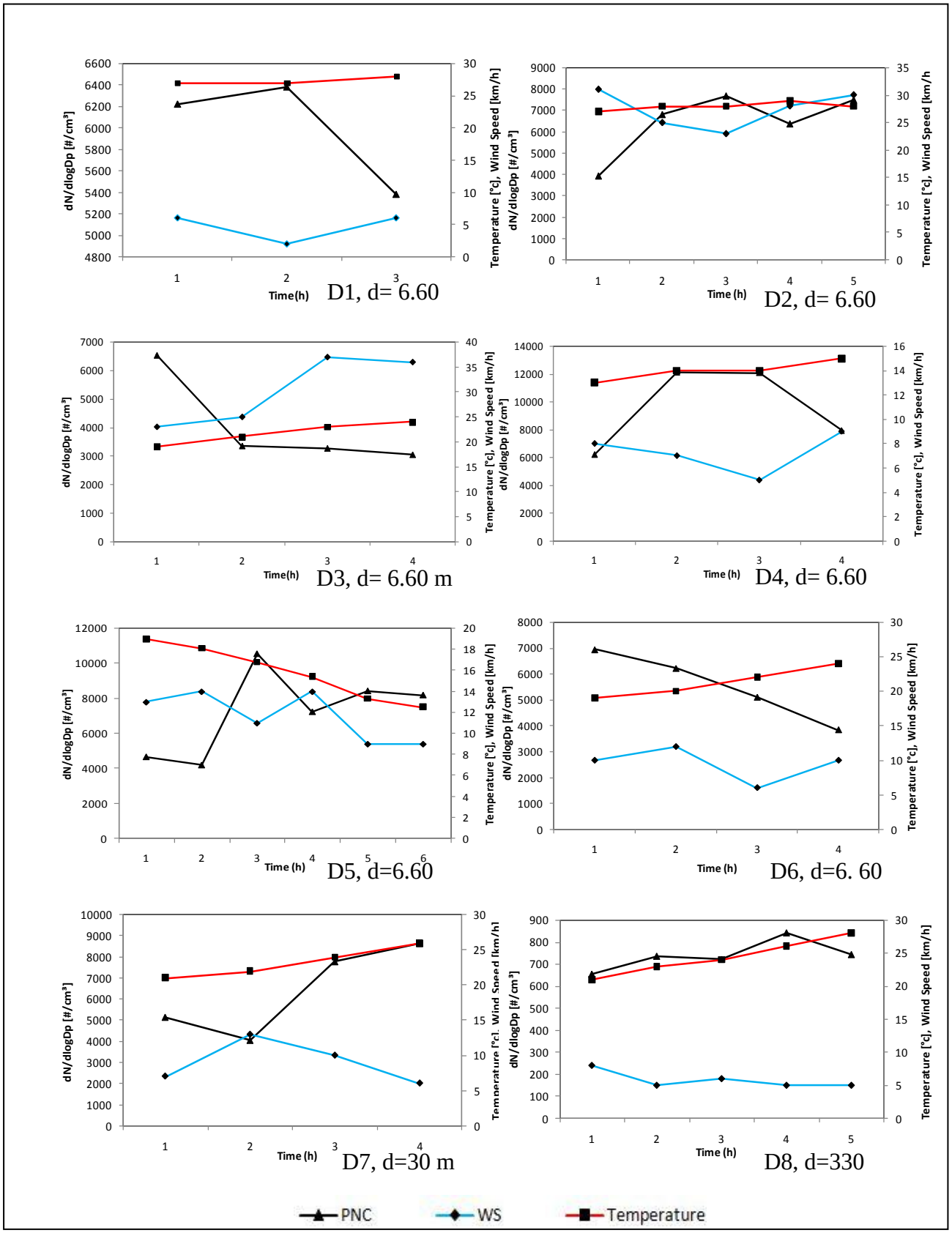

Figure 2. 4: climatologically parameters effect on PNCs during sampling days.

On the other hand, Schneider *et al.* (2015) pointed out that $PNDs$ are centered at $\sim 14\,nm$, $\sim 30\,nm$ and $\sim 105\,nm$. Along the same lines, Kumar *et al.* (2008) evaluated the effect of wind speed on nanoparticle dispersion in several directions using a particle spectrometer ($DMS500$). They found that PND peaks appeared at $15\,nm$ and $87\,nm$ in a street canyon. However, in this study, the bimodal distribution source was not well specified but could be explained by tyre wear, brake wear and exhaust emissions. Sampling measurements were in fact recorded close to a road segment characterized by a signalized crosswalk and bus station. Consequently, several acceleration and deceleration maneuvers were included, where vehicles accelerated after a red traffic light turned green. More specifically, Dahl *et al.* (2006) revealed that tyre wear was the source of the highest particle number concentrations at $15\,nm$ and $50\,nm$. In addition, Mamakos*et al.* (2019) found that the highest particle number concentrations caused by brake wear were positioned at $10\,nm$. Furthermore, a study carried out by Rymaniak*et al.* (2017) demonstrated that the highest peak in exhaust particle number emissions appeared at $10.8\,nm$. In the current study, the average measurement time was variable from one day to another that may induce non-consistent average PND actually.

A slight difference in $PNDs$ from one study to another may be explained by the use of different measurement tools or a focus on different road types and/or different traffic volumes and climatic conditions (i.e. relative humidity, wind speed, wind direction, etc.).

2. 3.2. Effect of height on $PNCs$ and $PNDs$

In order to examine the effect of height on $PNDs$, two measurement days ($D2\ and\ D3$) were considered with two heights: $h1 = 2.03\,m$ (horizontal position), and $h2 = 2.82\,m$ (vertical position) above the road pavement. Figure 2.5 shows the $PNDs$ in both horizontal and vertical pipe positions with various wind directions and speeds. The urban study area is characterized by a high nanoparticle number with channel size diameters in nucleation mode primarily in $10.75\,nm$, reaching up to $5.61.10^3\ \#/cm^3$ at height $h1$, and $3.23.10^4\ \#/cm^3$ at height $h2$ (Fig. 2.5). This finding is due to the role of thermal plume rise and the high number of buses, whereby the tailpipe height of an HDV is practically at $2.70\,m$ above ground (He and Dhaniyala, 2012). Particle number concentrations ($PNCs$) increase when the height increase is less than $5\,m$ above ground. Along these lines, a number of studies have affirmed that PNCs increase significantly with height under all wind speed conditions at heights closer to the pavement (below $3.4\,m$) (see, for instance, He and Dhaniyala, 2012; Imhof et *al.*, 2005;

Zhu and Hinds, 2005). Overall, these findings contend that particles with a diameter smaller than 30 nm are strongly influenced by height, as validated by Quang et *al.* (2012).

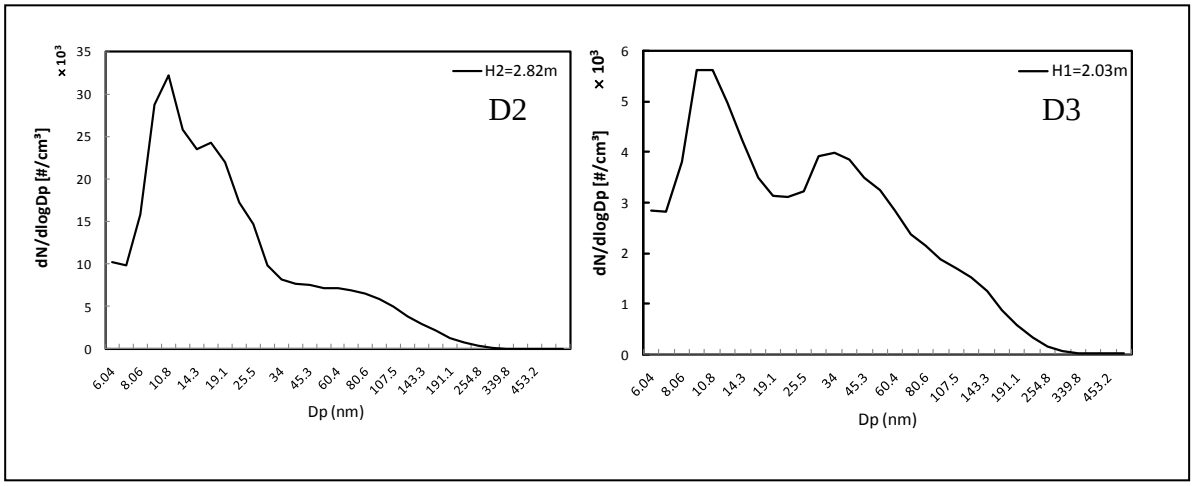

Figure 2. 5: Nanoparticle number distributions, PNDs, at various heights

The resultant increase with a diameter of less than 30 nm (nucleation mode) while decreasing above 30 nm would in fact suggest that this mode is correlated with the new particle formation event tied to the amount of global radiation. It can be concluded that a significant correlation exists between $PNCs$ and channel size Dp at $h1 = 2.03\,m$ on rush hour period. This relationship can be explained by the negative linear equation ($y1 = -207.7\,x + 6,618$) with a reliability coefficient of $R^2 = 50.7$, where $PNCs$ increase inversely proportional to particle diameter (Fig. 2.6a).

The strong correlation between $PNCs$ and channel size D_p at $h2 = 2.82\,m$ can be explained by the negative linear equation ($y2 = -327.9\,x + 9{,}332$) with a reliability coefficient of 62.4 % (Fig. 2.6b). This latter finding explains the high particle number in both nucleation and Aitken modes and the low particle number in the accumulation and coarse modes. Moreover, it is important to note that a high PNC has appeared in the nucleation mode, as validated by several studies (see Kukutschová*et al.*, 2011; Wahlström*et al.*, 2010b).

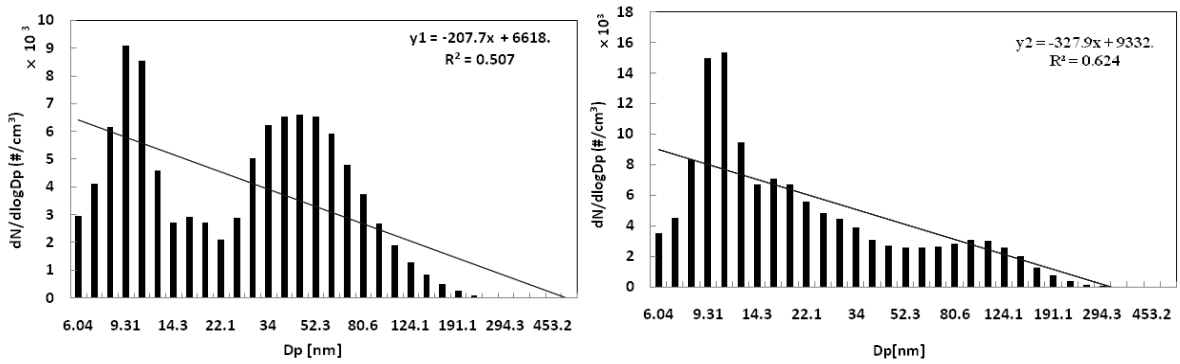

(a) Correlation between PNC and channel size at height $h1 = 2.03\,m$

(b) Correlation between PNC and channel size at height $h2 = 2.82\,m$

Figure 2. 6: Correlation between PNC and channel size.

2.3.3. Effect of distance and traffic conditions on $PNCs$

This section seeks to investigate the effect of distance from the source and traffic conditions on $PNCs$. To this end, three measurement days were considered with different distances. Measurement times started at around $8\,am$ and lasted until $1\,pm$, with a $1\,min$ time step. Results reveal that tremendous peaks appeared in the morning, especially during morning rush hour (mostly from $8{:}00$ to $9{:}00$) (Fig. 2.7). Figure 2.7a displays three peaks during the period from 8 to $9{:}30\,am$ due to the high traffic volume, with a distance $d1 = 6.60\,m$ between the road traffic and the sampling site. However, at a distance $d2 = 30\,m$ (as depicted in Fig. 2.7b), a succession of peaks occurs over the $8 - 9\,am$ period. Beyond this period, PNC peaks decline. It is worth noting that on the second measurement day, the $PNCs$ were lower than those measured on $D1$ due to the greater distance between source (road traffic) and sampling site.

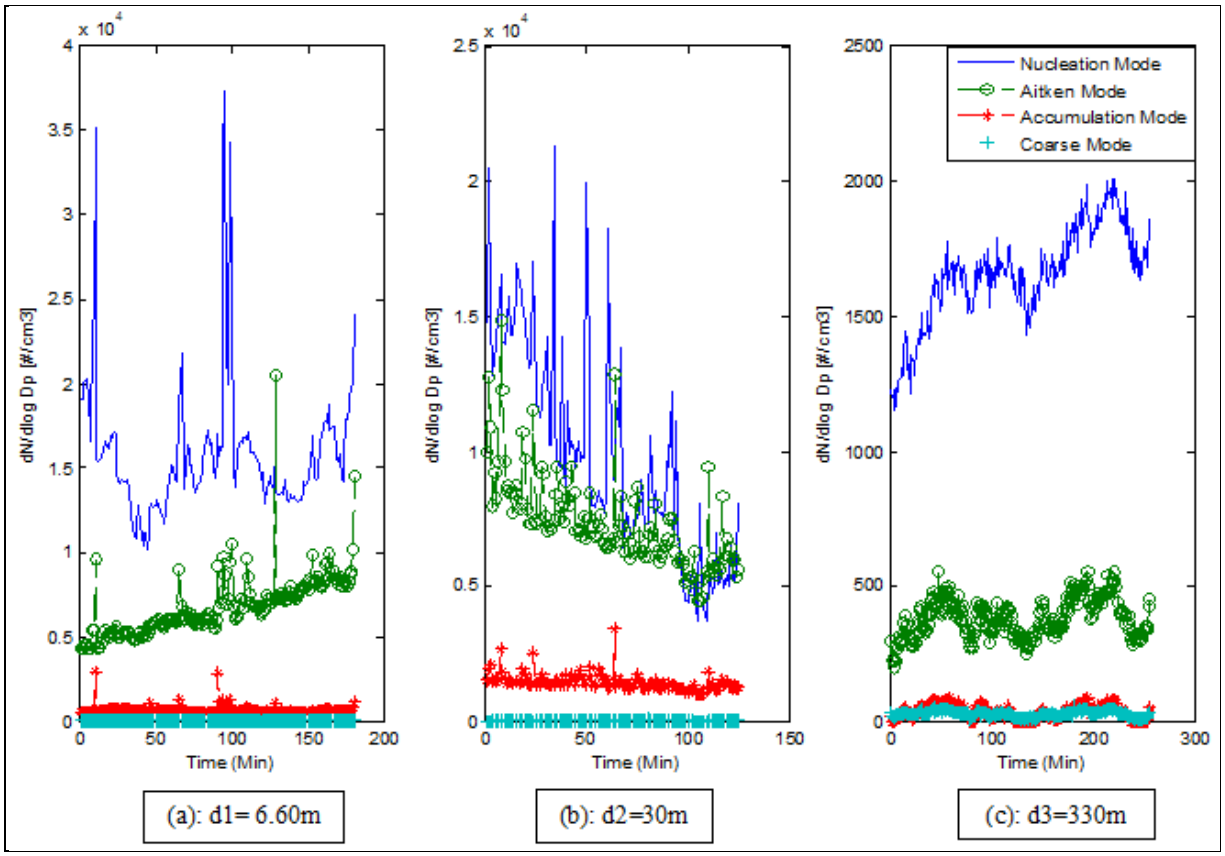

Figure 2. 7: PNCs at various distances from the road traffic

As illustrated in Figure 2.7c, the third measurement day with a distance $d3 = 330\,m$ from the road traffic was characterized by low $PNCs$ compared to the other two days and by a curve with steady peaks, since the sampling measurement position was located far from the road. The experimental results demonstrate that the relationship between $PNCs$ and distance from the source could be explained by a negative linear polynomial model with 95 % confidence bounds and high reliability coefficient of 96.69 % (Eq.2.1). More specifically, $PNCs$ are found to decrease with increasing distance from the source (road traffic) and *vice versa*, which is in close agreement with previously published results (see Choi and Paulson, 2016; Goel and Kumar, 2016; Kittelson*et al.*, 2004; Zhu *et al.*, 2002). As shown in Figure 2.8, the relationship between $PNCs$ and road traffic - sampling site distance is derived as follows:

$f(x) = p1 \times x + p2$ (Eq.2.1), where:

$p1 = -15.83\ (-53.06, 21.4), p2 = 5{,}733\ (-1{,}397, 1.286\ e + 04)$

Figure 2.8 indicates that the PNC decreases equal roughly six-times its maximum in the case of distance $d3 = 330\,m$ from the road compared to recordings with distance $d1 = 6.60\,m$ from the same emission source.

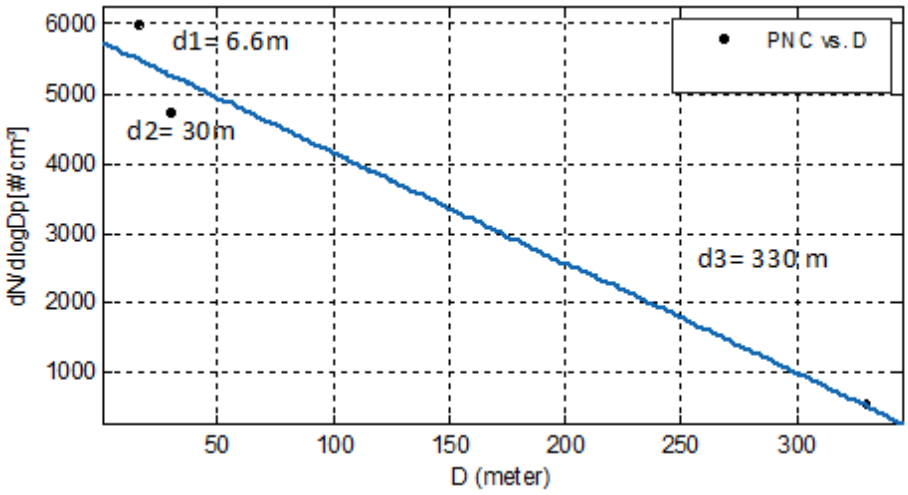

Figure 2. 8: PNC vs. distance from the source

Hitchins *et al.* (2000) reported that the concentrations of fine and ultrafine particles decreased by about half from their maximum at distances of 100 and 150 m from the source.

It can generally be concluded from these recorded results that both traffic and distance greatly influence particle number concentrations.

2. 4. Concluding remarks

The current chapter has provided the results of an experimental study conducted in the urban sector of Bron (in the Lyon Metropolitan Area) at two-heights ($h1 = 2.03\,m$ and $h2 = 2.82\,m$) above the road level and at three distances ($d1 = 6.60\,m$, $d2 = 30\,m$ and $d3 = 330\,m$) from the emission source. Real-time continuous measurements of both particle number concentrations and distributions were recorded using the Fast Mobility Particle Sizer ™ ($FMPS$™) Spectrometer (Model 3091) with size-resolved particles in the range of $5.6 - 560\,nm$. In this study, particles were classified into four distinct modes, namely nucleation ($6.04 - 30\,nm$), Aitken ($30 - 100\,nm$), accumulation ($100 - 300\,nm$), and coarse ($300 - 560\,nm$). The impact of wind at various speed and direction on particle number concentrations (PNCs) was measured and analyzed. In addition, the effects of distance from the source and traffic conditions on nanoparticles were investigated experimentally and thoroughly discussed. It was demonstrated that PNC values are inversely

proportional to the distance between road traffic and sampling site. Moreover, $PNCs$ are very high in the vicinity of the traffic zone, predominantly during rush hour since the sampling site connects the city center with a business activity area. In this circumstance, practically all workers commute at the same time, which increases traffic density. Furthermore, PNC increases significantly with an increase in height of less than $2.82\ m$ above the ground. With heights $2.03\ m$ and $2.82\ m$ above the ground, the urban study area is characterized by high nanoparticle number with channel size diameters in nucleation mode ($10.75\ nm$). The average PND values revealed typical bimodal distributions for each wind speed and direction, with a strong nucleation mode peak at $\sim 10.75nm$ and an Aitken mode peak between 22.07 and $52.33\ nm$. The magnitude of $PNCs$ is changed according to wind speed and direction, accounting for a much higher variation in the nucleation and Aitken modes than in the accumulation mode. These latter results explained by a greater variation being attributed to the larger effect of increased dilution on particles in the nucleation and Aitken modes than in accumulation.

Chapter 3: Continuous real-world measurements of exhaust and non-exhaust vehicle emissions over different traffic areas

3. 1. Introduction

Section1 : vehicle exhaust PNCs

Diesel-powered vehicles constitute the major source of road vehicle pollution in the European Union (EU). Urban areas generate considerable human activity and large proportion of pollution that induces significant adverse environmental impacts, not to mention health effects by virtue of penetrating into the deep lung (Stone et al., 2017). Furthermore, they raised risk of lung cancer mortality through the mechanisms of inflammation and oxidative stress (Sun *et* al., 2010; Valavanidis et al., 2008). In fact, small-diameter particles account for a higher deposition fraction in the human respiratory system, in addition to exhibiting a larger specific surface area (Giechaskiel et al., 2015). Epidemiological analyses have consistently confirmed a significant relationship between PM, pollution and the number of cardiovascular and respiratory tract disease victims (e.g. Kim et al., 2012; Skrzypek et al., 2013). Furthermore, (Oviedo and Sabogal, 2020) revealed that the transport is strongly associated with the life of citizens and human health. Road traffic PM emissions can be subdivided into exhaust and non-exhaust emission components (Charron et al., 2019), with the exhaust PM emissions being produced from tailpipes as a consequence of incomplete fuel combustion inside the engine combustion chamber. PM adversely affects human health in two ways, namely a diminished capacity of the respiratory tract to remove such deposits and a PM deposition mechanism acting in the respiratory tract, both of which are highly correlated with PM size (Mainka and Zajusz-Zubek, 2019). In general, particulates suspended in air ranged between 0.005 and $100\ \mu m$. In practical terms, suspended particles are classified as either ultrafine / alveolic fraction ($<\ 0.1\ \mu m$) or fine / thoracic fraction ($<\ 2.5\ \mu m$). Both classification types tend to deposit in the area of the bronchi and trachea, as well as in pulmonary alveoli; in contrast, the coarse or inhalable fraction ($2.5 - 10\ \mu m$) tends to deposit in the area of the throat, nose and larynx of the respiratory tract (Bernstein et al., 2008; Lippman et al., 1980). The smaller PM ($<\ 1\ \mu m$) exerts a larger negative effect on human health, targeting asthma and the respiratory system (Mei et al., 2018). Despite these negative externalities, until now $PM1$ has not been frequently quantified since it lies outside the focus of air quality standards. In an absolute majority of countries, data relating to $PM1$ concentration levels and its various

features are restricted (Agudelo-Castañeda and Teixeira, 2014; Titos et al., 2014; Zajusz-Zubek et al., 2017).

Road transport is the main contributor of fine particulate mass ($PM2.5$) emissions in Europe, which contribute by 11 % of the total amount (EEA, 2018). The urban traffic proportion of total particulate matter levels has been determined to lie between 5% and 80% (Pant and Harrison, 2013), while it can reach 90% on busy roads (Kumar et al., 2014). Approximately 20% of the European Union's (EU) 2010 urban population lived in areas characterized by a daily air quality PM standard whose diameter was smaller than 10 μm (50 $\mu g/m^3$) (Belkacem et al., 2020; EEA, 2014). Furthermore, rural areas cover about half of Europe and account for 20 % of its population.

As regards air quality management, the responsibility for improving air lies with the authorities managing the urban road environment. The basic approval procedure for road vehicles had been carried out on a roller dynamometer test bench within a clearly prescribed New European Driving Cycle ($NEDC$). This cycle has since been replaced by the Worldwide Harmonized Light Vehicles Test Procedure ($WLTP$) (DELPHI, 2017). In order to obtain information on particle emissions into the atmosphere under real-world conditions, laboratory measurements must be validated by field measurements, which happen to be more consistent and reliable. Stationary measurements are well adapted to provide relevant data for specific measurement sites (urban, rural, suburban, motorway, etc.) yet are less well adapted to continuously study the contribution of individual vehicles under actual driving conditions. Real-world road measurements are thus critical to improving the scientific knowledge of road traffic particle emissions. Several commercial tools are available for real-world particle measurements; one such real-time aerosol monitor is the Optical Particle Counter ($OPCGRIMM^{TM}$) analyzer, series 1.108 Portable Aerosol Spectrometer. This $OPCGRIMM^{TM}$, ref. EDM 1.108, has the capability to simultaneously measure particulates ranging in aerodynamic diameter size from 0.35 μm to 22.5 μm across 15 channels (Kundu and Pal, 2015; Peters et al., 2006). Furthermore, several studies have demonstrated that the $GRIMM$ monitor is an accurate tool compared with the filter dynamic measurement system ($FDMS$) (e.g.Grimm and Eatough, 2009) and other particulate matter instruments (Cheng 2008; Omidvarborna et al., 2020; Qiu et al., 2019). Very few studies have compared continuous real-world diesel vehicle exhaust PMC and PNC measurements over different traffic areas, including urban, rural, motorway and national roads.

Section 2: non-exhaust emissions

Road traffic is the main source of ambient air quality and particulate matter in the atmosphere degradation. The total non-exhaust PM ($PM2.5$ and $PM10$) induced by light duty vehicles (LDVs) worldwide will increase by $53.5\,\%$ along with transport demand in 2030 as compared to 2017 ($OECD$ 2020). Road, tire and brake wear emissions have developed from $39\,\%$ of $UKPM10$ road traffic emissions in 2000 to $73\,\%$ in 2018 and from $26\,\%$ in 2000 to $67\,\%$ in 2018 for $PM2.5$ ($COMEAP$ 2020). Resuspension and wear part can be considered as non-exhaust emissions. Atmospheric Particulate Matter $PM2.5$ or fine PM are considered to cause $412{,}000$ premature deaths per year including $33{,}200$ in France (European Environment Agency 2019). The particles induced from road dust, tire, road surface and brake wear are emitted with a diameter $<10\ \mu m$, inducing a significant health risk for the human body. Despite the important burden of non-exhaust particle (NEP) emissions on public health and environment, few regulations target them explicitly (OECD, 2020). This is due to the lack of uniform technique/protocol of measurements. According to the UK National Atmospheric Emissions Inventory ($NAEI$), the $NEPs$ are strongly higher than exhaust emissions for both $PM2.5$ and $PM10$. The impact on NEP emissions remains unclear, as the evolution of the advanced propagation of regenerative braking systems (e.g., the energy recovery mechanism employed in electric vehicles that makes resistance braking through the vehicle's engine acting as a generator to transform kinetic energy into electrical energy) will probably mitigate brake wear emissions.

Coarse and fine particles from non-exhaust sources have been related with short-term morbidity and mortality (Meister et al. 2012; Ostro et al. 2011). $PM10$ can easily penetrate into bloodstream, lungs and hearts (Environmental Protection Agency, 2017). However, in order to contribute to a productive and healthy indoor air environment, vehicle ventilation systems should be equipped with filters that are able to remove $PM1$ particles, since the smallest particles are the most harmful to human health like; pulmonary inflammation and asthma exacerbation (Shao et al. 2017; Niu et al. 2020). It has been demonstrated that regularly exposure to nanoparticles may harmfully affect human health (Feng et al. 2020). A comparative study by Zwozdziak et al. 2016 demonstrated that PM1 has greater effect on lung function parameters as compare to $PM2.5$ for school children aged between 13 and 14 years. In order to realize a sustainable environment and mobility, it is important to quantify not only particle mass concentration but also particle number concentration. Given the pronounced

negative impacts of particulate matter on human public health, it is incumbent on authorities on to mitigate these emissions. Disc brakes are the most frequent type of braking system for the recent technological vehicle generation, including an abatable brake pad, which works on the brake disc (Grigoratos and Martini 2015). Particles are engendered from the frictional wear during the braking action, but the fraction of this PM (less than $10\ \mu m$) is not yet fully mastered (Grigoratos and Martini 2014). In fact, the composition of brake friction material is frequently proprietary/confidential and can be influenced on manufacturer and the tire of brake system (e.g. ceramic, non-asbestos organic, semi-metallic, etc.) (Thiyagarajan et al. 2015; Grigoratos and Martini (2014, 2015)). There is diversity of commercial brake friction materials which exceeds 200 ingredients. Tire and road wear particle emissions are induced when tires associate with the road surface through abrasion and friction (Grigoratos et al. 2018; Kesarkar et al. 2020). These particles are internally comprised and mixed both the embedded road materials, depending on the type of road surface (e.g. concrete/asphalt) and the tread rubber (Grigoratos et al. 2014). Tire compositions are multiple and their proprietary data make it complicated to estimate the tire tread composition. They generally contained a mixture of synthetic and natural rubbers ($40-60\ \%$), vulcanization agents ($2-5\ \%$), fillers ($20-35\ \%$), textile and metal reinforcements ($5-10\ \%$), process oils ($12-15\ \%$) and additives ($5-10\ \%$) (Panko et al. 2019; Baensch-Baltruschat et al., 2020). Road vehicle dust resuspension emissions are engendered by different mechanisms: turbulent micro-eddies, subsequent and attachment of material from the tire and the road surface due to high-speed airflows, and movement of the vehicle as air is expelled from the tire (AQEG 2019; Harrison 2020). Various sources participate to the composition of road dust resuspension, which makes quantifying and separating the different emission sources quite difficult (Harrison 2020; Furger et al. 2020). Nevertheless, particle size distribution of resuspension is over $10\ \mu m$, of which crustal and soil material reveale the dominant components in road dust (Amato et al. 2014; Huang et al. 2020).

Even though highly developed, vehicle technologies have been made for mitigating PM emissions from motor exhausts, no actions have been taken to reduce the non-exhaust proportion of emissions, inducing in turn a substantial increase of total emissions. The relative contribution of road and tire wear particles is anticipated to gradually multiply at short-medium-long term (Mathissen et al. 2011). Tire wear particles can also be constituted as evaporative emissions -resulting to the heating of the tire followed by coagulation and condensation (Jekel 2019). The emissions of tire road wear particles ($TRWPs$) constitute a

major non-exhaust particles source (Grigoratos and Martini 2015; Kwak et al. 2013), including road surface wear and tires as well as resuspension of road dust. Practically, in road transport, the most primary fine particles are produced from the exhaust, whereas coarse particles are mainly induced from non-exhaust sources (Grigoratos and Martini 2014). Some studies have shown the peak of the PN distributions in the ultrafine mode, while they are not pronounced under normal driving conditions (Grigoratos and Martini 2014). The change in particle emissions is due to many factors, such as traffic conditions, meteorological, ambient particulate pollution, variation in tire composition and texture, driving style, and road surface features (Dahlet al. 2006; Gustafsson et al. 2008; Grigoratos et al. 2018; Park et al. 2018).

In order to take complete and real information about particle measurements, laboratory control methods become insufficient measurement tools. For this reason, laboratory measurements have been enhanced through on-road-real driving emissions (RDE) (Belkacem et al. 2021). In addition, laboratory studies are not suitable to represent the entire vehicle fleet, as tires and brakes that can change significantly between the performance and manufacturers specifications. Meanwhile there may be dissimilarities between real-world and simulations conditions, including emissions driving styles.

A number of studies have been done towards characterizing the non-exhaust particles (NEP) on road (Kwak et al. 2013; Harrison et al., 2012) or in laboratory measurements (Gustafsson et al. 2008; Grigoratos et al. 2018; Foitzik et al. 2018). In addition, some studies have focused on evaluating the effect of acceleration and deceleration maneuvers, without taking into account the real traffic conditions (real driving conditions) (e.g.Kwak et al. 2014) or with a predefined test cycle (e.g. Pelkmans and Debal 2006). The latter mentioned conditions may not reflect real particle number concentrations. Fundamentally, this study tends to measure real $NEPs$ in different road segment areas of Lyon - France; urban, rural, and motorway. In fact, implementing similar measurements and sampling methodologies are needed to provide comparative results. The parameters that were changed from one to another sampling day were; road type, vehicle speed and acceleration/deceleration maneuvers, while keeping the same driver during all measurement days. Thus, instantaneous particle emissions are applied in individual level analysis because they provide accurate spatial and temporal analyses. Finally, this research measured the effect of real vehicle speed and acceleration/ deceleration maneuvers on NEP concentrations in urban, rural and motorway areas.

Thus, the aim of this chapter to estimate, investigate and compare real-world, micro-scale continuous exhaust and non-exhaust particle mass concentrations and number by optical size, from roughly 0.35 to 22.5 μm, under actual measurement conditions for light-duty vehicles (LDVs) in order to improve road mobility within the framework of environmental sustainability. Measurements were conducted in Lyon (France) using $GRIMM$ analyzer series 1.108. The instantaneous speed profiles and locations were simultaneously recorded by the global positioning system 747 Pro (GPS). To the best of the authors' knowledge, the current research is the first comprehensive initiative evaluating both fine and coarse particles on major roads in Lyon (urban, rural, motorway, $RN6$) under actual traffic conditions. The critical situation here has been correlated with medium-to-long term effects on the population as well as with air quality.

Section 1: Vehicle Exhaust emissions

3. 1. 1. Materials and Methods

3. 1.1.1. Study areas

Measurements took place during July 2019 in the vicinity of Lyon (France). Lyon is France's second largest conurbation and third largest city; it is located in central eastern France between Paris and Marseille, in the Auvergne-Rhône-Alpes Region. The National Institute of Statistics and Economic Studies ($INSEE$) has estimated the population at 515,695 as of 2016, with location coordinates of $45°45′35″$ North, $4°50′32″$ East. The total mileage traveled for all sampling day measurements was approximately 203 km, including both forward and backward directions. This large population number underscores the importance of this research through exposing the human body to different types of road traffic air pollution (specifically for urban, suburban and rural roads). Diesel vehicle exhaust particulates were collected during either the morning or evening period, depending on climate conditions (Table 3.1).

Table 3. 1: Related data for all sampling measurement days

Measurement day	Direction	Road type	Distance (km)	Min. temp. ($°C$)	Max. temp ($°C$)	Mean temp. ($°C$)	Precipitation (mm)
D1	Forward	Urban	16	20.5	32	26.25	No
	Backward		16				
D2	Forward	Suburban +Rural	32.5	19.1	31.7	25.4	No
	Backward		32.5				
D3	Forward	Motorway	35	16.9	27.6	22.25	No
	Backward		39.6				
D4	Forward	RN6 National Highway	16	16.1	28.2	22.15	No
	Backward		16				

The registration year of the light utility vehicle used for sampling days was 2001, which corresponds to the $Euro\ 3$ class, since in Europe vehicle tailpipe emissions are regulated according to Euro class. Emission thresholds are identified for compounds regulated in the year that a vehicle category is introduced on European roads: $pre-1992$ ($Euro\ 0$), $1992-95$ ($Euro\ 1$), $1996-99$ ($Euro\ 2$), $2000-04$ ($Euro\ 3$), $2005-08$ ($Euro\ 4$), $2009/2011$-13 ($Euro\ 5a/b$) and $2014-present$ ($Euro\ 6$). Measurements have mainly been obtained in urban (Bron-Décines-Meyzieu), suburban-rural (Saint-Just Chaleyssin-Corbas), motorway ($A46$) and national highway ($RN6$, along the ring road) (Fig. 3.1).

The mileage traveled was not the same on all sampling days, depending on the road type (urban, suburban-rural, motorway, $RN6$). Fig. 3.1a depicts the first day's itinerary of mobile sampling measurements on an urban road. The operating mode was adjusted according to the speed, idle acceleration and time via the global positioning system (GPS) under real-world monitoring with a $1-s$ resolution. The itinerary extended from Bron (urban area) to Meyzieu (suburban) passing through Décines (semi-urban).

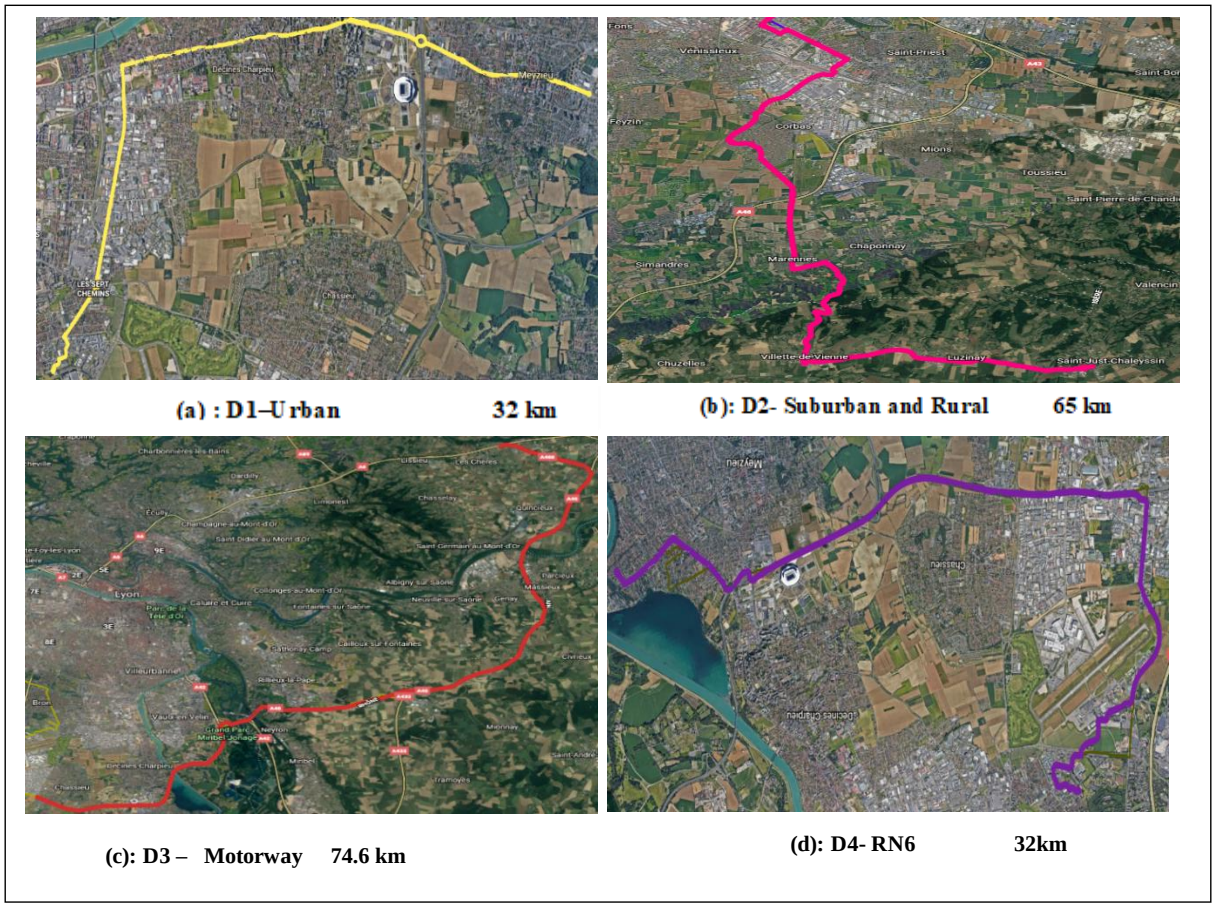

Figure 3. 1: Road map of the various study areas

Fig. 3.1b illustrates the suburban and rural road itinerary (Saint-Just, Corbas). Fig. 3. 1c represents the third day's mobile sampling itinerary along the $A46$ motorway. According to the official website of France's Ministry for the Ecological and Inclusive Transition (http://www.dir.centre-est.developpement-durable.gouv.fr/donnees197de-trafic-r87.html), the average traffic volume traveling on the $A46$ amounted to 85,760 vehicles per day, with 19 % composed of $HDVs$. Fig. 3.1d indicates the fourth day's mobile sampling itinerary along $RN6$ (ring road section). In all sampled measurements, the current study has taken into account both forward and backward directions. The average traffic volume traveling on the RN6 amounted to 36,369 vehicles per day, with 6 % composed of $HDVs$. Table 3.1 lists detailed information on all the mobile measurements, including time, road type, mileage traveled and direction. Four days of measurements were processed in order to evaluate the exhaust particulate mass and particle number for the four tested road types, again in both directions. Trip duration varied according to road type.

3.1. 1.2. Experimental set-up and data recording

Several studies were conducted to measure the particulate matter (PM) in close proximity to specific road segments (at the macroscopic scale), while not being focused on the microscopic PM exhaust emissions (at the vehicle scale). Particulate matter concentrations ($PM10, PM2.5$ and $PM1$), particle number concentrations (PNC) were estimated within the $0.35 - 22.5\ \mu m$ diameter size range using the $GRIMM$ series 1.108 Aerosol Spectrometer. The mobile measurements were programmed to record at a time resolution of 6 seconds, which yielded sufficiently detailed data in particle concentrations of urban, rural, motorway and national road particles that were unclear in laboratory or fixed-site measurements (Fig. 3.2). It was used also to estimate the exhaust PM concentrations ($PM1, PM2.5, PM10$) at a flow rate of $1.2\ l\ min^{-1}$. This portable optical particle counter was selected due to its ease of operation, light weight and effectiveness for the time resolution of continuous particulate measurements. Within the aerosol classification, particle counts ranged between 1 and $2{,}000{,}000 particles.l^{-1}$, while the mass measurements could vary from 0.1 to $100{,}000\ \mu g.m^{-3}$. The $GRIMM$ efficiency for radial symmetric sampling is influenced by wind speed. A study has compared the GRIMM 1.108 response with 6 other devices, namely: $TEOM1400$, spectrometer $TSI\ APS\ 3321$, $GRIMM\ 1.109$, $LIGHTHOUSE\ HH3016IAQ$, $GLA\ 5000\ PVC$, and $GLA\ 5000\ PVC$. Results showed very good conformity between $GRIMM$ and the six tested devices (INRS, 2012).

Figure 3. 2: Field study set-up (Exhaust emissions)

Diesel particle concentrations were measured with a $GRIMM$ series 1.108 Aerosol Spectrometer. This analyzer had been calibrated by its manufacturer using dolomite dust. Measurements were conducted on four different road segments in the vicinity of Lyon (France). Thirty minutes were required before starting the trip in order to load all necessary tools inside the light utility vehicle. Battery charging lasted between four and five hours. All team members exercised caution not to exceed five hours of charging, which would have caused the battery to discharge. Moreover, before initiating each sampling measurement, zero calibrations were regulated on both the $GRIMM$ 1.108 aerosol spectrometers and GPS. Next, a blank test was run for a $10 - min$ duration using a filter in order to eliminate any stale lingering particles in the $GRIMM$ pipe. In this manner, one team member ensured that the

standby button was activated before taking measurements. The GPS time was synchronized with the $GRIMM$ time on a daily basis. The pipe connected to the $GRIMM$ device was placed in front of the tailpipe of the light utility vehicle of a $4\ cm$ distance and with a diameter of 1 cm. Diesel exhaust particle measurements were recorded under real-world traffic conditions on various road segment types. Most studies measure particle exhaust in the laboratory with a standard driving cycle (e.g. $NEDC, WLTP$) (Andersson et al., 2007). In contrast, this driving cycle does not take into account the actual traffic, climate conditions, "blackheads" (e.g. unforeseen collision) or driver behavior. The time spent during this research to cover the various segments varied from 1 hour $2\ min$ to $1\ hour\ 24\ min$ depending on the traffic conditions and road segment type. Before starting the sampling process, all team members installed the necessary tools inside the light utility vehicle, including the $GRIMM$ series 1.108 Aerosol Spectrometer and the GPS. In addition, one staff member verified that all tools had been secured, so as to avoid their damage during vehicle operations. Different itineraries were followed by the driver as a function of the selected destination. After finishing sampling measurements, a team member activated the $GRIMM$ standby button and then recorded the data on the laptop. Lastly, 30 minutes were needed to return the tools to the laboratory.

3.1. 2. Results and discussion

3.1.2.1. Particulate mass concentrations

- Diurnal variations of PM10, PM2.5 and PM1concentrations

Table 3.3 shows the correlation between $PM10, PM2.5$ and $PM1$ concentrations on various road segments. $PM10, PM2.5$ and $PM1$ rates exhibit high correlation between fine, $PM2.5$, $PM1$ ($PM_{2.5\text{-}1}$) and coarse particulates ($PM10$) across all road types. This high correlation between $PM_{2.5\text{-}10}$, $PM_{1\text{-}10}$ and $PM_{2.5\text{-}1}$ may be explained by the fact that emission sources were the same for all mobile sampling measurements (i.e. road traffic sources) (Janssen et al. 2013). Fig. 3. 3 provides the diurnal variations of $PM10, PM2.5$ and $PM1$ concentrations for the summer season.

Table 3. 2: Correlation between $\boldsymbol{PM10}, \boldsymbol{PM2.5}$ ***and*** $\boldsymbol{PM1}$ concentrations

Description	Best-fit equation	R^2	Sampling measurement day
$PM2.5$ vs. $PM10$	y1 = 0.784x1 - 3.446	0.876	D1
	y 2= 0.891x2 - 4.999	0.934	D2
	y3 = 0.845x3- 5.063	0.968	D3
	y4 = 0.780x4 - 2.443	0.905	D4
$PM1$ vs. $PM10$	y1 = 0.618x1 - 8.576	0.725	D1
	y2 = 0.628x2 - 6.494	0.761	D2
	y3= 0.500x3 - 3.635	0.939	D3
	y4 = 0.462x4 - 1.716	0.825	D4
$PM2.5$ vs. $PM1$	y1= 1.119x1 + 10.01	0.941	D1
	y2 = 1.207x 2+ 7.867	0.888	D2
	y3 = 1.651x3 + 1.651	0.984	D3
	y4 = 1.575x4 + 2.511	0.957	D4

The first peak in all curves could be explained by incomplete combustion with short distances traveled during the first 2 km of the trip (roughly the first 5 min) and a cold engine (Chen et al., 2017; Zhu et al., 2016).

The highest average $PM10, PM2.5$ and $PM1$ values appeared on the urban national highway $RN6$ (along its ring road section) with recordings of $43.96, 31.85$ and $18.62\ \mu g/m^3$, respectively. In fact, the $RN6$ geometry features a curvature that requires more power from

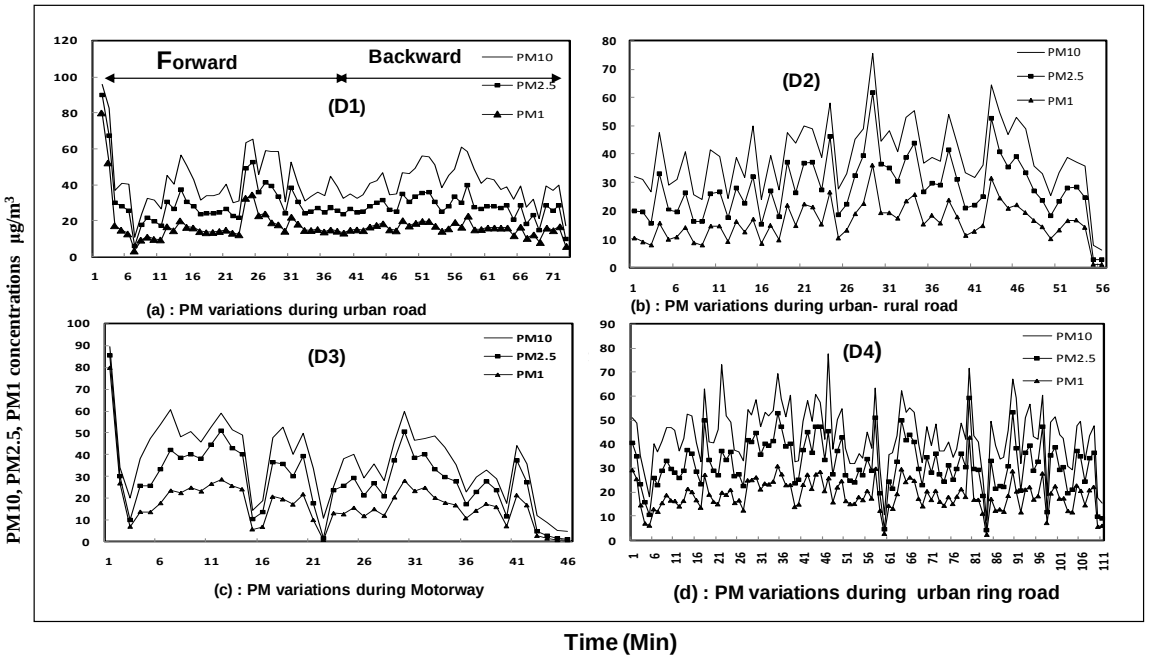

Figure 3. 3: Diurnal PM10, PM2.5 and PM1 variations across the tested road segment types

the engine and higher speed in order to ensure equilibrium in the middle of the roadway. Moreover, it is characterized by high traffic density, especially by the heavy vehicle category. The highest maximum $PM10, PM2.5$ and $PM1$ values occurred in the urban area with readings of $95.97, 89.97$ and $79.8\ \mu g/m^3$, respectively. These high rates are correlated with traffic volume, the presence of buildings and high inter-vehicular times, generating an accumulation of particle number concentrations inside the tailpipe. The particle adhesion phenomenon induces an increase in particle mass concentrations (PMC) but not PNC. In contrast, the lowest averages of $PM10, PM2.5$ and $PM1$ values were found in suburban and rural areas, with readings of $37.55, 26.66$ and $15.14\ \mu g/m^3$ (Table 3.3). During suburban-rural driving, road conditions are in fact characterized by very fluid traffic inducing a

reduction in the inter-vehicular time. Furthermore, the presence of fewer buildings favors a dispersion phenomenon. Fig 3. 4a displays $PM10, PM2.5$ and $PM1$ variations throughout

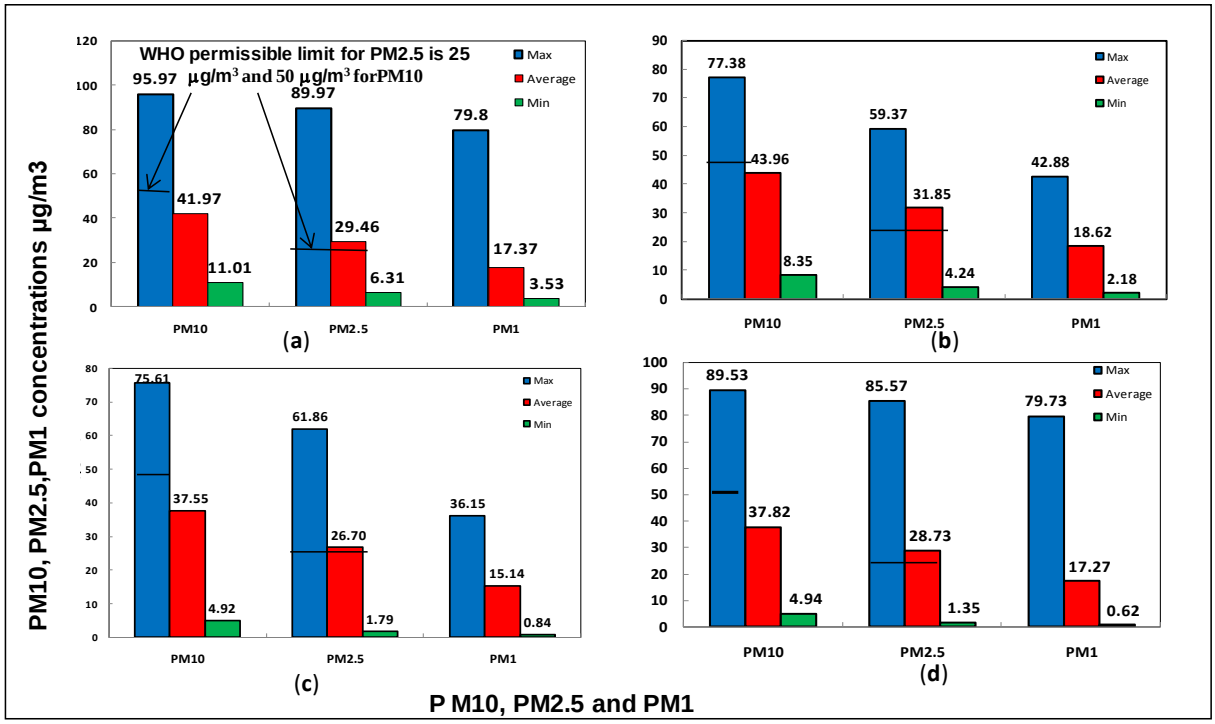

Figure 3. 4: PM10, PM2.5 and PM1 concentrations over four sampling sites in Lyon

the urban road segment, where the minimum – maximum range of $PM10, PM2.5$ and $PM1$ concentrations were $11.01 - 95.97\ \mu g/m^3$, $6.31 - 89.97 \mu g/m^3$ and $3.53 - 79.8\ \mu g/m^3$, respectively. Furthermore, the average values of $PM10, PM2.5$ and $PM1$ were calculated at 41.97, 29.46 and 17.37 $\mu g/\ m^3$, respectively (Table 3.3). These results are significantly lower than those obtained by (Hussein et al., 2019), whose average $PM10$ and $PM2.5$ equaled 89 and 60 $\mu g/m3$. The measurements from the previously reported study were conducted in the Middle East and North Africa ($MENA$) Region, characterized by a large area of arid/desert terrain in its southeastern part, which is not all the case for Lyon (site of the present study). In fact, dust storms and sand originate from three main regions: the Arabian Peninsula, North Africa, and the Levant. In addition, measurement periods differed for the two compared studies.

Table 3. 3: Min, Max and average concentrations of $\boldsymbol{PM10, PM2.5\ and\ PM1}$

PM variation	$PM10\ (\mu g/m^3)$			$PM2.5\ (\mu g/m^3)$				$PM1\ (\mu g/m^3)$			
	Min	Max	Mean± SD	Min	Max	Mean± SD	PM2.5/ PM10 (%)	Min	Max	Mean± SD	PM1/ PM10 (%)
D1	11.01	95.97	41.97± 13.46	6.31	89.97	29.46 ± 11.27	70.19	3.53	79.8	17.37± 9.77	41.38
D2	4.92	75.61	37.55± 13.45	1.79	61.86	26.66 ± 11.55	71.01	0.84	36.15	15.14± 6.94	40.33
D3	4.94	89.53	37.82± 16.98	1.35	85.56	28.72± 15.67	75.93	0.62	79.73	17.27± 12.23	45.66
D4	8.35	77.38	43.96± 12.54	4.24	59.37	31.85± 10.28	72.45	2.18	42.88	18.62± 6.38	42.35

The current study was performed during summer, while the Hussein et al. study took place in the spring. With the particle mass concentration being strongly influenced by temperature, it increases during spring and decreases in summer, as found by (Bilalet al., 2019). Moreover, (Bilal et al., 2019) demonstrated that the average urban $PM2.5$ was between 23.15 and $24.10\ \mu g/m^3$, i.e. close to the value obtained in the present study ($29.46\ \mu g/m^3$). Fig. 3.4b reveals $PM10, PM2.5$ and $PM1$ variations throughout the suburban-rural road segments, where the minimum - maximum range of $PM10, PM2.5$ and $PM1$ concentrations were $4.92 - 75.61\ \mu g/m^3$, $1.79 - 61.86\ \mu g/m^3$ and $0.84 - 36.15\ \mu g/m^3$, respectively. Furthermore, the average $PM10, PM2.5$ and $PM1$ values were $37.54, 26.66$ and $15.14\ \mu g/m^3$, respectively (Table 3. 3). The average $PM2.5$ value was slightly higher than that obtained by (Bilal et al., 2019) ($18.20\ \mu g/m^3$). These reported rates are lower than those obtained in urban areas, as demonstrated, for example by Hand et al., (2019) and Li et al., (2014). Fig. 3.4c shows $PM10, PM2.5$ and $PM1$ variations throughout the motorway segment, where the minimum - maximum $PM10, PM2.5$ and $PM1$ concentrations varied between $4.94 - 89.53\ \mu g/m^3$, $1.35 - 85.56\ \mu g/m^3$ and $0.62 - 79.73\ \mu g/m^3$, respectively. For this road type, the average $PM10, PM2.5$ and $PM1$ values were $37.82, 28.72$ and $17.27\ \mu g/m^3$.

Lastly, Fig. 3. 4d presents the $PM10$, $PM2.5$ and $PM1$ variations over the $RN6$ highway (along the ring road), where the minimum - maximum mass concentrations varied from $8.35 - 77.38\ \mu g/m^3$, $4.24 - 59.37 \mu g/m^3$ and $2.18 - 42.88\ \mu g/m^3$, respectively. The average $PM10, PM2.5$ and $PM1$ for $RN6$ were $43.96, 31.85$ and $18.62\ \mu g/m^3$ (Table 3.3). The standard deviations (SD) remained low during all measurement days, as concluded by Srimuruganandam and Nagendra, (2010) who explained that particle mass $PM1, PM2.5$ and $PM10$ displayed a similar response around the dataset average (Table 3. 3).

As far as the authors' knowledge is of concern, no previous study in Lyon has simultaneously compared a continuous $PM1, PM2.5$ and $PM10$ series on urban, rural, motorway and national roads under real-world conditions (i.e. traffic, climate, driver behavior, etc.). For this reason, our findings have been compared with results obtained from other studies conducted abroad, which has led to inaccurate comparisons due to differing climate conditions, traffic volumes, road signage and geometry, etc. Furthermore, the principal reasons for each dissimilarity in the literature might be changes in experimental methods, especially the absence of a standard protocol.

- PM2.5/PM10 and PM1/PM10 average concentration ratios

Compared with $PM10$ and $PM2.5, PM1$ must receive greater attention due to its longer atmospheric lifetime, health risks and smaller size (Dominici et al., 2014). $PM1$ acts as a carrier of toxic substances and penetrates deep into the lungs (McEntee and Ogneva-Himmelberger, 2008). An emergency solution is therefore required to prevent against this harmful phenomenon in order to ensure a sustainable community. Since coarse and fine particles were both produced from various sources, the $PM2.5/PM10$ ratio can furnish critical information associated with particle source (Speranza etal., 2014). High $PM2.5/PM10$ ratios indicate low proportion of coarse particles originating from anthropogenic sources (e.g. vehicle exhaust). In contrast, low $PM2.5/PM10$ ratio values suggest the strong participation of coarse particles, which might be influenced by natural sources (e.g. dust storm, increased solar radiation) and traffic (Alam et al., 2011; Sugimoto, 2016). The $PM2.5/PM10$ values ranged between $71.01\ \%$ and $75.93\ \%$, which is nearly the same interval found in urban areas by Giugliano et al.,(2005). In the present study, $PM1/PM10$ ratios were low, varying between $40.33\ \%$ and $45.66\ \%$; this fact underscores that the crustal elements lie mainly in the coarse fraction (Alam et al., 2011; Titos et al., 2014). Figure 3.4 shows the minimum, maximum and average $PM1, PM2.5$ and $PM10$ concentrations for

all investigated sites. The $PM2.5$ and $PM10$ values greatly exceeded the $WHO's$ recommended maximum concentrations of 25 $\mu g/m^3$ for PM 2.5 and 50 $\mu g/m^3$ for $PM10$ (on a $24-h$ basis). PM1 is still not regulated in the European Union (EU) despite its high rates, reaching 79.8 $\mu g/m^3$ in the Lyon conurbation. Regardless, these $PM1$ measurements contribute to accurate prediction of anthropogenic particles (Perrone et al., 2013), representing a major portion of $PM2.5$ and, practically speaking, may even be more harmful than $PM2.5$. In this context, the contribution of $PM1$ in $PM10$ and $PM2.5$ has limited coverage in the literature despite the fact that PM size dependence is a good indicator for air quality monitoring. In addition, with its small size, $PM1$ easily contributes to penetrating into the human cardiovascular and respiratory systems, causing an increase in blood coagulability and lung disease. Particulate matter emissions are heavily influenced by local ambient temperature, inducing catastrophic phenomena like acid rain. Particulate matter may become deposited on the water or ground and carried by wind over long stretches. Exposure to both ambient $PM2.5$ and $PM1$ are also strongly correlated with the increase in the number of emergency hospital visits. $PM1$ is thus the main cause of most health effects from $PM2.5$ (Chen et al., 2017). These damaging implications should be assessed, controlled and regulated immediately.

3.1.2.2. Particle Number Concentration (PNC)

Fig. 3.5 presents the $PNCs$ on the various road segments (urban, rural, motorway, $RN6$). The $PNCs$ were divided into particle numbers with a diameter greater than and less than 1 μm ($PNC > 1$) and ($PNC < 1$).

This figure illustrates that both $PNC > 1$ and $PNC < 1$ μm alongside a road are shaped like exponential functions. The $PNCs$ with a diameter less than 1 μm are too high, reaching $8.12 \cdot 10^7 cm -^3$ with a particle diameter of 0.35 μm on the motorway. Whenever the particle diameter exceeded 1 μm, the PNs decreased rapidly. It is worth pointing out that this trend stems from large particles being eliminated faster due to the sedimentation phenomenon. The particle number from the vehicle tailpipe was actually characterized by a small diameter; consequently, as particle diameter increases, particle number decreases and vice versa. Fig. 3.5a reveals that on the urban road, the majority of sampled particles have diameters smaller than 0.35 μm and extend to $5.6 \cdot 10^6 cm^{-3}$. In contrast, $PNCs$ trend tend to zero with a

diameter above 3.5 μm since particles $<$ 2.5 µm are mainly generated by vehicle tailpipe exhaust emissions (Pant et al., 2015).

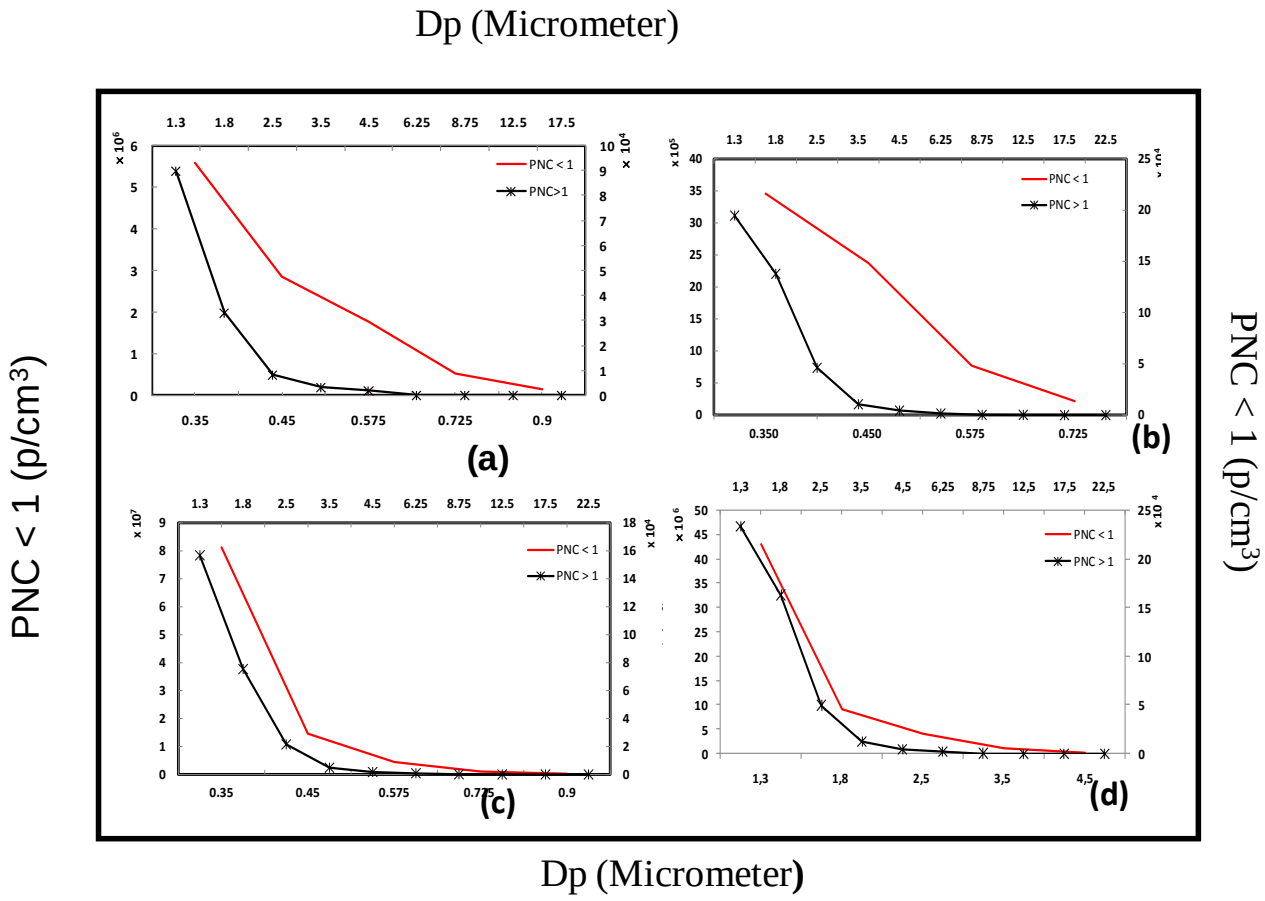

Figure 3. 5: PNC during all road segment types

Results showed that human health is seriously endangered as pedestrians and cyclists are directly exposed to these harmful particulates. Villafuerte et al., (2017) found that the maximum $PNCs$ in urban exhaust emissions were slightly higher than $1.1 \cdot 10^5$. cm^{-3}, which is considerably lower than the values obtained in this study. In fact, the present study was in fact conducted using the $Euro\ 3$ tailpipe exhaust emissions, while the aforementioned research was tested with $Euro\ 6$. The average vehicle exhaust for urban $PNCs$ equals $7.4 \cdot 10^5\ cm^{-3}$, which is much higher than the value of $3.7 \cdot 10^4 cm\ -^3$ obtained by Patton et al., (2012) due to both traffic volume and a different pollution source. These authors indeed measured $PNCs$ in a residential area renowned for its low traffic volume; moreover, they revealed that the main pollution source in the study area was residential heating. Fig. 3.5b shows that on the rural road, the behavior of the PNC curve follows the same pattern as the urban $PNCs$ for diameters smaller and larger than 1 μm. However, the maximum rural $PNCs$

are lower than their urban counterparts, which is in agreement with Cazier etal., (2016). The rural $PNCs$ present a mean of $5.15 \cdot 10^5\ cm^{-3}$. Fig. 3.5c illustrates that motorway $PNCs$ follow the same trends as the two-previous road types. However, the maximum motorway $PNCs$ $(8.12 \cdot 10^7)$ were higher than on urban or rural roads, as found by Kontses et al., (2020), due to a high constant speed (e.g. Banerjee and Christianb, 2019). This outcome could, in fact, be anticipated due to the high turbulence produced from the traffic generated at high speed with a dry climate. Furthermore, the exhaust emissions include in large part a mixture of road surface wear and dust. The on-road average exhaust PN concentration along the motorway was $6.7.10^6\ cm^{-3}$ (Table 3. 4). Fig. 3.5d demonstrates that in $RN6$, the PNC curve follows the same trends as the last three road types discussed previously. In contrast, the maximum national road $PNCs$ were less than motorway $PNCs$ and greater than the rural and urban $PNCs$, which reached as high as $4.3 \cdot 10^7 cm^{-3}$ due to a high constant speed and a heavy-duty vehicle (Table 3.4).

Table 3. 4: Mean particle number concentrations

Sampling day	Mean
D1	$7.4.10^5$
D2	$5.15.10^5$
D3	$6.7.10^6$
D4	$3.9.10^6$

The geometry of the national road happens to be characterized by a high curvature radius, thus requiring more power in order to ensure vehicle equilibrium in the roadway axis (to handle the centrifugal force).

In conclusion, motorway $PNCs$ exhibited the highest rates compared to the other three road types due to a high constant speed, which is in agreement with several studies (e.g. Geller et al., 2005; Imhof et al., 2005; Maricq et al., 1999; Simonen et al., 2019). However, rural $PNCs$ displayed the lowest rates compared to the other three road types due to several factors,

namely: low traffic volumes, few acceleration/deceleration maneuvers, short inter-vehicle times (i.e., free-flow conditions), and limited obstacles (buildings) to promote the dispersion phenomenon. The minimum particle number recorded was very low, with large-sized diameters ($> 10\ \mu m$), since exhaust particles are essentially ultrafine or fine particles. Keep in mind this analysis is limited given that the $OPC\ GRIMM^{TM}$ (ref. EDM 1.108) is inappropriate for accurately assessing the number of ultrafine particles (below $100\ nm$), for which the number concentration should be higher.

The current study has faced many of the difficulties inherent in comparing results obtained with those in the literature. Many reasons can be cited, including: (1) Only a few studies have focused on measuring the $PNCs$ of tailpipe exhaust emissions at the micro-scale under real-world conditions on urban, suburban-rural, motorway and national (ring) roads; (2) To the best of the authors' knowledge, no previous study has ever compared $PNCs$ across the various road types using micro-scale measurements in the Lyon region despite its dense population; and (3) No study has ever focused on comparing diesel tailpipe exhaust $PM1, PM2.5$ and $PM10$ measurements in urban, suburban-rural, motorway and national roads under actual traffic conditions of Lyon -France.

4.1.2.3. Influence of vehicle speed

In order to assess the effect of vehicle speed/ acceleration on the evolution of nanoparticles in the size range of $0.35 - 22.5\ \mu m$, simultaneous measurements are executed using the global positioning system $747Pro$ (GPS) for vehicle speed and particle size distribution at $4\ cm$ distance from the exhaust with the $GRIMM$ analyzer, series 1.108. Variations of total number concentration with abrupt acceleration and deceleration maneuvers of diesel vehicles for both forward and backward directions are depicted from Fig. 3.6. The first peak observed in all curves is due to incomplete combustion with short distances traveled during the first $2\ km$ of the trip and a cold engine (Chen et al., 2017; Zhu et al., 2016). Then, it is observed that the total number concentration increases even for sharp deceleration maneuvers. In fact, this is due to in homogeneity in the engine mixture throughout sharp deceleration and related change in fuel-air mixture. Similar results have been revealed in on-field measurements obtained by (Banerjeea and Christian, 2019; Giechaskiel et al., 2007) on diesel vehicle. They demonstrated that the total particle number concentrations over deceleration maneuvers related to the increase in Air/ Fuel (A/F) ratio leading to a reduction in the available surface area of solid particles.

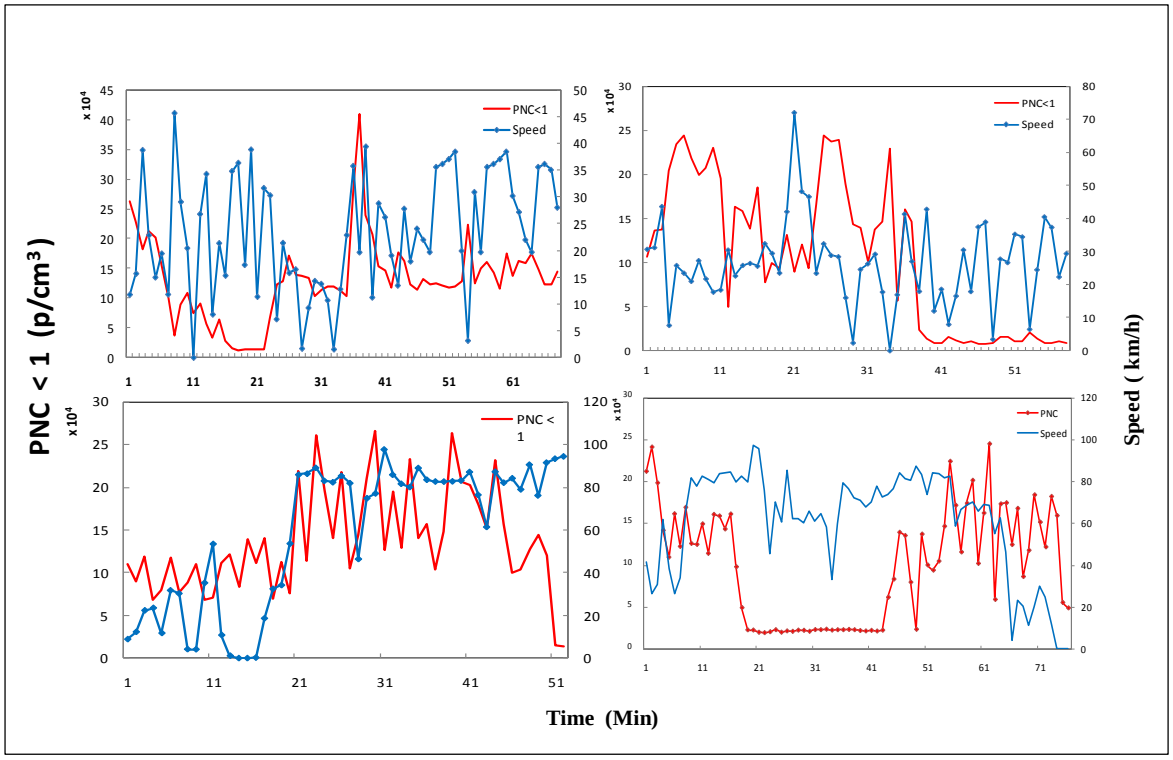

Figure 3. 6: Speed versus total number concentration recorded on-road from diesel vehicle

Section 2: Vehicle non-exhaust emissions

3.2. 1. Materials and methods

3.2.1. 1. Study areas

Measurements took place during July 2019 in the vicinity of Lyon (France). The total mileage traveled for all sampling day measurements was approximately 172 km, including both forward and backward directions. This large population number underscores the importance of this research through exposing the risk to the human body to different types of road traffic air pollution (specifically for urban, and rural roads). Non-exhaust particle concentrations including; resuspension, bake, tire and road surface wear were collected either during the morning or evening period, depending on climate conditions (Fig. 3.7).

Figure 3. 7: Field study set-up (non-exhaust emissions)

Measurements have mainly been obtained in urban (Bron-Décines-Meyzieu), rural (Corbas-Saint-Just Chaleyssin) and motorway ($A46$) (Fig. 3.8). The mileage traveled was not the same on all sampling days, it depended upon the road type (urban, rural or motorway).

Fig. 3.8a depicts the first day's itinerary of mobile sampling measurements on an urban road. The operating mode was adjusted according to the speed, idle acceleration and time via the global positioning system (GPS) under real-world monitoring with a $1-s$ resolution. The itinerary was extended from Bron to Meyzieu. Fig. 3.8b illustrates the rural itinerary (Corbas-Saint-Just Chaleyssin). Fig. 3.8c represents the third day's mobile sampling itinerary along the $A46$ motorway. In all sampled measurements, the current study has taken into account both forward and backward directions.

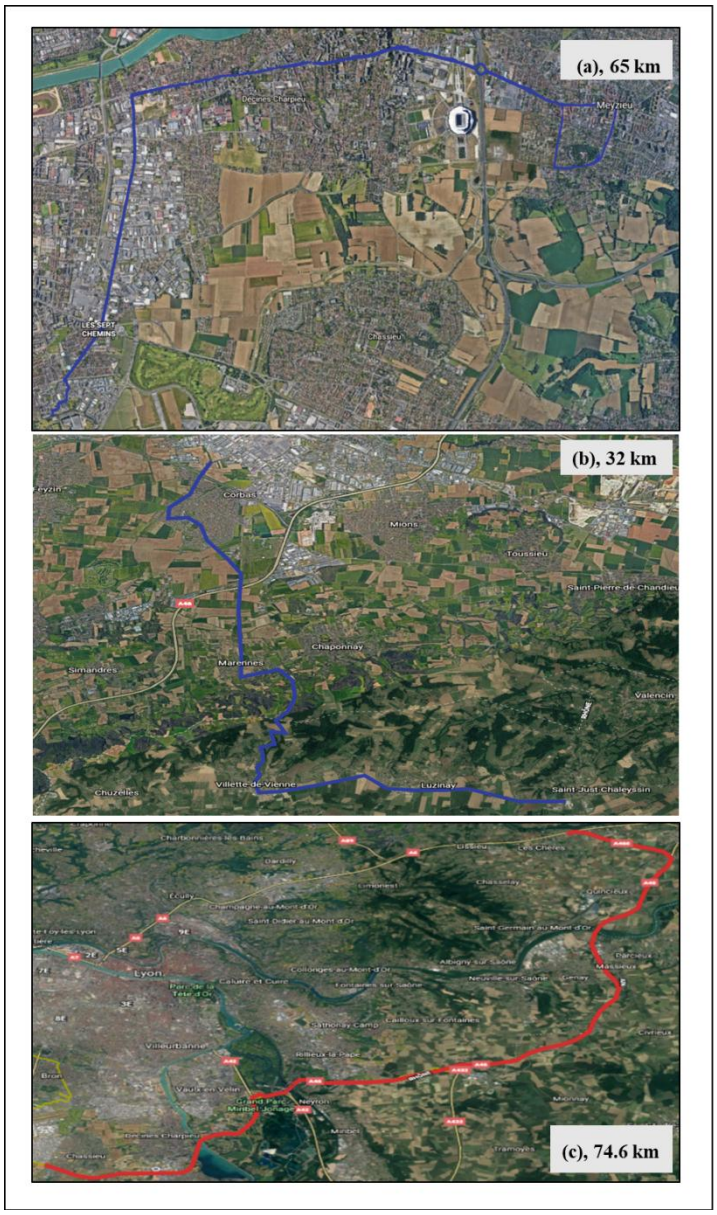

Figure 3. 8: Road map of the various study areas

Table 3.5 lists detailed information on all the mobile measurements, including time, road type, mileage traveled and direction. Three days of measurements were processed in order to evaluate non-exhaust particle concentrations for the three tested road types, again in both directions. Trip duration varied according to road type.

Table 3. 5: Related data for all sampling measurement days

Measurement day	Direction	Road type	Distance (km)	Min. temp. ($°C$)	Max. temp ($°C$)	Mean temp. ($°C$)	Precipitation (mm)

D1	Forward	Urban	33	17	30	20	No
	Backward		32				
D2	Forward	Rural	15	17	31	21	No
	Backward		16				
D3	Forward	Motorway	35	18	32	24	No
	Backward		39.6				

3.2.1.2. Instrumentations

The same instruments have been used in the section of estimating vehicle exhaust PNCs (section 1).

3.2.1.3. Sampling and measurement strategies

Non-exhaust particle emissions (resuspension, tire, brake and road surface wear) were investigated under real-time driving conditions (continuous speed profiles, with different mileages varying between 32 up to around 75 km). The summer tire (dimension $185/75R16C$) was chosen to study variation in wear and particle emission between different tires and roads under real-time conditions. Sampling measurements have been conducted under dry weather conditions ($T = 17-32\,°C$ with 23 %– 67 % humidity) and moderate wind speed ($< 30\ km.h^{-1}$). The same driver was kept and maintained for all the experimentations in order to maintain the same driving style and conditions throughout all sampling days. Instantaneous speed profiles and instantaneous acceleration profiles were recorded at $1\ Hz$ frequency regardless of driving conditions. The scientific instrument was installed behind the utility car. The $GRIMM$ was chosen due to its small size and light weight comparatively to other atmospheric particle instruments (for example, $PEMS, FMPS$). In fact, heavy instruments may provide inaccurate data due to their weight on vehicle engine efficiency. A $GRIMM$ did not require power generators due to built-in battery that lasts between six- to eight-hours continuous operations. Furthermore, the highest $TRWPs$ are generally recorded in accumulation and coarse modes (Kim and Lee 2018; Beji et al. 2020). In addition, sampling

measurements were registered under real-time driving characterized by high acceleration and deceleration maneuvers.

The inlet sampling probe was fixed in the axis of the wheel 5 cm from the ground, 10 cm behind the tire and with a diameter of 1 cm. PM can be divided into $PM1, PM2.5$ and $PM10$ which are particles with aerodynamics smaller than 1 μm, 2.5 μm and 10 μm respectively.

Measurements were conducted on three different road segments in the vicinity of Lyon (France). Thirty-minutes were required before starting the trip in order to load all necessary tools inside the light utility vehicle. All staff members exercised caution not to exceed five hours of charging, which would have caused the battery to discharge. Moreover, before initiating each sampling measurement, zero calibrations were regulated on both the $GRIMM1.108$ aerosol spectrometers and the GPS.

3.2. 2. Results and discussion

3.2.2.1. Particle number distributions under various driving conditions

Studies have reported the generation of ultrafine particles with diameters of $30 - 60\ nm$ and particle with diameter sizer lower than 30 nm for studded and non-studded tires, respectively (Dahl et al. 2006; Foitzik et al. 2018), equally with the emission of a coarse fraction (Kwak et al. 2013; Kim et al. 2018). The vehicle of the actual study was fitted with summer tires. Fig. 3.9 presents $PNCs$ on various road segments (urban, rural and motorway). $PNCs$ were too high with a diameter less than 1 μm, which reaches up to $1.85.10^{7}.cm^{-3}$ on motorway. Whenever the particle diameter exceeded 1.3 μm, PNs decreased rapidly. It is worthy pointing out that this trend stems from large particles being eliminated faster due to the sedimentation phenomenon. We shall precise that during all measurement days, $PNCs$ were characterized by a bimodal distribution at coarse mode with 0.35 and 1.3 μm, respectively. It was found that cold start emissions (about the first 2 km of the trip) were composed of non-volatiles particles (coarse mode particles). However, in other available published studies dealing with measurement of $PNCs$ with an optical diameter ranging from 6 nm to 22.5 μm, it was shown that bimodal distribution centered at approximately 200 nm and a coarse peak at 2 μm (Beji et al. 2020).

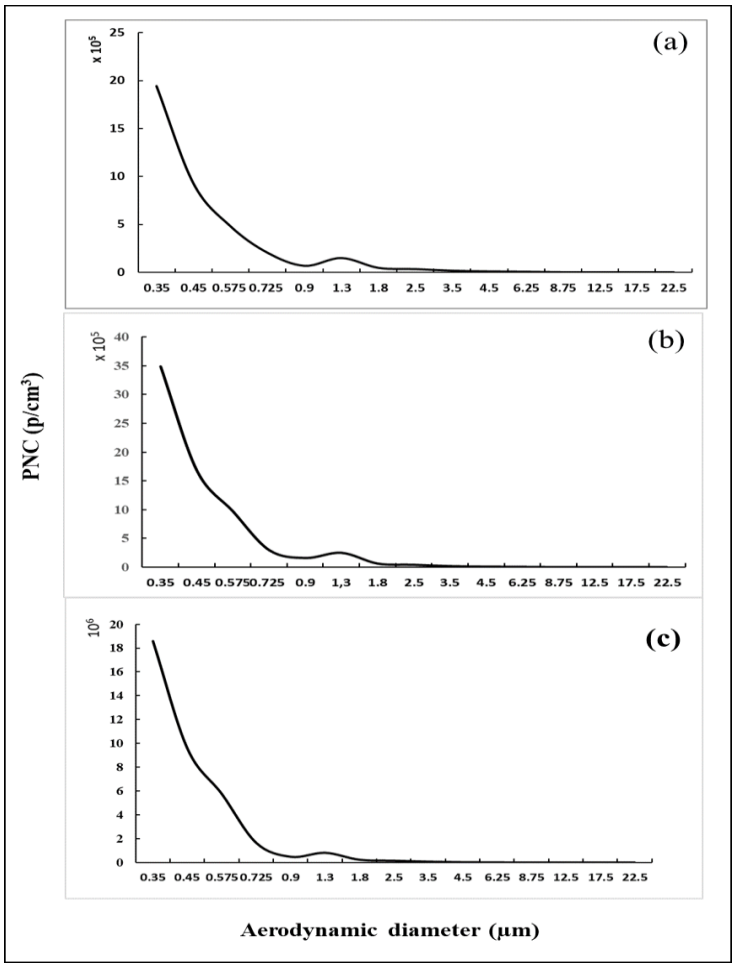

Figure 3. 9: Non-exhaust particle size distributions under real driving conditions in (a) urban, (b) rural and (c) motorway areas

This slight difference in modal size could be explained by the sampling methods, traffic conditions and the instrumental properties inherent or not all non-exhaust factors are taken into account in this analysis.

Fig. 3.9a reveals that on the urban road, the majority of sampled particles have diameters smaller than 0.35 μm and extend to $1.9.10^{6} cm^{-3}$, followed by a second light peak at 1.3 μm that reaches $1.49.10^{5} cm^{-3}$. The same trends are shown in Fig. 3.9b, the highest particle concentrations appeared at 0.35 m with $3.4.10^{6}\ cm^{-3}$ in rural area. The high concentration on rural road as compared to urban road is mainly due to high vehicle speed. Fig. 3.9c illustrates particle size distributions on motorway. The maximum motorway $PNCs$ were higher than those found in both urban and rural zones, which are as high as $1.85.10^{7} cm^{-3}$ due to high speed, pavement materials and abrupt vehicle acceleration and deceleration maneuvers.

Generally, concrete roads (motorway) are more pollutant than asphalt roads (urban - rural), as outlined by Pant and Harrison (2013). They demonstrated that concrete surfaces cause more tire abrasion than asphalt surfaces; PM emissions are 1.4 to 2 times higher for concrete roads than for asphalt roads. However, this result remains relative and depends upon the tire type, drive behavior and climate conditions.

3.2.2. 2. Effect of vehicle speed on PM concentrations

In real-time measurements, different instantaneous speed profiles depending on road type (urban, rural and motorway) were taken into account to investigate the effect of vehicle speed on PM mass. Fig. 3.10 shows the average $PM10, PM2.5$ and $PM2.5/PM10$ ratios. It is worth noting that the increase of PM and $PM2.5/PM10$ ratio is related to driving speed conditions. In fact, the highest PM and $PM2.5/PM10$ ratio appeared on motorway due to high vehicle

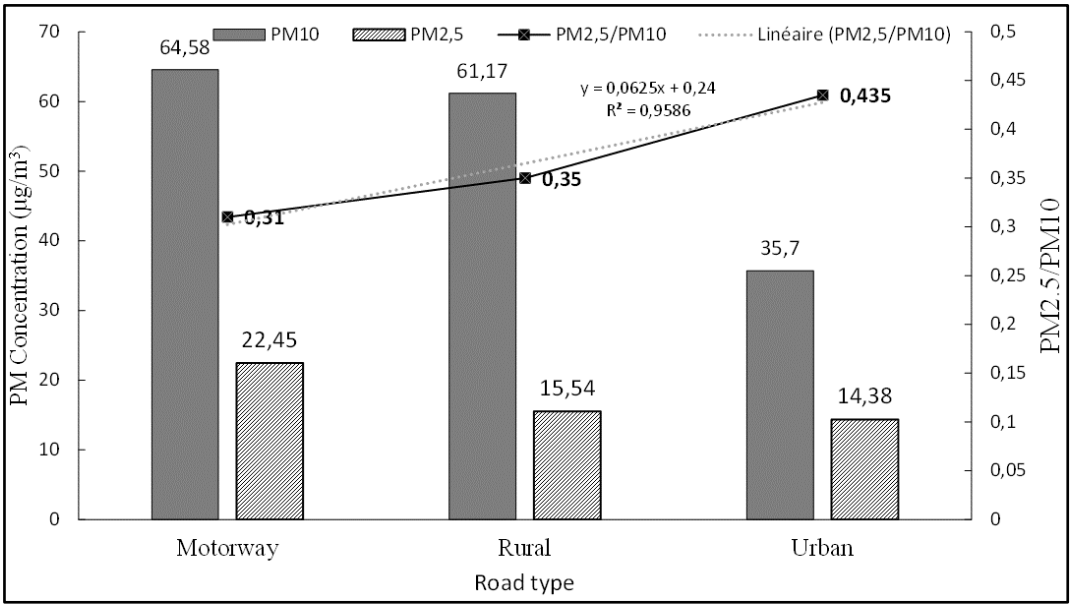

Figure 3. 10: Average particulate PM concentrations, PM2.5/PM10 ratio

speed (V^{9}_{m1}= $89.82 km.h^{-1}$). In contrast, the lowest PM and $PM2.5/PM10$ ratio were found on urban road (V^{10}_{m2}= $34.95\ km.h^{-1}$) as validated by several studies (i. e. Grigoratos et al. 2018; Kim and Lee 2018; Beji et al. 2020). A linear relationship was obtained between $PM2.5, PM10, PM2.5/PM10$ ratio and the driving speed with high coefficient of determination R^2 of $0.85, 0.84$ and 0.96, respectively. The relative contribution of $PM2.5$ to

[9] V_{m1}= Average speed in motorway expressed in km/h
[10] V_{m2}= Average speed in urban road expressed in km/h

$PM10$ (the ratio $PM2.5/PM10$) varied from $0.31\ to\ 0.435$. However, Kim and Lee 2018 reported lower values compared to our obtained results, where they reported 0.24 up to 0.32 as the contribution of $PM2.5$ to $PM10$. This is because particulate matter from road traffic is induced also from resuspension in addition to tire, brake and road wear, which is not the case in laboratory measurements. Indeed, particulate matter resuspension could be defined as fresh produced particles from abrasion and stress as well as older located road dust refreshed and transported into the atmosphere.

The results show that PM and $PM2.5/PM10$ ratio were positively correlated with vehicle speed. In fact, $PM2.5$ and $PM2.5/PM10$ ratio continuously increased as vehicle speed increased depending on road type. Particles occur through volatilization and by shearing (Kreider et al. 2010) and friction forces. In fact, shearing forces mechanism practically induces in coarse particles, whereas volatile mechanism produces smaller fine particles via the evaporation (Kim and Lee. 2018).

Under real-time measurements, shear stress acting on tire tread was wide, mostly on motorway due to high speed and the state of the tire. Indeed, the used tire in this experience was not put into circulation for the first time. Contrary to what was found by Kim and Lee. (2018), a limited shear stress was acting on tire tread with low $PM10$ particles. This can be explained by the difference in experimentation as in this current study we took into account all real driving conditions including road dust emissions induced by mechanical vibration sieve (Wang et al. 2012), which is not the case for laboratory measurements. In this study, non-exhaust $PM10$ concentration presents $64.58\ m.cm^{-3}$, which is larger than the World Health Organization (WHO) permissible limit ($50\ \mu g.m^{-3}$). The pronounced volatilization process related to high speed were produced on motorway as well as on rural roads (ring). In fact, the selected rural road geometry features a curvature that requires more power from the engine and higher speed in order to ensure equilibrium in the middle of the roadway. Moreover, it is characterized by high traffic density, especially by heavy vehicle category. Here we notice that the increase in non-exhaust PM concentration is strongly related to the increase in vehicle speed and vice-versa as validated by several studies (i. e. Hussein et al. 2008; Grigoratos et al. 2018; Kim and Lee 2018; Beji et al. 2020). This might be due to turbulence air streams, suspension, increasing road wear of accumulated particles and high proportion of heavy-duty vehicles ($HDVs$). In fact, Wagner et al. 2018conducted a review paper where they outlined that $HDVs$ produced approximately ten times more TWP than passenger cars and light duty vehicles ($LDVs$).

3.2. 2.3. Vehicle speed effect on particle concentrations

In order to investigate the effect of vehicle speed on particles evolution (in terms of concentration number) induced from non-exhaust in the range of $0.35 - 22.5\,\mu m$, simultaneous assessment is taken out applying the GPS for vehicle speed on different road surface types (urban, rural and motorway). The variation in total number of non-exhaust concentrations versus vehicle speed in urban, rural and motorway is provided in Fig. 3. 11 (a,b) and Fig. 3. 11c, respectively. The maximum and minimum $PNCs$ appeared on motorway and urban were $1.85.10^{7}$ and $1.9.10^{6}.cm^{-3}$, respectively. These findings may be explained by the high speed on motorway resulting in substantial increase of $PNCs$ as outlined by Béji et al. (2020). Obviously, this result highlights an increase in the coarse particles at high speed. This is because more shear stresses and turbulent air streams developing at the road tire pavement interface resulted in an increase in particle concentrations. Consequently, a remarkable change took place in the super micron fraction of the wheel rear ambient aerosol. This current work as well as other available published studies have confirmed that vehicle speed is an important parameter to be considered to accomplish strategies to mitigate non-exhaust particle emissions from road traffic (i. e. Dahl et al. 2006; Gustafsson et al. 2008; Hussein et al. 2008; Foitzik et al. 2018).

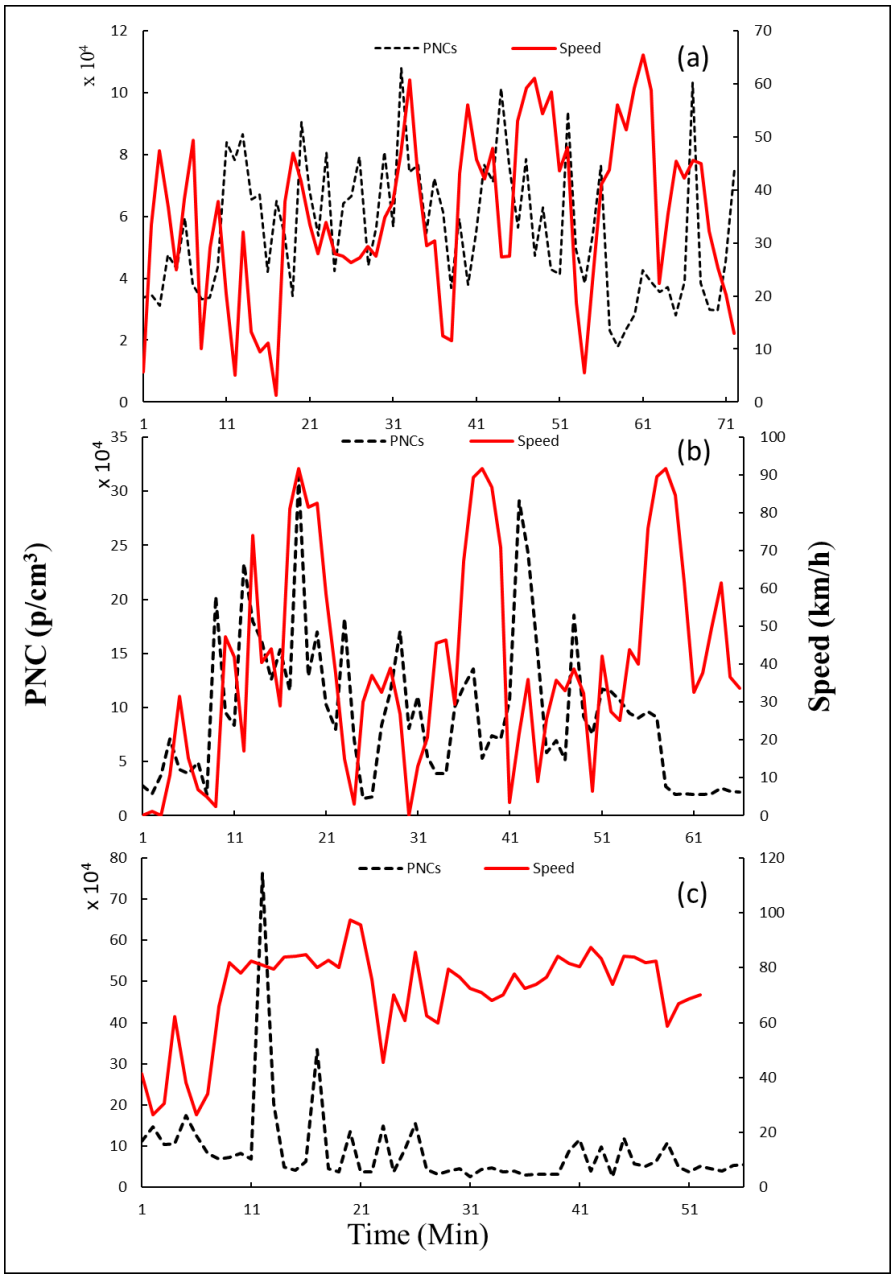

Figure 3. 11: Vehicle speed versus total particle number concentrations (PNCs) recorded in urban, rural and motorway areas

3.2.2.4. Positive and negative vehicle acceleration effect on non-exhaust particle concentrations

In order to evaluate the influence of vehicle speed on non-exhaust PNCs, it is important to include acceleration and deceleration (A/D) maneuvers in the analysis. In specific road geometry (curvature with sharp radius, speed bumps, etc.), traffic conditions (congested traffic, accident, etc.) and driver behavior (aggressive driving) both acceleration and

deceleration maneuvers can engender a pronounced effect on non-exhaust emissions (Luhana et al., 2004). Significant non-exhaust particle concentrations were registered in coarse mode during A/D cycles (Fig. 3.12).

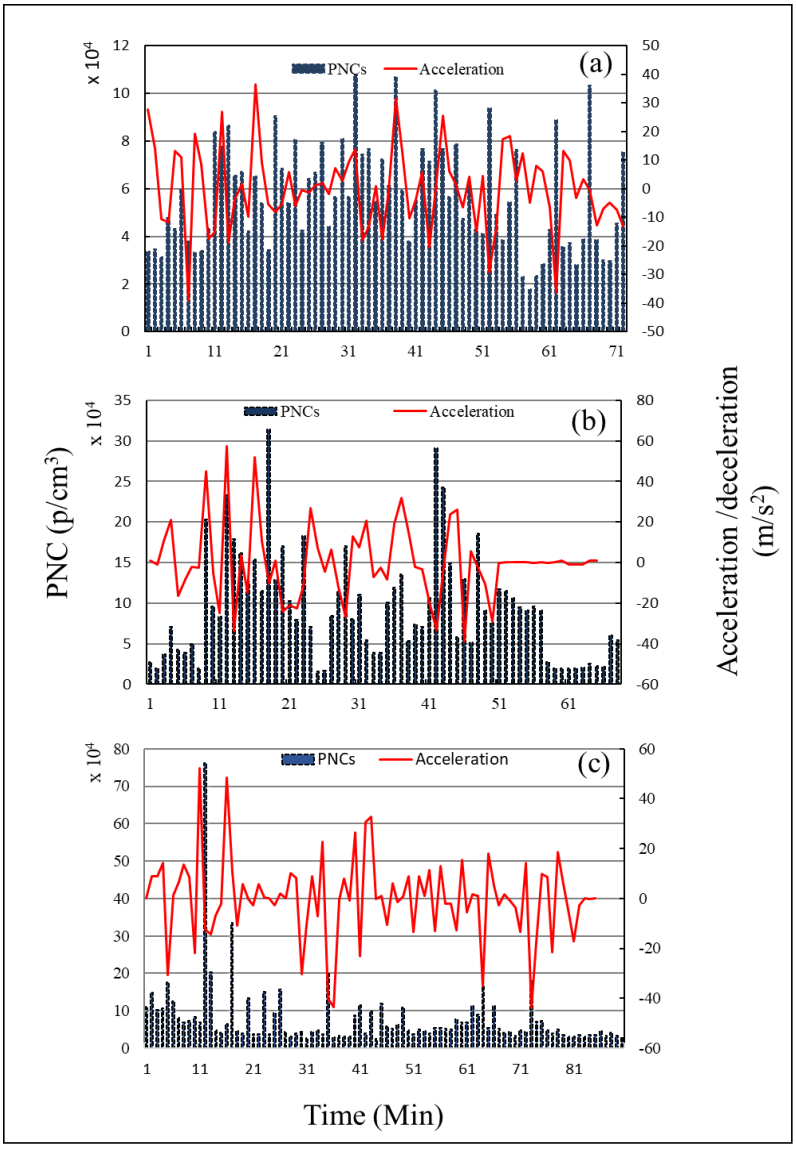

Figure 3. 12: Evolution of non-exhaust PNCs versus positive and negative acceleration in (a) urban, (b) rural and (c) motorway areas.

Fig. 3.12a shows NEP concentrations versus positive and negative acceleration in urban area. It demonstrates several negative acceleration maneuvers due to speed bumps, pedestrian crossing and traffic light. Abrupt positive vehicle acceleration $[10 - 38\, m.s^{-2}]$ induced abundant NEP concentrations. This significant increase in particles rate that varies from $1.79.10^4$ to $1.07.10^5$.cm^{-3} may be explained by different generation mechanisms like tire wear under elevated temperature or related with a more abundant road dust fragmentation. Fig. 3.12b illustrates NEP concentrations versus positive and negative acceleration in rural area.

The geometry of the rural road is generally characterized by a high curvature change radius, thus requiring more A/D maneuvers. The rural NEP concentrations were 3 times higher when comparing the vehicle positive acceleration passing from (-24) to $(+57.13)$ $m.s^{-2}$. In contrast, with stable speed where the positive and negative vehicle acceleration were around zero, it showed a significant decrease in NEP concentrations. Rural road is characterized by sharp rate of positive and negative vehicle due to road geometric (curvatures) and road maintenance during measurement days. Fig. 3.12c indicates motorway NEP concentrations versus positive and negative acceleration maneuvers. The NEP concentrations were 11 times higher when comparing the vehicle negative acceleration passing from $(+52)$ to (-12) $m.s^{-2}$. The significant increase in NEP concentrations with sharp positive and negative vehicle acceleration maneuvers suggests that an aggressive driving produces more abundantly tire road wear particles than with an economic driving style (Boulter 2005; Kwak et al. 2013).

Despite that, the urban area is distinguished by a high rate of vehicle A/D maneuvers, while not admitting the highest particle emissions. This is because in urban area generally the speed does not exceed 50 km/h, which cannot generally engender a sharp vehicle A/D maneuvers. Unlike to motorway and rural roads, with a sudden vehicle A/D maneuvers can engender an extreme A/D rates.

3. 3. Concluding remarks

In the present chapter, mobile micro-scale, real-world measurements of exhaust $PM1$, $PM2.5$, $PM10$ and PN on four distinct road types (urban, rural, motorway, $RN6$ national road) in the Lyon region have been investigated. In order to examine particles within the $0.35-22.5$ μm range, we compared both on-road diesel particle mass and number among various road types. Results indicated similar pattern (exponential trends) in particle number concentrations over four road types for both particle diameters both smaller and greater than 1 μm. The highest average vehicle exhaust particle number concentration was recorded on the motorway, at $6.7 \cdot 10^6$, where the highest value was found at 0.35 μm. The particle counts thus exceeded WHO's permissible limit for both $PM2.5$ and $PM10$, i.e. at 25 $\mu g.m^{-3}$ and 50 $\mu g.m^{-3}$. These results demonstrate that particle mass is heavily influenced by stop-and-go traffic; Moreover, PN. $PM1$ concentrations are not yet regulated in the EU, despite its high mass rates and hazardous health effects (e.g. cardiovascular and respiratory problems, cancer), in reaching as high as 79.8 $\mu g.m^{-3}$on motorway. The study of exhaust emissions underscores the usefulness of evaluating the contribution of individual vehicles. Consequently, on-road experiments

under actual driving conditions are critical to improving the scientific understanding of traffic-related air pollution in urban, suburban and rural areas.

In addition to mobile micro-scale, real-world measurements of exhaust $PM1$, $PM2.5$, $PM10$ and PN, this chapter has been investigated the $NEPs$ (resuspension, tire, road surface and brake wear) under different road traffic areas.

To recapitulate, in motorway real-time driving conditions, NEP concentrations are higher in comparison with induced particles in rural and urban areas due to high speed, pavement materials and abrupt vehicle acceleration and deceleration maneuvers. NEP concentrations were characterized by a bimodal distribution at coarse modes with 0.35 and 1.3 μm ranges, respectively, within the three selected measurement days. Large coarse of NEP concentrations were formed from the road dust resuspension, under stress of the tire with the pavement. Information gathered on the key parameters assessing non-exhaust particles in real-time measurements can be employed to issue recommendations considered to mitigate non-exhaust particle emissions and ensure sustainable mobility. Speed, sharp positive and negative vehicle acceleration maneuvers have a pronounced effect on NEP concentrations. Linear relationship was found between PM ($PM2.5$, $PM10$ and $PM2.5/PM10$) ratio and the driving speed with high coefficient of determination, R^2. The relative contribution of $PM2.5$ to $PM10$ (the ratio $PM2.5/PM10$) varied from 0.31 to 0.435. The abundant increase in $NEPs$ with abrupt positive and negative vehicle acceleration maneuvers propound that irrational driving generates more significantly tire road wear particle concentrations than with rational (or economic) driving style.

Moreover, our results showed that NEP concentrations can vary with driving style and traffic conditions. In addition, it has been demonstrated that tire road wear can engender substantial particles with respect to mass and/or number particle concentration. Furthermore, $NEPs$ could be significant contributors to particles in motorway area. Further researches using different tire types and pavement materials in real-time measurements should be conducted to definitively define the effects of $NEPs$ on human health, climate change and environment impact.

Chapter 4. Modeling of particle number exhaust and non-exhaust emissions

4. 1. Introduction

Nanoparticles have dangerous effects on ambient air quality (Watson, 2002), human health (Tang et al., 2017; Belkacem et al., 2021) and environmental impact (Silva et al., 2021). Nanoparticles recorded a remarkable increase in recent years. Diesel-powered vehicles reveal the major source of road vehicle pollution in the European Union. Urban road traffic areas engender various human activities and pollution that reveals considerable adverse environmental impacts (Stone et al., 2017; Belkacem et al., 2020). Particles with small size diameter displaying larger specific surface area and reveal high disposition fraction in the respiratory system (Giechaskiel et al., 2015). According to Epidemiological analyses, a pronounced relationship exists between pollution, the number of cardiovascular and respiratory tract disease victims and particle number concentrations ($PNCs$) (Kim et al., 2012; Skrzypek et al., 2013). Atmospheric pollutants issues are not a simple problem for assessing the emission sources. The complexity of particle exhaust emissions in the atmosphere is largely depending on driver behavior. In fact, the total number concentration is strongly influenced by sudden acceleration/deceleration maneuvers of the vehicle (Carnevale et al., 2016).

Exhaust emissions being generated from tailpipes are mainly due to incomplete fuel combustion inside the engine chamber. This is because, modeling ambient air pollutants and $PNCs$ is a critical research area for mitigating road transport emissions on environment. $ANNs$ were frequently applied for the simulation of the ambient air pollution and environment induced from road traffic. Benedetti et al., 2016 and Khayatian et al., 2016 demonstrated the great potential of $ANNs$ for predicting and modeling such problems. However, restricted research has been focused on simulating continuous real time $PNCs$ from road traffic using $ANNs$. (Antonopoulos et al., 2017; Vakili et al., 2017) and differentiate complex patterns in database without understanding required interconnectivity among input and output variables (Lu et al., 2016). $ANN's$ accuracy do not only depend on the quantity of data but also on the quality of data. The number of hidden layers and the architecture are the major factors that influence on the performance of the model. The extreme number of neurons in the hidden layer can generate an overfitting or underfitting, which creates in turn errors in

the estimated models. This case can be presented in the training stage. The number of neurons in the hidden layer is resolved by error and trial approach, which begins with one neuron then incremented one by one (Alp and Cigizoglu, 2007; Arjun and Aneesh, 2015). The optimum number of neurons is determined practically by error and trial method rehashing 10 times at arbitrarily selected data points (Feng et al., 2015). The optimum number of neurons was chosen based on the least performance error as estimated by the coefficient of determination R^2 (Arjun and Aneesh, 2015) and Root Mean Square Error ($RMSE$) (Arjun and Aneesh, 2015; Abdullah et al., 2016a).

$PNCs$ were recorded in Lyon (France) using Grimm analyzer series 1.108. The locations and instantaneous speed profiles were simultaneously gathered by the global positioning system 747 Pro (GPS). After that, we make the simulation of $PNCs$ from urban road traffic by $ANNs$, MLP and $GRNN$. The model efficiency is assessed by applying statistical parameters; mean absolute percentage error ($MAPE$), coefficient of determination, (R^2) and Root mean squared error ($RMSE$). Finally, this study tends to compare the performance between the two-chosen ANNs methods.

4.2. Artificial neural network models for ambient air pollution prediction

Research studies in the field of emissions and ambient air pollution forecasting and predicting using artificial neural networks ($ANNs$) has been developed greatly in recent years. However, the improvement of ANN models provides levels of accuracies given the black-box nature of ANNs. In fact, ambient air quality in urban areas has been assigned to premature mortalities and chronic diseases of vulnerable members of the public (World Health Organization, 2016). Recently, ANNs have been greatly applied in many short- and long-term predicting and forecasting applications (e.g. Cabaneros et al., 2017; Lightstone et al., 2017; Rahimi, 2017). Moreover, more practitioners resorted to data -driven methods such as ANNs as alternatives to physics-based or traditional deterministic approaches, such as the examples of Community Multiscale Air Quality model ($CMAQ$) (Mueller and Mallard, 2011), Weather Research and Forecasting Model with Chemistry ($WRF/Chem$) (Chuang et al., 2011), the Urban Airshed Model (UAM) (Chang and Cardelino, 2000). In fact, deterministic approaches are reactive to several factors, including the quality and scale of the parameters participated computationally

expensive and dependent on rich databases of several input variables, of which some may not be available (Jiang et al., 2017; Sun et al., 2013)

4. 2.1. Methods applied for ANN model development

There are several accessible guidelines in the literature to make available future modelers with a systematic way of estimating ANN models. The model elaboration process is subdivided into eight major steps: data collection, data pre-processing, selection of input variables, data splitting, selection of model architecture, determination of model structure, model training, and model validation (Maier et al., 2010).

4. 2.1.1. Data collection

Black-box models like ANN models are data-dependent, practically complicate to integrate them with prior knowledge. Accordingly, the efficiency of ANN models depends on the form and type applied to train them. In fact, the choice of various types of predictor variables plays a pivotal role in the model efficiency since ambient air pollution is a complex function of emissions and meteorology (colls, 2001). There is an abundance of predictor variables that have been examined in previous environmental modeling applications including emissions, meteorological variables (wind direction, wind speed, relative humidity), traffic, etc. (Cabaneros et al., 2019) and vehicle speed.

4. 2.1.2. Data pre-processing

Data pre-processing is an important step in the estimation of ANN models. In fact, it tends to preliminary techniques that refer at assessing the representation of the gathered data. The two prevalent data pre-processing techniques in the area of environment and air pollution modeling that are contain missing data imputation and normalization. Normalization is applied to make sure that all predictors fall in equivalent range. This is a primordial step in model development as inputs with wide values disproportionately mask the effect of the other inputs with smaller ones. This measure should also be considered to coordinate the range of the predictors to those of the transfer function of the hidden layer (Cabaneros et al., 2019). Missing data induced from many factors like faults in data acquisition or errors in measurements and insufficient sampling. The simplest method to classify this problem is the substitution of missing data with the average of the entire dataset. However, this method is

highly inadvisable as this can disorder the inherent structure of the basic dataset, which can decrease the performance of the estimated model (Plaia and Bondi, 2006).

4. 2.1.3. Selection of predictors

The selection of the most appropriate ANN model predictors for a forecasting problem is an important step. The performance of the ANN strongly relies on the manner and form of which predictor variables are being fed into the model. However, the absence of the pertinent explanatory variables prevents the model from accurately approximating the underlying dynamics between target and predictors variables (Maier and Dandy, 2000). Several approaches are available in literature for selecting the most significant predictor variables of a given model. These approaches are divided into two major categories, known as model-based and model-free approaches. Model-based approaches execute input variable selection by resolving the impact of a candidate model predictor on the general model performance. In the other hand, model free approaches execute input selection without depending on the performance of the estimated ANN models (Maier et al., 2010).

4. 2.1.4. Data splitting

The division of data is an important step in the elaboration of ANN models. In fact, this is executed out by parting the available data into three subsets; training, validation and test sets. The first subset (e.g. training) is employed for calibrating network biases and weights, as well as for computing the gradient. The second subset (e.g. validation) is employed to block the network training before overfitting appears. In fact, the error in the validation subset assesses the network performance/efficiency during training subset. When this error tends to increase for much iteration, the training is terminated, and the bias and weights values that induced the minimum error are then employed as the final trained network biases and weights (Hagan et al., 1995). The third subset (e.g. testing) is employed to resolve the generalization capability of the developed model. In fact, the error from this subset is employed to compare the predictive efficiency of different models. Data splitting can be divided into supervised and unsupervised approaches. Supervised approaches tend to divide the input variables into three-subsets that take into account the statistical properties of each subset. However, unsupervised approaches do not take the statistical parameters of the data subsets into consideration, and only stratified unsupervised approaches tend to ensure that the statistical parameters of the subsets are identical (Maier et al., 2010).

5.2.1.5. Selection of model architecture

There are two-popular network architectures appropriate for forecasting and function approximation, namely the recurrent networks and feed forward (Hagan et al., 1995). In a feed forward network, data transfers in a unique direction from the input to the output layer. Among the most efficient feed forward ANNs are general regression neural networks ($GRNN$s), radial basis function networks ($RBFN$), extreme learning machine (ELM) and ward neural networks. In addition, the most popular feed forward ANNs are the Multilayer perceptron (MLP) for non-linear function (Shahraiyni and Sodoudi, 2016)

4.2.1.6. Determination of model structure

The determination of model structure including the number of nodes in each layer and the number of layers is an important step in ANN model development. The input variable layer is where the final network findings are calculated. Therefore, the number of target and input nodes are dependent on the number of target and predictors variables, successively. Finally, another layer in addition to the input and output layers, is known as hidden layer. It is in the hidden layer where the underlying dynamics between target and predictors variables is captured. When the number of nodes is sufficient, the ANN can estimate almost any function. ANNs may be developed by one or more hidden layers. The use of very limited number of hidden layers can lead to model underfitting, while the opposite situation results model overfitting (Samarasinghe, 2006). A standard method that estimates the optimal number of neurons and hidden layers still remain unspecified, which can be considered as the initial difficulty in ANN model building. For this, there are several employed approaches to correct these weaknesses, namely, ad-hoc, stepwise trial-and-error and global (Cabaneros et al., 2019).

5. 2.1.7. Model training

Training a model of ANN is the process of evaluating the association weights between the inter-associated nodes of the network. Due to the connection of the node biases and weights that an ANN can be qualified to estimate complex outputs. Training ANN model is usually carried out in a supervised manner. Before training, ANN biases and weights are typically initialized. Initial weighting is usually chosen randomly from a uniform distribution (Hagan et al., 1995). In the training process, the ANN is frequently accorded with the intended network

response for every input pattern as the network biases and weights are adjusted until the target outcome (Cabaneros et al., 2019).

4.2.1.8. Model validation

The performance of ANN model is typically evaluated using a quantitative error metric. However, ANN models should not be evaluated simply on their predictive error, but through their potentiality to capture underlying dynamics between target and predictors variables (Kingston et al., 2005a, b). In fact, the performance of the ANN models is based on three essential aspects of model validity; structural validity, predictive validity, and replicative validity (Gass, 1983; Humphrey et al., 2017). Metrics evaluating replicative validity perceive to it that a predicted model approximates both utilized data and those observed in previous ANN model (Gass, 1983). Recognized methods under this category include variance and means, maximum and minimum, goodness-of-fit-fit testing, analysis of variance, correlation and regression analysis (Wu et al., 2014).

Section1: Modeling of particle exhaust emissions based on real-time measurements

4. 1.1. Experimental protocol

4. 1.1.1. Study area and data

Measurements took place during July 2019 in urban (Bron -Meyzieu) – France (Fig.4.1). More details have been shown on sampling measurements, materials and methodology in chapter 4/section 1.

Figure 4. 1: Field area

4.1.1.2. Methodology

This study started by gathering the $PNCs$ of exhaust emissions and vehicle speed under continuous real-time measurements using the $GRIMM$ series 1.108 Aerosol Spectrometer and GPS (747 Pro), respectively. After that, the data has been filtered and analyzed, then synchronized to obtain a step of time $1\ min$ for both vehicle speed and particle number concentrations. Subsequently, two $ANNs$ models (Multi-Layer Perceptron (MLP) and General Regression Neural Networks ($GRNN$)) have been chosen to predict particle number concentration from real-time exhaust emissions in urban French area. In fact, the same input variables have been selected for both MLP and $GRNN$ that present vehicle speed and positive/negative vehicle acceleration maneuvers. $PNCs$ measured by the Grimm have been considered as the Target for $ANNs$ models (MLP and $GRNN$). Finally, this study tends to compare Grimm and $ANNs$ outputs. Then, the test was ended when the error reached its minimum. The flow chart methodology that was followed to model the continuous vehicle exhaust $PNCs$based on real experimental details summarized in Figure 4.2.

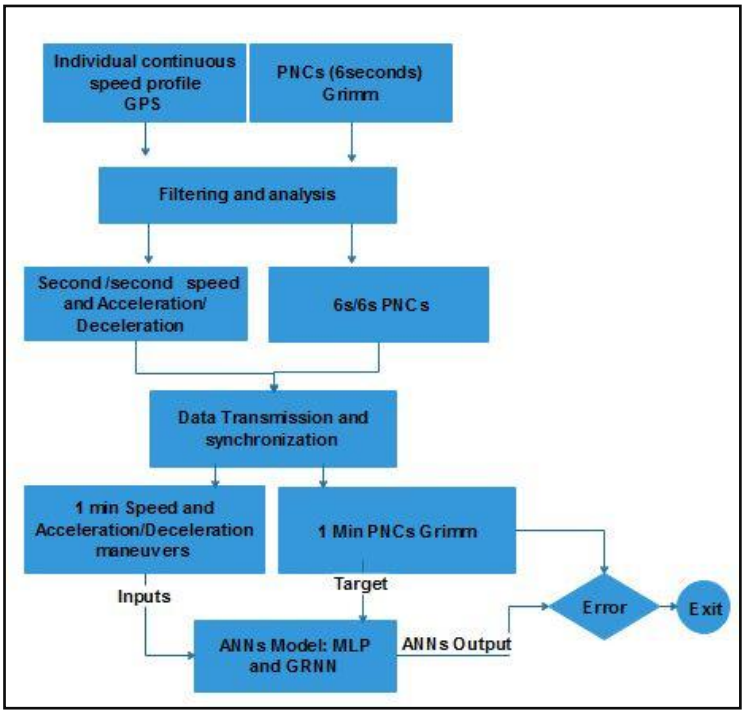

Figure 4. 2: Flow chart Methodology for exhaust PNCs

4.1.2. Artificial Neural Networks ($ANNs$)

$ANNs$ are among the most efficient computational models that practically approximate the same behavior as human brain. $ANNs$ have been extensively applied for forecasting and predicting in ambient air pollution, due to their accuracy and reliability to estimate any non-linear function (Nielsen et al.,2015). $MLPs$ are among the most applied architectures of the feed-forward networks employed by researchers (Maier et al., 2010). In this section, the $GRNN$ and MLP were chosen to model and predict particle number exhaust emissions.

- Multi-Layer Perceptron (MLP)

The Feed Forward topologies are among the most used Multi-Layer Perceptron (MLP) models in air pollution prediction. The input variables produce input signals, then they are transferred to the network starting from the left side (Input layer) to the right side of the $GRNN$ architecture (output layer) passing by the pattern layer. The input vector is multiplied by weights vector. This information has been recapitulated by the neuron in the patter layer, which includes bias (Fig 4.3).

$$y_0 = \sum_{i=1}^{n} w_i \times x_i + b \quad (4.1)$$

The non-linearity of model is produced when it is proceeding through the transfer or activation function.

$$f(x) = \frac{1}{1+e^{-x}} \quad (4.2)$$

Then

$$y_0 = f[\sum_{i=1}^{n} w_i \times x_i + b] \quad (4.3)$$

Where, y_0= output, w_i= weight vector,x_i = scaled input vector, b=bias, f=transfer function and x= total sum of weighted inputs.

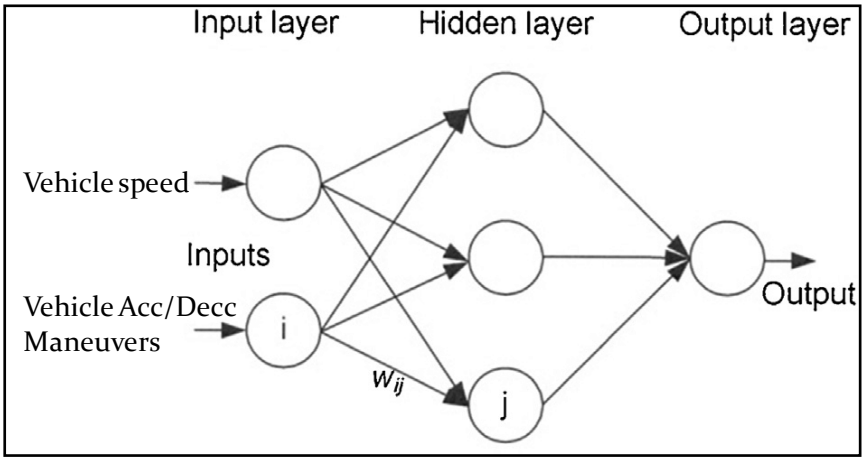

Figure 4. 3: Architecture of Multi-Layer Perceptron

When the error signal is calculated, the method of model fitting terminates. The difference between output and target is employed to calculate the error signal in the model, which corresponds to the input variable. The corresponding equation for MLP containing several neurons number is specified as shown in Eq (4.4):

$$y_0 = f\left[\sum WO_{kj}\left(\sum_{i=1}^{n} WI_{ij}\, x_i + b_1\right) + b_2\right] \tag{5.4}$$

Where, WI_{ij} = weight of input layer, WO_{kj} = weight of output layer, b_1 = bias in the inputlayer and b_2 = bias in the output layer.

There are no standard methods to determine the minimum and maximum number of neurons in the hidden layer (Sun et al., 2008). Few researchers have recommended the range of the optimal number of neurons in the hidden layer. In fact, the appropriate number of neurons ranges from $2\sqrt{M} + N$ to $2M + 1$; where, N and M are the number of output and input nodes, respectively (Fletcher and Goss, 1993). In the other side, (Voukantsis et al. 2011) demonstrated that the diverse number of neurons were proven in MLP models by applying the following formulas; $\frac{M}{2} - 2$ up to $\frac{M}{2} + 2$. Furthermore, a study suggested and demonstrated that the number of neurons should not be greater than twice the number of inputs (Sun et al., 2008).

The transfer or activation function has an important participation in ANN by generating a non-linear decision through non-linear blends of weighted input variables. The transfer function is able to transform the input signals into output signals. This transfer function reveals the non-linearity in the MLP model, and then opposes it with the linear model. The

sigmoid function has been chosen as the transfer function in this study. All implementations and computations were performed using $MATLAB$.

$$f(x) = \frac{1}{1+e^{-x}} \qquad (4.5)$$

- General Regression Neural Network ($GRNN$)

$GRNN$ requires few time-consuming as compare to the other iterative training networks. In fact, it selects an approximate function that connects the input and the output variables directly based on the training data. In addition, their algorithms are characterized by a flexible network structure setting, high fault and robustness tolerance when updating values of the parameters (Kumar and Malik, 2016; Bendu et al., 2016)

$GRNNs$ are based on a standard statistical technique known as kernel regression (Specht, 1991). $GRNNs$ comprise of four main layers including; output, summation, pattern and input layers from right to left (Fig.4.3). It is based on Equation (4.1)

$$E\left(\frac{y}{X}\right) = \frac{\int_{-\infty}^{\infty\infty} y\, f\,(x,y)dy}{\int_{-\infty}^{\infty\infty} f\,(x,y)dy'} \qquad (4.6)$$

Where, $\boldsymbol{y}$ =the output of the predictor, x = the input vector of the predictor, $E\left(\frac{y}{x}\right)$ = the predicted value of output, $\boldsymbol{x}$ = the input vector, $f(x,y)$ =the joint probability density function of x and y.

In the present research, the $GRNN$ architecture of exhaust PNC was present in (Fig. 4.4)

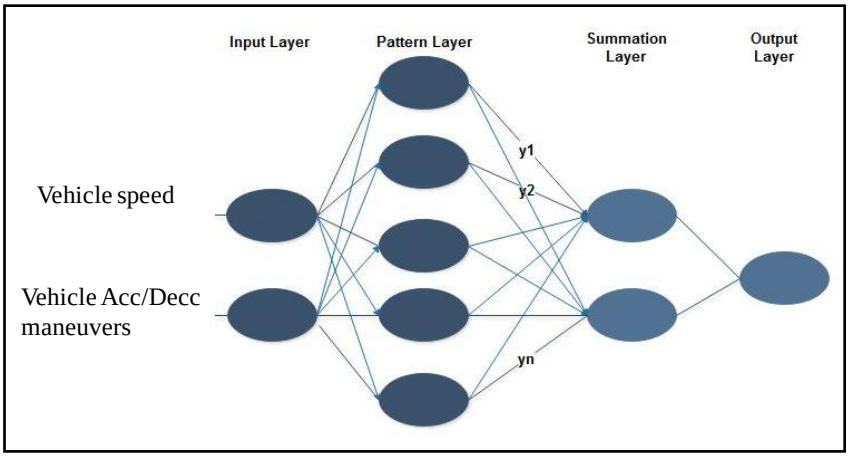

Figure 4. 4: Architecture of General Regression Neural Network (GRNN)

4.1.3. Performance Indicators

The comparison between $GRNN$ and MLP networks can be performed by specifying an objective function, which tends to minimize the total error between the measured (target) and predicted (calculated) $PNCs$ values, such as, coefficient of determination (R^2), root-mean-square error ($RMSE$) and mean absolute percentage error ($MAPE$) (Eqs. 4.4-4.6). The aforementioned parameters are applied measure of the gaps between measured $PNCs$ by the Grimm and the predicted values by models. If a good model is predicted whenever $R^2$is close to 1, and RMSE and MAPE are minimal.

The selected performance indicators are:

$$R^2 = 1 - \left(\frac{\sum_{i=1}^{n}(Target_{\,i} - Output_{\,i})^2}{\sum_{i=1}^{n} Target_{\,i}^{\,2}}\right) \quad (4.7)$$

$$RMSE = \sqrt{\frac{1}{n}\sum_{i}^{n}(Target_i - Output_i)^2} \quad (4.8)$$

$$MAPE = \frac{1}{n}\sum_{t=1}^{n}\left|\frac{(Target_{\,i} - Output_{\,i}}{Target_{\,i}}\right| \quad (4.9)$$

n = samples size, Target = measured$PNCs$ and *Output*= predicted value by $GRNN$ or MLP model.

4. 1.4. Results and discussion

4. 1.4.1. ANN Architecture

The standard $ANNs$ model architecture is constituted by output layer, one/more hidden layers and input layer passing from right to left (Khoshnevisan et al. 2014). In the present research, two-different architectures have been considered ($GRNN$ and MLP).$GRNN$ model was based on two-input variables including vehicle speed and vehicle acceleration/deceleration maneuvers, one hidden layer, a spread value equal to 0.7 and a single output node (particle number concentration) $(2, 0.7, 1)$. MLP was based on the same output and inputs of $GRNN$as well as one hidden layer with three neurons. In order to ensure accurate comparison, the same hidden layer number (one hidden layer) has been chosen for the two-selected methods (MLP and $GRNN$).

4. 1.4.2. Efficiency of the predicted models

The 70 sets of sampling were dividedrandomly as follows: 49 (about 70%) for training, 11 (about 15 %) for validation and 10 (about 15 %) for testing data. The performance of the trained networks was evaluated, using several statistical parameters which are; $RMSE$, R^2, and $MAPE$. These parameters and coefficients are estimated using MATLAB® packageTable 4.1.

Table 4. 1: The performances of each model

Models	$\boldsymbol{RMSE}$ **(**$\boldsymbol{p/cm^3}$**)**	$\boldsymbol{R^2}$	$\boldsymbol{MAPE}$ **(%)**
MLP	4.8×10^4	0.80	20.4
$GRNN$	3.9×10^3	0.98	1.08

The measured and predicted exhaust $PNCs$ by $GRNN$ and MLP models are shown in Figure 4.5. Comparison results demonstrated that MLP model exhibits lower accuracy than $GRNN$ model as found by (Chen et al., 2018; Abdullah et al., 2019). This can also be clearly observed.

Testing and training results revealed that ANN techniques performance is considered to be higher than that associated to regression models. The $GRNN$ method was created to have the finest method for forecasting particle number exhaust emissions in urban road traffic. This result is coherent with other pertinent literature. Comparison results of $GRNN$ with several other $ANNs$ models showed that $GRNN$ model provides accurate and efficient results (Antanasijevi´c et al., 2015). $MLPs$ are among the best $ANNs$, which reveals a noticeable performance, since the selected model could be specified by iterant settings calibration after adaptation in the model(Safari et al., 2016).

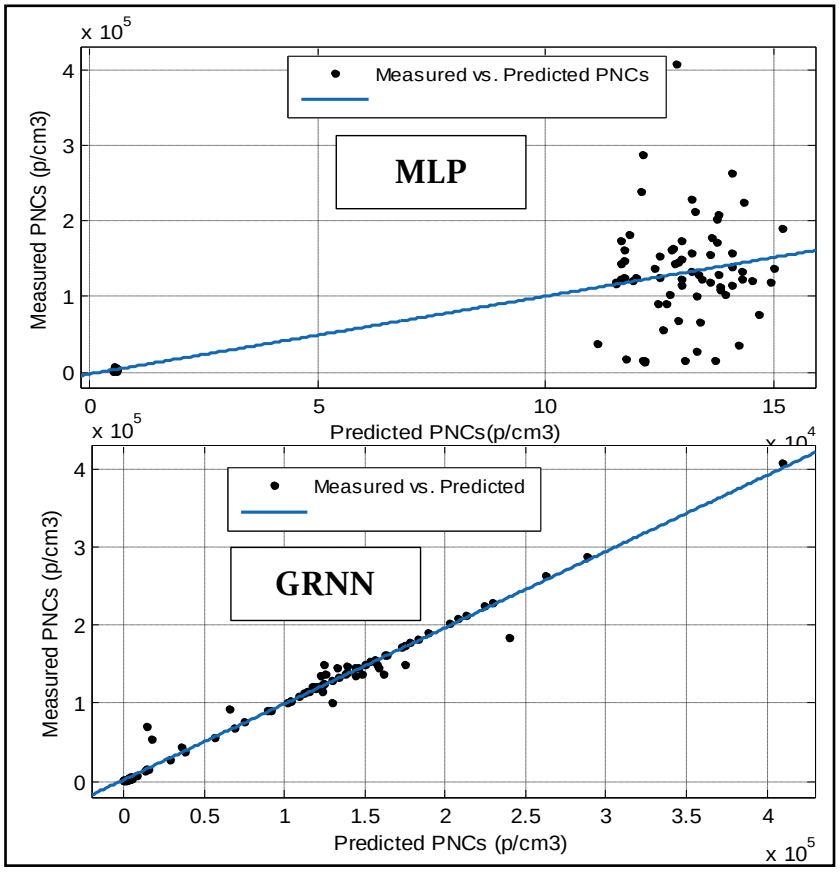

Figure 4. 5: Comparison between predicted PNCs by MLP and GRNN models

The issue of overtraining is frequently reliable, because a wide number of biases and weights is induced from many iterations. However, $GRNN$ model is a one pass learning network and does not require a repetitive strategy like MLP models.Indeed, $GRNN$ is able to solve overfitting issue to a wide margin. In conclusion, the $GRNN$ model can be preferred over the MLP model for estimating $PNCs$ induced from urban road exhaust emissions.

Section 2: Modeling of particle non-exhaust emissions based on real-time measurements

4. 2.1. Experimental protocol

4. 2.1.1. Study area and data

Measurements took place during July 2019 in urban area in the vicinity of Lyon (France) (Fig. 4.6). Lyon is France's second largest conurbation and third largest city; it is located in central eastern of France between Paris and Marseille, in the Auvergne-Rhône-Alpes Region.

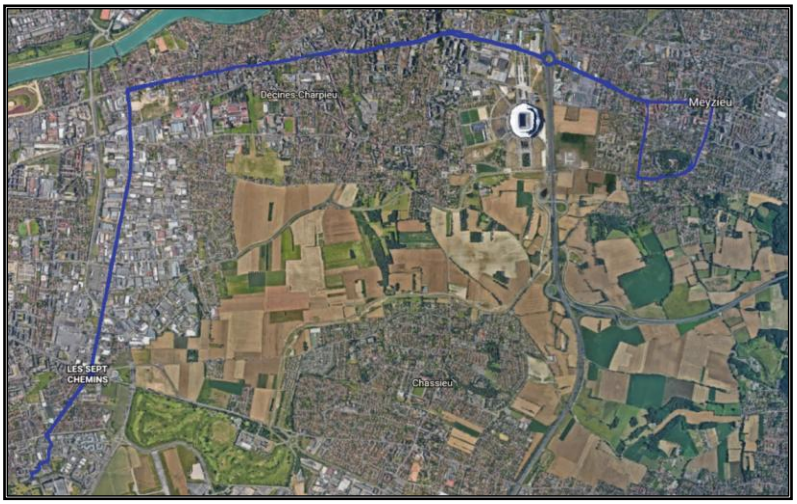

Figure 4. 6: Field area (non-exhaust)

The total mileage traveled for the present sampling day measurement was approximately $64\ km$. More details have been shown on sampling measurements, materials and methodology in chapter 3/section 2.

4. 2.1.2. Methodology

This study started by gathering the $PNCs$ of non-exhaust emissions (resuspension, tire, road surface and brake wear) and instantaneous vehicle speed under continuous real-time measurements using the $GRIMM$ series 1.108 Aerosol Spectrometer and GPS ($747\ Pro$), respectively. After that, the data has been filtered and analyzed, then synchronized to obtain a step of time $1\ min$ for both vehicle speed and non-exhaust particle number concentrations.

Subsequently, $ANNs$ model (General Regression Neural Networks ($GRNN$)) and Multiple Linear Regression (MLR) have been chosen to predict particle number concentration from real-time non-exhaust emissions in urban French area. In fact, the same input variables (vehicle speed and positive/negative vehicle acceleration maneuvers) have been selected for both MLR and $GRNN$. $PNCs$ measured by the $GRIMM$ have been considered as the target for MLR and $GRNN$ models. Finally, this study tends to compare $GRIMM$ output and $ANNs$ output. Then, the test was ended when the error reached its minimum. The flow chart methodology that was followed to model the continuous vehicle non-exhaust $PNCs$ based on real experimental data is summarized in Figure 4.7.

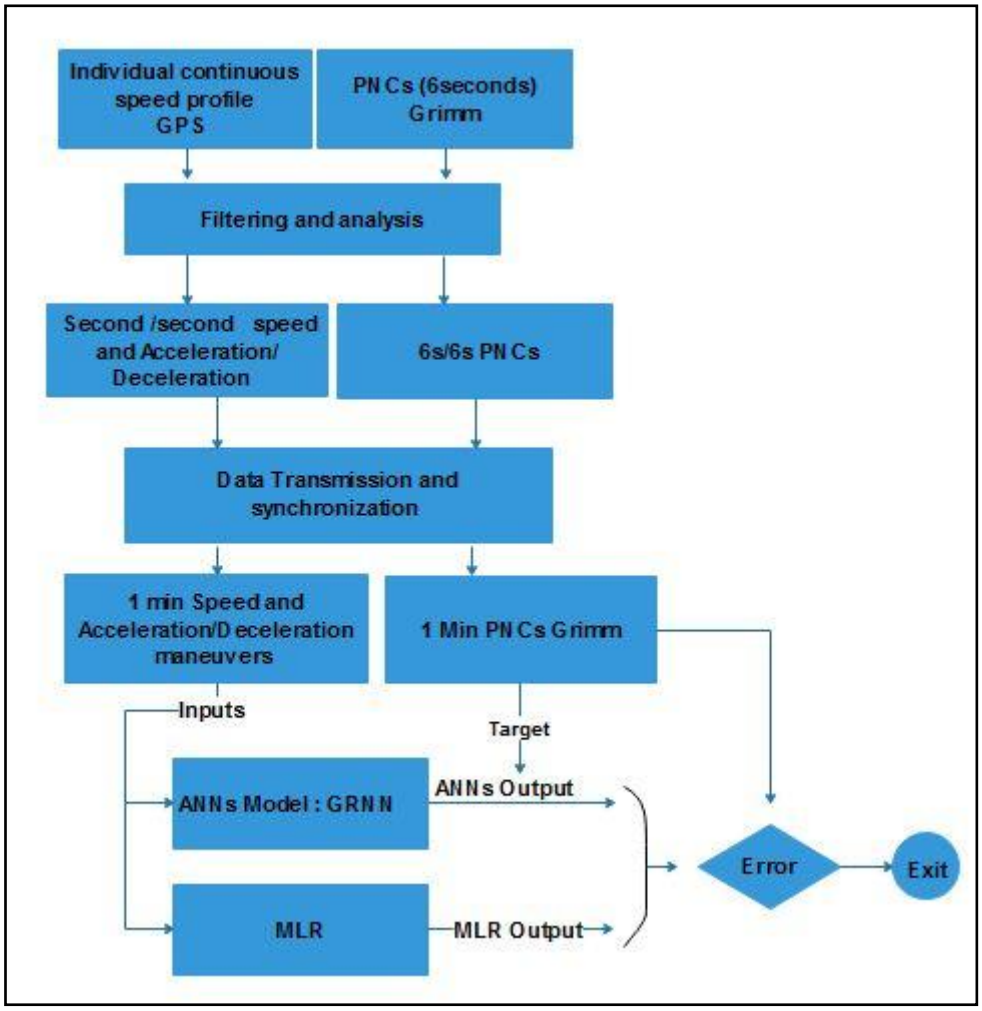

Figure 4. 7: Flow chart Methodology for non-exhaust PNCs

4. 2. 2. Multiple Linear Regression (MLR)

The regression analysis is the most commonly applied for predicting. The objective is to estimate a mathematical model that can be applied to predict the dependent variable based on the input variables (independent variables). The coefficient of correlation (R^2) is an indication to determine whether the information provides appropriate proof to demonstrate that the general models participate to the overall variance in data (Abdullah et al., 2016b).

The error indicated by $\varepsilon$is through to be frequently distributed with the mean 0 and changeσ^2 (constant). Uniformly, $\varepsilon$is through to be uncorrelated. In this study, it was agreed that MLR model has$k$independent variables and that there are "n " observations (Juneng et al., 2011). The regression model can be observed as:

$$Y_i = \beta_0 + \beta_1 x_{1i} + \cdots + \beta_k x_{ki} + \varepsilon_i \text{With, i= 1,…, n.} \quad (4.10)$$

Where, β_i = the model parameters to be predicted, x_i =the independent variables and ε= the stochastic error associated with the regression.

4. 2.3. Performance Indicators

- Multiple Linear Regression (MLR)

The major limit of the linear model is the multicollinearity between the independent variables. The main criterion for determining the validity of the results is the statistics parameter of R^2. However, R^2 rate is affected by the Perth data. Therefore, it is important to integrate other statistical parameters (Legates and McCabe, 1999). This is because, in the present research, we have added the $RMSE$, MSE and The Mean Absolute Deviation (MAD) for more accuracy in modeling (Ahmat et al., 2015).

$$MSE = \frac{1}{n}\sum_{i=1}^{n}(Target_i - output_i)^2 \quad (4.11)$$

$$MAD = \frac{\sum|Target_i - output_i)|}{n} \quad (4.12)$$

- General Regression Neural Networks – GRNN

The $GRNN$ has been also chosen to estimate the non-exhaust PNC emissions as in section 1 (estimating exhaust emissions). The same input variables were selected in the section of predicting exhaust emissions, which are vehicle speed and vehicle acceleration /deceleration maneuvers. More details have been shown in section 1.

4. 2.4. Results and discussion

- **Descriptive statistics**

The descriptive statistics showing the temporal variation of non-exhaust particle number concentration, which are less and more than 1 μmTable 5.2.

Table 4. 2: Descriptive statistics

Models	R^2	$RMSE$	MSE	MAD
$MLR1\_PNCs < 1$	0.689	11128.5	3.6×10^3	15.14
$GRNN1\_PNCs < 1$	0.969	751	3.6×10^2	0.425
$MLR2\_PNCs > 1$	0.701	1159.28	2.3×10^3	6.98
$GRNN2\_PNCs > 1$	0.978	19.13	5.08	0.02

- Multiple Linear Regression Model-*MLR*

The *MLR* models were designed and the models ' summary is represented in Table 5.2.*MLR* model is employed in this research to forecast the non-exhaust *PNCs*. The model has been commonly employed in many researchers (Goyal et al., 2006; Fernandez et al., 2012; Abdullah et al., 2019). The considered independent variables are vehicle speed and vehicle acceleration/deceleration maneuvers. The training results of *MLR* model in forecasting the non-exhaust *PNCs*minor and more than 1in urban French area are presented in Equations 4.13 and 4.14 and in Figure 4.8.

$$PNCs_{<1} = 238.26x_1 + 106.74\,x_2 + 6103.88 \quad (4.13)$$

$$PNCs_{>1} = 6.24x_1 + 4.74\,x_2 + 156.54 \quad (4.14)$$

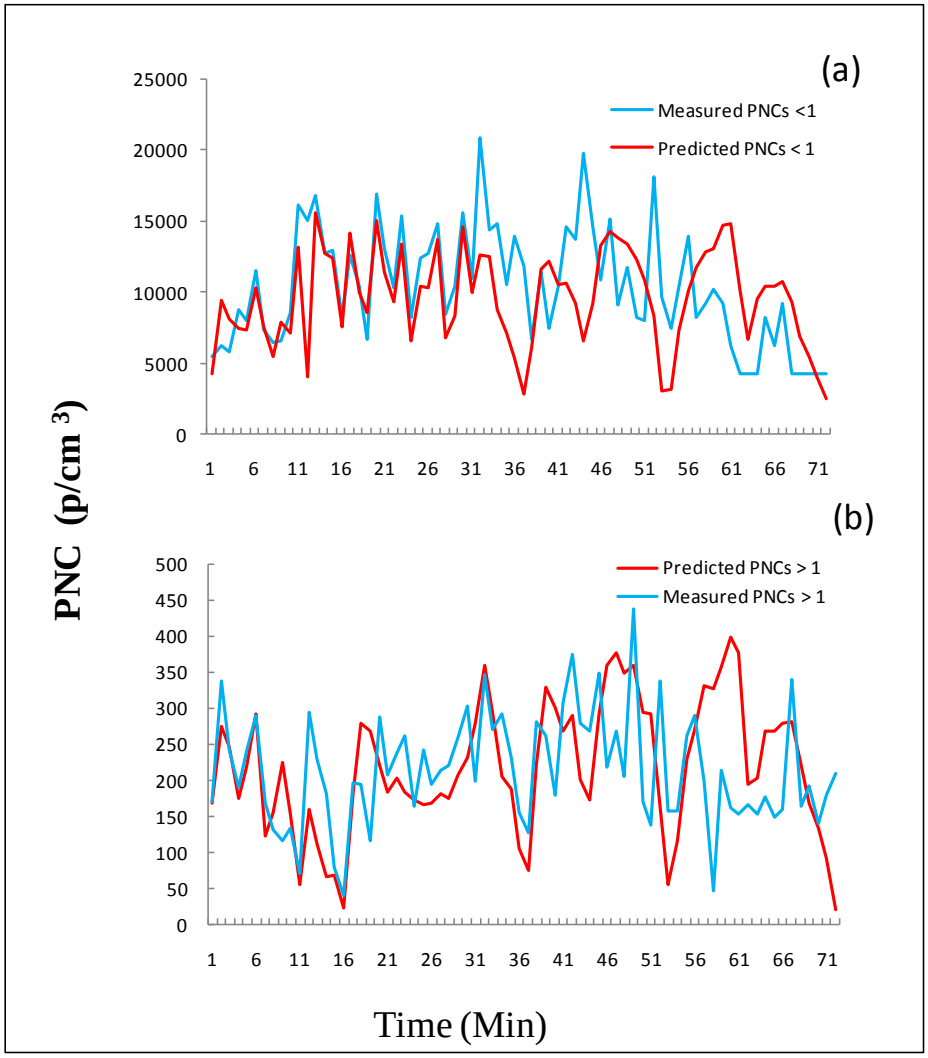

Figure 4. 8: Simulated and measured non-exhaust PNCs (p/cm3) using MLR model

Figure 4.8 illustrates the results of the testing phase of MLR for both less and more than $1\mu m$. For non-exhaust $PNCs$ less than one, the results are as follows; $R^2 = 0.68$, $RMSE = 128.5$, $MSE = 3.6 \times 10^3$ and $MAD = 15.14$. This model is less efficient than the $GRNN$ model. Many assumptions should be taken into account to apply the MLR. This makes it very complicated to use. MLR is not applied since these assumptions tend to engender sophisticated statistical calculations (Fig.4.8a). Consequently, it decreases the accuracy of the presented model. Similarly, for non-exhaust $PNCs$ more than one, the model is less efficient than the $GRNN$ model (Fig. 4.8b).

- General Regression Neural Networks – $GRNN$

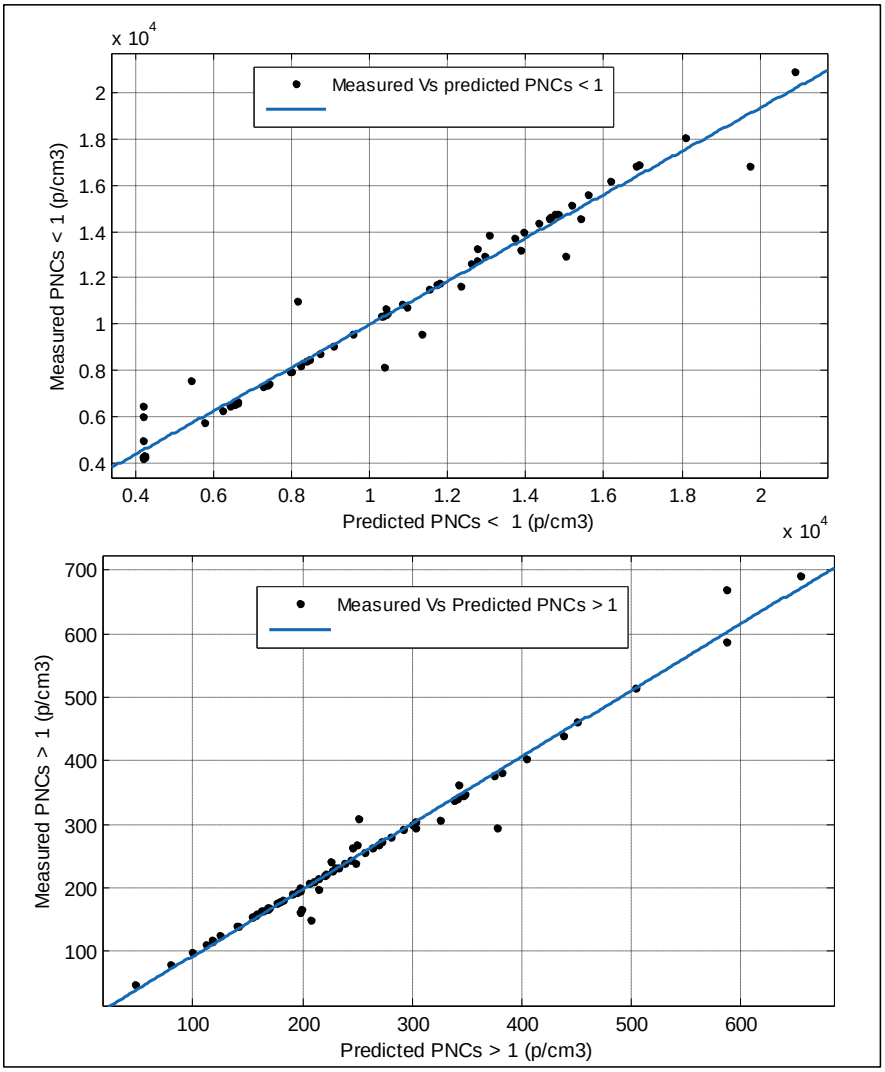

Figure 4. 9: Simulated and measured non-exhaust PNCs ($\boldsymbol{p/cm^3}$) using GRNN model

Testing and training results revealed that ANN techniques performed more efficient to the MLR model. The $GRNN$ method was produced to have the finest tool for forecasting particle number non-exhaust emissions in urban French road traffic area. This result is coherent with other pertinent literature. High similarity between measured $PNCs$ (for both less and more than $1\mu m$) by $GRIMM$ analyzer and $PNCs$ predicted by $GRNN$ (Fig. 4.9). Comparison results of $GRNN$ with several other $ANNs$ models showed that $GRNN$ model provides accurate and efficient results (Antanasijevi´c et al., 2015; Zhang et al., 2020).

4.3. Conclusion

In the first section of this chapter, $ANNs$ (MLP and $GRNN$) are applied to predict vehicle exhaust $PNCs$ from French urban road traffic based on real-time measurements. The performance of observation models was evaluated and compared by statistical indexes, namely $RMSE$, $MAPE$ and R^2. The performance of the $GRNN$ model is quite higher compared to that of MLP model. Furthermore, results proved that $GRNNs$ characterized by significant potential to predict the exhaust $PNCs$from urban road traffic. Furthermore, forecasting the non-exhaust $PNCs$ could increase and improve the public health. In section 2, $GRNN$ and MLRmodels were applied to forecast the non-exhaust $PNCs$ in French urban road traffic based on real-time measurement by $GRIMM$ analyzer. The overall results suggested that the $GRNN$ models have higher accuracy and efficiency than MLP and MLR models in predicting non-exhaust $PNCs$ in French urban road traffic. The analysis of $GRNN$, MLR and MLP models justified that vehicle speed and vehicle acceleration/deceleration maneuvers have an important impact on $PNCs$.This is because the statistical models need more attention, since they are powerful tools to evaluate the particle exhaust emissions engendered from urban road traffic giving new insights into consideration of vehicle technologies' conception and ensure a sustainable mobility and environment.

Conclusions and Recommendations for Further Research

• Conclusions

This dissertation introduces the measurements of continuous $PNCs$ and $NEPs$ under real traffic conditions and the ambient nanoparticles in urban area. The conclusions of this research can be divided into three categories:

- The influence of urban road traffic on nanoparticles: Roadside measurements

This study assesses the continuous ambient $PNCs$ in urban road traffic, taken into account several parameters, which are traffic volume, wind speed and direction, height above the road surface and distance from the source. The results substantiate that:

- The ambient $PNCs$ are inversely proportional to the distance between road traffic and sampling site.

- $PNCs$ are very high in the vicinity of the traffic zone, predominantly during rush hour since the sampling site connects the city center with a business activity area.

- PNC increases significantly with an increase in height of less than $2.82\ m$ above the ground. With heights $2.03\ m$ and $2.82\ m$ above the ground, the urban study area is characterized by high nanoparticle number with channel size diameters in nucleation mode ($10.75\ nm$).

-The average PND values revealed typical bimodal distributions for each wind speed and direction, with a strong nucleation mode peak at $\sim 10.75\ nm$ and an Aitken mode peak between 22.07 and $52.33\ nm$.

- Continuous real-world measurements of exhaust and non-exhaust vehicle emissions over different traffic areas

This study measures and analysis the continuous real-world measurements of exhaust and non-exhaust emissions in different road traffic areas. The results reveal that:

- Similar pattern (exponential trends) in particle number concentrations over the four road types for both particle diameters both smaller and greater than 1 μm.

- The highest average exhaust $PNCs$ were recorded on the motorway, at 6.7×10^6, where the highest value was found at $0.35 \mu m$.

- The particle counts exceeded WHO's permissible limit for both $PM2.5$ and $PM10$, i.e. at 25 $\mu g/m^3$ and 50 $\mu g/m^3$.

- Particle mass is heavily influenced by stop-and-go traffic

- The NEP concentrations in motorway are higher as compare to particles induced in rural and urban areas, due to high speed, pavement materials and abrupt vehicle acceleration and deceleration maneuvers.

-The NEP concentrations were characterized by a bimodal distribution at coarse modes with 0.35 and 1.3 m ranges respectively within the three selected measurement days.

- Vehicle speed, sharp positive and negative acceleration maneuvers have a pronounced effect on NEP concentrations.

- A linear relationship was found between PM ($PM2.5$, $PM10$ and $PM2.5/PM10$) ratio and the driving speed with high coefficient of determination R^2.

-TheNEP concentrations can vary with driving style and traffic conditions.

- **Recommendations for Further Research**

The following areas should be taken into account to extend the present research work on vehicle exhaust and non-exhaust emissions.

- Future research should include the physicochemical analysis in order to distinguish between each source of NEP (resuspension, brake, tire and road surface wear).

- Focusing on roadside and board devices able to warning drivers and identifying situations prone to NEP emissions to adjust their speed.

- Focusing more on the technological aspects of vehicles systems for both exhaust and non-exhaust vehicles including

- Development of sensors allowing sensing nanoparticles with size diameter $<23\ nm$ that are emitted from braking system before their dispersion in atmosphere;
- Implementation of ultrafine particle aspirator for the brakes;
- Identification of the chemical composition of particles induced from friction between pad and brake disc;
- Integration of a particle filter with a size diameter $<7\ nm$ since exhaust particles are very ultrafine.

In addition to technological vehicles, it is worthy to implement severe regulations with very expensive penalties. Moreover, it is important to put in place an efficient traffic management system like prohibit polluting vehicles from entering to the city center.

- investigating in a sustainable road with optimum pavement materials and reducing the intervention works of rehabilitation and maintenance or applied in an optimum period. Moreover, it is worthy to ensure an efficient drainage system in order to avoid the long-time exposure of pedestrians and cyclists to nanoparticles especially in the developing countries. In the same direction, the impact of nanoparticles on geochemical cycle is one of the environment challenging issue that may require more attention by researchers. In fact, the interaction of these nanoparticles when diffused with the soil and its geochemical interaction with the soil matrix as a receptor will constitute a future research axis on which we aim to investigate experimentally with electrochemical techniques for nanoparticles detection and theoretically with the derivation of the chemical reactions series that may take place.

References

Abdullah S, Ismail M, Ahmed A N, Abdullah A M., 2019. Forecasting particulate matter concentration using linear and non-linear approaches for air quality decision support. Atmosphere 10(11), 667.

Abdullah, S., Ismail, M., Fong, S.Y., Ahmed, A.N., 2016a. Neural network fitting using Lavenberq Marquardtalgorithm for PM10 concentration forecasting in Kuala Terengganu. J. Telecommun. Electron. Comput. Eng. 8, 27–31.

Abdullah, S., Ismail, M., Fong, S.Y., Ahmed, A.N., 2016b. Evaluation for long term PM10 forecasting using multilinear regression (MLR) and principal component regression (PCR) models. Environ. Asia. 9, 101–110.

Ahmat, H.,Yahaya, A.S., Ramli, N.A., 2015. The Malaysia PM10 analysis using extreme value. J. Eng. Sci. Technol.10, 1560–1574.

Agudelo-Castañeda, D.M., & Teixeira, E.C., 2014. Seasonal changes, identification and source apportionment of PAH in PM 1.0. Atmos. Envionm, *96*, 186–200.

Air Quality Expert Group (AQEG). 2019. Non-Exhaust Emissions from Road Traffic; Defra:385 London, UK.

Akyüz, M., Çabuk, H., 2009. Meteorological variations of PM2.5/PM10 concentrations and particle-associated polycyclic aromatic hydrocarbons in the atmospheric environment of Zonguldak, Turkey. Journal of Hazardous Materials 170, 13-21.

Alam, K., Blaschke, T., Madl, P., Mukhtar, A., Hussain, M., Trautmann, T., Rahman, S., 2011. Aerosol size distribution and mass concentration measurements in various cities of Pakistan. J. Environ. Monit. 13(7), 1944-1952.

Al-Dabbousa, A. N., Kumar, P., 2014. The influence of roadside vegetation barriers on air borne nanoparticles and pedestrians exposure under varying wind conditions. Atmospheric Environment 90, 113- 123.

Aldrin, M., Haff, I.H., 2005. Generalized additive modelling of air pollution, traffic volume and meteorology. Atmospheric Environment 39, 2145-2155.

Alp, M., Cigizoglu, K., 2007. Suspended sediment load simulation by two artificial neural network methods usinghydrometeorological data. Environ. Model. Softw 22, 2–13.

Amaral, S. S., De Carvalho, J. A., Costa, M. A. M., Pinheiro, C., 2015. An overview of particulate matter measurement instruments. Atmosphere 6(9), 1327-134.

Amato, F., Cassee, F.R., Van Der Gon, H.A.D., Gehrig, R., Gustafsson, M., Hafner, W., Harrison, R.M., Jozwicka, M., Kelly, F.J., Moreno, T., 2014. Urban air quality: The challenge of traffic non-exhaust emissions. J. Hazard. Mater. 275, 31–36

Andersson, J., Giechaskiel, B., Muñoz-Bueno, R., Sandbach, E., & Dilara, P. (2007). Particle Measurement Programme (PMP) Light-duty Inter-laboratory Correlation Exercise (ILCE_LD) Final Report. Luxembourg: Office for Official Publications of the European Communities; 163p. Report No. EUR 22775 EN.

Antonopoulos, V. Z., AntonopoulosA. V., 2017. Daily reference evapotranspiration estimates by artificial neural networks technique and empirical equations using limited input climate variables. Comput. Electron. Agric 132, 86–96.

Antanasijevi´c D, Pocajt V, Risti´c M, Peri´c-Gruji´c A., 2015. Modeling of energy consumption and related GHG (greenhouse gas) intensity and emissions in Europe using general regression neural networks. Energy 84, 816–824

Araujo, J.A., Barajas, B., Kleinman, M., Wang, X., Bennett, B.J., Gong, K.W., Navab, M., Harkema, J., Sioutas, C., Lusis, A.J., Nel, A.E., 2008. Ambient particulate pollutants in the ultrafine range promote early atherosclerosis and systemic oxidative stress. Circ. Res.102(5), 589-596.

Arjun, K.S., Aneesh, K., 2015. Modelling studies by application of artificial neural network using Matlab. J. Eng.Sci. Technol. 10, 1477–1486.

Arnold, F., Pirjola, L., Rankko, T., Abdul-khalek, I., Kittelson, D., Brear, F., 1999. The influence of Dilution Conditions on Diesel Exhaust Particle Size Distribution Measurements.International Congress and Exposition Detroit, Michigan, 1-4 March, 01-1142.

Baensch-Baltruschat, B., Kocher, B., Stock, F., Reifferscheid, G., 2020. Tyre and road wear particles (TRWP)—A review of generation, properties, emissions, human health risk, ecotoxicity, and fate in the environment. Sci. Total Environ. 733,137823.

Banerjee, T., & Christian, R. A., 2019. Effect of operating conditions and speed on nanoparticle emission from diesel and gasoline driven light duty vehicles. Atmospheric Pollution Research, 10, 1852-1865.

Barrios, C.C., Domínguez-Sáez, A., Rubio, J.R., Pujadas, M., 2012. Factors influencing the number distribution and size of the particles emitted from a modern diesel vehicle in real urban traffic. Atmospheric Environment 56, 16-25.

Bealey, W. J., McDonald, A. G., Nemitz, E., Donovan, R., Dragosits, U., Duffy, T. R., Fowler, D., 2007. Estimating the reduction of urban PM10 concentrations by trees within an environmental information system for planners. J. Environ. Manage. 85(1), 44-58.

Beji, A., Deboudt, K., Khardi, S., Muresan, B., Flament, P., Fourmentin, M., Lumière, L., 2020. Non-exhaust particle emissions under various driving conditions: Implications for sustainable mobility. Transp. Res. D Transp. Environ.81, 102290.

Belkacem, I., Khardi, S., Helali, A., Slimi, K., Serindat, S., 2020. The influence of urban road traffic on nanoparticles: Roadside measurements. Atmos. Environ. 242, 117786.

Belkacem I, Helali A, Khardi S, Chrouda A, Slimi K., 2021. Road traffic nanoparticles characteristics: sustainable environment and mobility. Geosci. Front, DOI: 10.1016/j.gsf.2021.101196.

Benedetti M, Cesarotti V, Introna V, Serranti J (2016) Energy consumption control automation using Artificial Neural Networks and adaptive algorithms: proposal of a new methodology and case study. J. Appl. Energy, 165, 60–71.

Bendu, H., Deepak, B., Murugan, S., 2016. Application of GRNN for the prediction of performance and exhaust emissions in HCCI engine using ethanol. Energy Convers. Manag. 122, 165–173

Bernstein, J.A., Alexis, N., Bacchus, H., Bernstein, I.L., Fritz, P., Horner, E., Li, N., Mason, S., Nel, A., Oullette, J., Reijula, K., Reponen, T., Seltzer, J., Smith, A., Tarlo, S.M., 2008. The health effects of non-industrial indoor air pollution. Journal of Allergy and Clinical Immunology, *121*, 585–591.

Bergmann, M., Kirchner, U., Vogt, R. Benter, T., 2009.On-road and laboratory investigation of low-PM emissions of a modern diesel particulate filter equipped diesel passenger car. Atmos. Environ. 43(11), 1908-1916.

Bischof, O., 2015. Recent developments in the measurement of low particulate emissions from mobile sources: a review of particle number legislations. Emiss. control sci. technol. 203-2212.

Bilal, M., Nichol, J. E., Nazeer, M., Shi, Y., Wang, L., Kumar, K. R., Ho, H.Ch., Mazhar, U., Bleiweiss, M.P., Qiu, Z., Khedher, K. M., Lolli, S., 2019. Characteristics of Fine Particulate Matter (PM2. 5) over Urban, Suburban, and Rural Areas of Hong Kong. Atmosphere 10 (9), 496.

Boulter PG., 2005. A review of emission factors and models for road vehicle non-exhaust particulate matter. TRL report PPR065. TRL Limited, Wokingham.

Brown, D. M., Stone, V., Findlay, P., MacNee, W., Donaldson, K., 2000. Increased inflammation and intracellular calcium caused by ultrafine carbon black is independent of transition metals or other soluble components. Occup. Environ. Med. 57, 685 –691.

Brown, D. M., Wilson, M. R., MacNee, W., Stone, V., Donaldson, K., 2001. Size-dependent pro-inflammatory effects of ultrafine polystyrene particles: a role for surface area and oxidative stress in the enhanced activity of ultra-fines. Toxicol. Appl. Pharmacol. 175, 191– 199.

Brugge, D., Durant, J.L., Rioux, C., 2007. Near-highway pollutants in motor vehicle exhaust: a review of epidemiologic evidence of cardiac and pulmonary health risks. Environ. Health. 6, 23.

Bukowiecki, N., Dommen, J., Prévôt, A. S. H., Weingartner, E., Baltensperger, U., 2003. Fine and ultrafine particles in the Zürich (Switzerland) area measured with a mobile laboratory: an assessment of the seasonal and regional variation throughout a year. Atmos. chem. phys. *3*(5), 1477-1494.

Cabaneros, S.M.S., Calautit, J.K.S., Hughes, B.R., 2017. Hybrid artificial neural networkmodels for effective prediction and mitigation of urban roadside NO2 pollution.Energy Procedia 142, 3524–3530.

Cabaneros, S.M.S., Calautit, J. K., Hughes, B. R., 2019. A review of artificial neural network models for ambient air pollution prediction. Environ. Model. Softw. *119*, 285-304.

Caulfield, B., Brazil, W., Ni Fitzgerald, K., Morton, C., 2014. Measuring the success of reducing emissions using an on-board eco-driving feedback tool. Transp. Res. D. Transp. Environ. 32, 253–262.

Carpentieri, M., Kumar, P., 2011. Ground-fixed and on-board measurements of nanoparticles in the wake of a moving vehicle. Atmos. Environ.*45*(32), 5837-5852.

Casati, R., Scheer, V., Vogt, R., Benter, T., 2007. Measurement of nucleation and soot mode particle emission from a diesel passenger car in real world and laboratory in situ dilution. Atmos. Environ.41, 2125-2135.

Cazier, F., Genevray, P., Dewaele, D., Nouali, H., Verdin, A., Ledoux, F., et al. (2016). Characterisation and seasonal variations of particles in the atmosphere of rural, urban and industrial areas: organic compounds. Journal of Environmental Sciences, *44*, 45-56.

Chalupa, D.C., Marrow, P.E., Oberdorster, G., Utell, M.J., Frampton, M.W., 2004. Ultrafine particle deposition in subjects with asthma. Environ. Health. Perspect. 112, 879-882.

Chang, M.E., Cardelino, C., 2000. Application of the Urban Airshed Model to forecastingnext-day peak ozone concentrations in Atlanta, Georgia. J. Air Waste Manag. Assoc.50 (11), 2010–2024.

Charron, A, Harrison, R.M., 2003. Primary particle formation from vehicle emissions during exhaust dilution in the roadside atmosphere. Atmos. Environ.37, 4109-4119.

Charron, A., Polo-Rehn, L., Besombes, J.L., Golly, B., Buisson, Ch., Chanut, H., 2019. Identification and quantification of particulate tracers of exhaust and non-exhaust vehicle emissions. *Atmospheric Chemistry and Physics, 19,* 5187–5207.

Chen, G., Li, S., Zhang, Y., Zhang, W., Li, D., Wei, X., He, Y., Bell, M.L., Williams, G., Marks, G.B., Jalaludin, B., Abramson, M.J., Guo, D.Y., 2017. Effects of ambient PM1 air pollution on daily emergency hospital visits in China: an epidemiological study. The Lancet Planetary Health, *1*(6), 221-229.

Chen, L., Liang, Z., Zhang, X., Shuai, S., 2017. Characterizing particulate matter emissionsfrom GDI and PFI vehicles under transient and cold start conditions. *Fuel, 189,* 131–140.

Cheng, Y.H., 2008. Comparison of the TSI Model 8520 and Grimm Series 1.108 portable aerosol instruments used to monitor particulate matter in an iron foundry. *Journalof Occupational and Environmental Hygiene, 5,* 157–168.

Che, H., Zhang, X., Li, Y., Zhou, Z., Qu, J., Hao, X., 2009. Haze trends over the capitalcities of 31 provinces in China, 1981-2005. Theor. Appl. Climatol. 97, 235-242.

Cheng, M.T., Tsai, Y.I., 2000. Characterization of visibility and atmospheric aerosols in urban, suburban, and remote areas. Sci. Total Environ. 263, 101-114.

Choi, W., Paulson, S. E., 2016. Closing the ultrafine particle number concentration budget at road-to-ambient scale: Implications for particle dynamics. Aerosol. Sci. Tech. 50(5), 448-461.

Choi, W., Winer, A. M., Paulson, S. E., 2014. Factors Controlling Pollutant Plume Length Downwind of Major Roadways in Nocturnal Surface Inversions. Atmospheric Chemistry and Physics14, 6925–6940.

Chuang, M.T., Zhang, Y., Kang, D., 2011. Application of WRF/Chem-MADRID for real time

air quality forecasting over the South eastern United States. Atmos. Environ. 45 (34), 6241–6250.

Carnevale, C., Finzi, G., Pederzoli, A., Turini, E., 2016. Volta, M. Lazy learning-based surrogate models for air quality planning. Env. Model. Softw. 83, 47–57.

Cazier, F., Genevray, P., Dewaele, D., Nouali, H., Verdin, A., Ledoux, F., et al. (2016). Characterisation and seasonal variations of particles in the atmosphere of rural, urban and industrial areas: organic compounds. *Journal of Environmental Sciences, 44*, 45-56.

Charron, A., Polo-Rehn, L., Besombes, J.L., Golly, B., Buisson, Ch., Chanut, H., 2019. Identification and quantification of particulate tracers of exhaust and non-exhaust vehicle emissions. *Atmospheric Chemistry and Physics, 19,* 5187–5207.

Chen, G., Li, S., Zhang, Y., Zhang, W., Li, D., Wei, X., He, Y., Bell, M.L., Williams, G., Marks, G.B., Jalaludin, B., Abramson, M.J., Guo, D.Y., 2017. Effects of ambient PM1 air pollution on daily emergency hospital visits in China: an epidemiological study. *The Lancet Planetary Health, 1*(6), 221-229.

Chen, L., Liang, Z., Zhang, X., Shuai, S., 2017. Characterizing particulate matter emissionsfrom GDI and PFI vehicles under transient and cold start conditions. *Fuel, 189,* 131–140.

Chen Z, Ye X, Huang P., 2018. Estimating carbon dioxide (CO2) emissions from reservoirs using artificial neural networks. Water 10(1), 26.

Cheng, Y.H., 2008. Comparison of the TSI Model 8520 and Grimm Series 1.108 portable aerosol instruments used to monitor particulate matter in an iron foundry. Journal of Occupational and Environmental Hygiene, *5*, 157–168.

Condurat, M., Nicuţă, A. M., Andrei, R., 2017. Environmental impact of road transport traffic. A case study for county of Iaşi road network. Procedia. Eng. 181, 123-130.

Condurat, M., Patterson, J., 2016. Welsh and Romanian policies for transition towards low carbon mobility. Cardiff, UK, February 2016. Proceedings of the international conference 'Smart energy Regions'. pp. 59-70, ISBN: 978-1-899895-32-6.

Colls, J., 2001. second ed. Air Pollution, vol 29 Spon Press, West 35th Street, New York,NY 10001.

Coudray, N., Dieterlen, A., Roth, E., Trouvé, G., 2009. Density measurement of fine aerosol fractions from wood combustion sources using ELPI distributions and image processing techniques. Fuel 88, 947–954.

Costa, M.A.M., Carvalho, J.A., Neto, T.G.S., Anselmo, E., Lima, B.A., Kura, L.T.U., Santos, J.C., 2012. Real-time sampling of particulate matter smaller than 2.5 μm from Amazon Forest biomass combustion. Atmos. Environ. 54, 480–489.

Committee on the Medical Effects of Air Pollutants (COMEAP). Statement on the Evidence for Health Effects Associated with Exposure to Non-Exhaust Particulate Matter from Road Transport; Committee on the Medical Effects of Air Pollutants: Chilton, UK, 2020. Eionet.

Dahl, A., Gharibi, A., Swietlicki, E., Gudmundsson, A., Bohgard, M., Ljungman, A., Blomqvist, G., Gustafsson, M., 2006. Traffic-generated emissions of ultrafine particles from pavement–tire interface. Atmos. Environ. 40, 1314–1323.

Dall'Osto, M., Beddows, D.C.S., Pey, J., Rodriguez, S., Alastuey, A., Harrison, R.M., Querol, X., 2012. Urban aerosol size distributions over the Mediterranean city of Barcelona,NE Spain. Atmospheric Chemistry and Physics 12, 10693–10707.

Delfino, R. J., Sioutas, C., Malik, S., 2005. Potential role of ultrafine particles in associations between airborne particle mass and cardiovascular health. Environ. Health. Perspect.113(8), 934-946.

DELPHI. 2017. Worldwide Emissions Standards—passenger cars and light duty vehicles—2017-2018. Available at: http://www.delphi.com/about/emissions_standards.

Deshmukh, D.K., Deb, M.K., Mkoma, S.L., 2013. Size distribution and seasonal variation of size-segregated particulate matter in the ambient air of Raipur city, India. Air. Qual. Atmos. Health. 6, 259–276.

Dominici, F., Greenstone, M., Sunstein, C.R., 2014. Particulate matter matters. Science, *344*, 257–259.

Donaldson, K., Tran, C. L., 2002. Inflammation caused by particles and fibers. Inhal. Toxicol. 14, 5–27.

Donaldson, K., Stone, V., Gilmour, P. S., Brown, D. M., MacNee, W., 2000. Ultrafine particles: mechanisms of lung injury. Philos. Trans. R. Soc. A. 358, 2741–2749.

Donaldson, K., Tran, L., Albert Jimenez, L.A., Duffin, R., Newby, D.E., Mills, N., MacNee, W., Stone, V., 2005. Combustion-derived nanoparticles: a review of their toxicology following inhalation exposure. Part. Fibre. Toxicol. 5-6, 553-560.

Donaldson, K., Stone, V., 2007.Toxicological properties of nanoparticles and nanotubes. Issues in environmental science and technology. Nanotechnology 24, 81–96.

Durbin, T., Johnson, K., Cocker, D., Miller, J., Maldonado, H., Shah, A., Ensfield, C., Weaver, C., Akard, M., Harvey, N., Symon, J., Lanni, T., Bachalo, W., Payne, G., Smallwood, G., Linke, M., 2007. Evaluation and comparison of portable emissions measurement systems and federal reference methods for emissions from a back-up generator and a diesel truck operated on a chassis dynamometer. Environ. Sci. Technol. 41, 6199–6204.

Duffin, R., Tran, C. L., Clouter, A., Brown, D., MacNee, W., Stone, V., Donaldson, K., 2002. The importance of surface area and specific reactivity in the acute pulmonary inflammatory response to particles. Ann. Occup. Hyg. 46, 242–245.

Easter, R.C., Peters, L.K., 1994. Binary homogeneous nucleation: temperature and relative humidity fluctuations, nonlinearity, and aspects of new particle production in the atmosphere. J. Appl. Meteorol. Clim. 33 (7), 775–784.

Edwards, R., Smith, K. R., Kirby, B., Allen, T., Litton, C. D., Hering, S., 2006. An inexpensive dual-chamber particle monitor: laboratory characterizationJ. Air. Waste. Manag. Assoc. 56 (6), 789-799.

Elsässer, M., Crippa, M., Orasche, J., Decarlo, P.F., Oster, M., Pitz, M., Cyrys, J., Gustafson, T.L., Pettersson, J.B.C., Zimmermann, R., 2012. Organic molecular markers and signature from wood combustion particles in winter ambient aerosols : Aerosol mass spectrometer (AMS) and high time-resolved GC-MS measurements in Augsburg, Germany. Atmos. Chem. Phys. 6113–6128.

European Environment Agency. 2019. Air quality in Europe - report 10 – 75. Available at: https://www.eea.europa.eu/publications/air-quality-in-europe-2019.

European Environment Agency. 2015. The European environment — state and outlook 2015 [WWW Document]. European Environment Agency. URL https://www.eea.europa.eu/soer. (Accessed 5.14.19).

E.U., 2008. Commission Regulation (EC) No 692/2008. Official Journal of the European Union 136.

European Environment Agency (EEA)., 2014. Air Quality in Europe-2014.Copenhagen: EEA Report No, 5 /2014. EMEP/EEA (2013). Air Pollutant Emission Inventory Guidebook. Copenhagen: European Monitoring and Evaluation Programme/European Environment Agency, 2013.

European Environment Agency (EEA)., 2018. Air quality in Europe - 2018 report.

Environmental Protection Agency, 2017. Particulate Matter (PM) Pollution: Health andEnvironmental Effects of Particulate Matter (PM) Health Effects.

European Environment Agency, 2015. The European environment — state and outlook 2019[WWW Document].

Feng, XL., Shao, LY., Xi, CX., Jones, TP., Zhang, DZ., BéruBé, KA., 2020, Particle-induced oxidative damage by indoor size-segregated particulate matter from coal-burning homes in the Xuanwei lung cancer epidemic area, Yunnan Province, China. Chemosphere 256,127058.

Feng, X., Li, Q., Zhu, Y., Hou, J., Jin, L., Wang, J., 2015. Artificial neural networks forecasting of PM2.5 pollution using air mass trajectory based geographic model and wavelet transformation. Atmos. Environ. 107, 118–128.

Fernandez, F.G., Palacios, P., Esteban, L.G., Garcia-Iruela, A., Rodrigo, B.G., Menasalvas, E., 2012. Prediction of MOR and MOE of structural plywood board using an artificial neural network and comparison with a multivariate regression model. Compos. Part B Eng. 43, 3528-3533.

Filonchyk, M., Yan, H., Yang, S., Hurynovich, V., 2016. A study of PM 2.5 and PM 10 concentrations in the atmosphere of large cities in Gansu Province, China, in summer period. J. Earth. Syst. Sci. 125(6), 1175-1187.

Fletcher, D., Goss, E., 1993. Forecasting with neural networks: An application using bankruptcy data. Inf. Manag. 24, 159–167.

Foitzik, M. J., Unrau, H. J., Gauterin, F., Dörnhöfer, J., Koch, T., 2018. Investigation ofultrafine particulate matter emission of rubber tires. Wear 394-395, 87-95.

Furger, M., Rai, P., Slowik, J.G., Cao, J., Visser, S., Baltensperger, U., Prévôt, A.S., 2020.Automated alternating sampling of PM10 and PM2.5 with an online XRF spectrometer.Atmos. Environ. 5, 100065.

Garg, B.D., Cadle, S.H., Mulawa, P.A., Groblicki, P.J., 2000. Brake wear particulate matter emissions. Environ. Sci. Technol. 34, 4463-4469.

Gass, S.I., 1983. Feature article-decision-aiding models: validation, assessment, and related issues for policy analysis.

Geller, M. D., Sardar, S. B., Phuleria, H., Fine, P. M., Sioutas, C., 2005. Measurements of particle number and mass concentrations and size distributions in a tunnel environment. Environ. Sci. Technol. *39*(22), 8653-8663.

Giechaskiel, B., 2018. Real Driving Emissions (RDE) Particle Number (PN) Portable Measurement Systems (PEMS) Calibration. Publications Office of the European Union.

Giechaskiel, B., Bonnel, P., Perujo, A., Dilara, P., 2019a. Solid particle number (SPN) portable emissions measurement systems (PEMS) in the European legislation: Review. Int. J. Environ. Res. Public. Health. 16, 4819.

Giechaskiel, B., Lahde, T., Suarez-Bertoa, R., Clairotte, M., Grigoratos, T., Zardini, A., Perujo, A., Martini, G., 2018. Particle number measurements in the European legislation and future JRC activities. Combustion engines 174 (3), 3-16.

Giechaskiel, B., Mamakos, A., Andersson, J., Dilara, P., Martini, G., Schindler, W., Bergmann, A., 2012. Measurement of automotive nonvolatile particle number emissions within the European legislative framework: a review. Aerosol. Sci. Tech.46, 719-749.

Giechaskiel, B., Maricq, M., Ntziachristos, L., Dardiotis, C., Wang, X., Axmann, H., Bergmann, A., Schindler, W., 2014a. Review of motor vehicle particulate emissions sampling and measurement: from smoke and filter mass to particle number. J. Aerosol. Sci.67, 48-86.

Giechaskiel, B., Manfredi, U., Martini, G., 2014b. Engine exhaust solid sub-23 nm particles. I. literature survey. SAE. Int. J. Fuels. Lubr. 7, 950-964.

Giechaskiel, B., Maricq, M., Ntziachristos, L., Dardiotis, C., Wang, X., Axmann, H., Bergmann, A., Schindler, W., 2014c. Review of motor vehicle particulate emissions sampling and measurement: From smoke and filter mass to particle number. J. Aerosol. Sci.67, 48–86.

Giechaskiel, B., Riccobono, F., Vlachos, T., Mendoza-Villafuerte, P., Suarez-Bertoa, R., Fontaras, G., Bonnel, P., Weiss, M., 2015. Vehicle Emission Factors of Solid Nanoparticles in the Laboratory and on the Road Using Portable Emission Measurement Systems (PEMS). Front. Environ. Sci. 3, 82.

Giechaskiel, B., Munoz-Bueno, R., Rubino, L., Manfredi, U., Dilara, P., DeSanti, G., 2007. Particle measurement programme (PMP): particle size and number emissions before, during and after regeneration events of a euro 4 DPF equipped light-duty diesel vehicle. SAE Technical Paper. 2007- 01-1944.

Giechaskiel, B., Zardini, A.A., Clairotte, M., 2019b. Exhaust gas condensation during engine cold start and application of the dry-wet correction factor. Appl. Sci.9, 2263.

Giugliano, M., Lonati, G., Butelli, P., Romele, L., Tardivo, R., Grosso, M., 2005. Fine particulate (PM2. 5–PM1) at urban sites with different traffic exposure. Atmos. Environ. 39(13), 2421-2431.

Gouriou, F., Morin, J. P., Weill, M. E., 2004. On-road measurements of particle number concentrations and size distributions in urban and tunnel environments. Atmos. Environ. 38 (18), 2831-2840.

Goel, A., Kumar, P., 2016. Vertical and horizontal variability in airborne nanoparticles and their exposure around signalized traffic intersections. Environ. Pollut. 214, 54-69.

Gomišček, B., Hauck, H., Stopper, S., Preining, O., 2004. Spatial and temporal variations of PM1, PM2.5, PM10 and particle number concentration during the AUPHEP—project. Atmos. Environ. *38*(24), 3917-3934.

Goyal, P., Chan, A.T., Jaiswal, N., 2006. Statistical models for the prediction ofrespirable suspended particulate matter in urban cities. Atmos. Environ. 40, 2068-2077.

Geller, M. D., Sardar, S. B., Phuleria, H., Fine, P. M., Sioutas, C., 2005. Measurements of particle number and mass concentrations and size distributions in a tunnel environment. *Environmental Science &Technology, 39*, 8653-8663.

Giechaskiel, B., Riccobono, F., Vlachos, T., Mendoza-Villafuerte, P., Suarez-Bertoa, R., Fontaras, G., Bonnel, P., Weiss, M., 2015. Vehicle Emission Factors of Solid Nanoparticles in the Laboratory and on the Road Using Portable Emission Measurement Systems (PEMS). Frontiers in Environmental Science, 3, 82.

Giechaskiel, B., Leonidas Ntziachristos, L., Samaras, Z., Casati, G.R., Scheer, V., Vogt, R., 2007. Effect of Speed and Speed-Transition on the Formation of Nucleation Mode Particles from a Light Duty Diesel Vehicle. SAE paper number, 2007-01-1110.

Giugliano, M., Lonati, G., Butelli, P., Romele, L., Tardivo, R., Grosso, M., 2005. Fine particulate (PM2. 5–PM1) at urban sites with different traffic exposure. Atmospheric Environment, *39*, 2421-2431.

Gramotnev, G., Ristovski, Z., 2004. Experimental investigation of ultra-fine particle size distribution near a busy road. Atmospheric Environment 38, 1767–1776.

Grigoratos, T., Gustafsson, M., Eriksson, O., Martini, G., 2018. Experimental investigation oftread wear and particle emission from tyres with different tread wear marking. Atmos.Environ. 182, 200–212.

Grigoratos, T., Martini, G., 2015. Brake wear particle emissions : A review. Environ. Sci.Pollut. Res. 22, 2491–2504.

Grigoratos, T., Martini, G., 2014. Non-Exhaust Traffic Related Emissions. Brake and TyreWear PM. 2014. Available online:https://publications.jrc.ec.europa.eu/repository/bitstream/JRC89231/jrc89231online%20final%20version%202.pdf (accessed on 5 November 2020).

Grigoratos, T., Martini, G., 2015. Brake wear particle emissions:a review. Environ. Sci.Pollut. Res. Int. 22, 2491–2504.

Grimm, H., Eatough, D.J., 2009. Aerosol Measurement: The Use of Optical Light Scattering for the Determination of Particulate Size Distribution, and Particulate Mass, Including the Semi-Volatile Fraction. Journal of the Air & Waste Management Association, *59*, 101–107.

Hand, J. L., Gill, T. E., Schichtel, B. A., 2019. Urban and rural coarse aerosol mass across the United States: Spatial and seasonal variability and long-term trends. Atmospheric Environment, *218*, 117025.

Harrison, R.M., 2020. Airborne particulate matter. Philos. Trans. R. Soc. A Math. Phys. Eng.Sci. 378, 2019031920

Harrison, R.M., Jones, A.M., Gietl, J., Yin, J., Green, D.C., 2012. Estimation of thecontributions of brake dust, tire wear, and resuspension to non-exhaust traffic particlesderived from atmospheric measurements. Environ. Sci. Technol. 46, 6523–6529.

Harris, S., Maricq, M., 2001. Signature size distributions for diesel and gasoline engine exhaust particulate matter. Journal of Aerosol Science 32, 749−764.

Harrison, R.M., Yin, J., Mark, D., Stedman, J., Appleby, R.S., Booker, J., Moorcroft, S., 2001. Studies of the coarse particle (2.5–10 μm) component in UK urban atmospheres. Atmospheric Environment 35, 3667-3679.

Harrison, RM., Dall'Osto, M., Beddows, DCS., Thorpe, AJ., Bloss, WJ., Allan, JD., Coe, H., Di Marco, CF., Smith, S., 2012b. Atmospheric chemistry and physics in the atmosphere of a developed megacity (London): An overview of the REPARTEE experiment and its conclusions. Atmos. chem. phys.12, 3065-3114.

Harrison, R. M., Jones, A. M., Beddows, D. C., Dall'Osto, M., Nikolova, I., 2016. Evaporation of traffic-generated nanoparticles during advection from source. Atmos. Environ. 125, 1-7.

Heal, M. R., Kumar, P., Harrison, R. M., 2012. Particles, Air Quality, Policy and Health. Chemical Society Reviews 41, 6606–6630.

He, M., Dhaniyala, S., 2012. Vertical and horizontal concentration distributions of ultrafine particles near a highway. Atmos. Environ. 46, 225-236.

Helland, A., Wick, P., Koehler, A., Schmid, K., Som, C., 2007. Reviewing the environmental and human health knowledge base of carbon nanotubes. Environ. Health. Perspect. 115 (8), 1125-1131, ISSN 0091-6765.

Hewitt, C. N., Ashworth, K., MacKenzie, A. R., 2020. Using green infrastructure to improve urban air quality (GI4AQ). Ambio 49(1), 62-73.

Hietikko, R., Kuuluvainen, H., Harrison, RM., Portin, H., Timonen, H., Niemi, JV., Rönkkö, T., 2018. Diurnal variation of nanocluster aerosol concentrations and emission factors in a street canyon. Atmos. Environ.189, 98-106.

Hinds, W.C., 1999. Aerosol technology: properties, behavior and measurement of Airborne particles. John Wiley & sons, U.K 483.

Hitchins, J., Morawska, L., Wolff, R., Gilbert, D., 2000. Concentrations of submicrometre particles from vehicle emissions near a major road ». Atmos. Environ. 34 (1): 51-59.

Huang, S., Taddei, P., Lawrence, J., Martins, M.A., Li, J., Koutrakis, P., 2020. Trace element mass fractions in road dust as a function of distance from road. J. Air Waste Manag. Assoc.70, 34001.

Huang R J, Zhang Y, Bozzetti C., …. ,2014. High secondary aerosol contribution to particulate pollution during haze events in China. Nature 514, 218–222.

Hujia, Z., Huizheng, C., Hiaoye, Z., Yanjun, M., Yangfeng, W., Hong, W., Yaqiang, W., 2013. Characteristics of visibility and particulate matter (PM) in an urban area of northeast China. Atmos. Pollut. Res. 4, 427-434.

Humphrey, G.B., Maier, H.R., Wu, W., Mount, N.J., Dandy, G.C., Abrahart, R.J., Dawson, C.W., 2017. Improved validation framework and R-package for artificial neural network models. Environ. Model. Softw 92, 82–106.

Hussein, T., Saleh, S. S. A., dos Santos, V. N., Abdullah, H., Boor, B. E., 2019. Black Carbon and Particulate Matter Concentrations in Eastern Mediterranean Urban Conditions: An Assessment Based on Integrated Stationary and Mobile Observations. *Atmosphere, 10,* 323.

Hussein, T., Johansson, C., Karlsson, H., Hansson, H. C., 2008. Factors affecting non-tailpipeaerosol particle emissions from paved roads: On-road measurements in Stockholm, Sweden. Atmos. Environ. *42*(4), 688-702.

Hussein, T., Karppinen, A., Kukkonen, J., Härkönen, J., Aalto, P.P., Hämeri, K., Kerminen,V.M., Kulmala, M., 2006. Meteorological dependence of size-fractionated number concentrations of urban aerosol particles. Atmos. Environ. 40, 1427–1440.

Hussein, T., Alghamdi, M. A., Khoder, M., AbdelMaksoud, A. S., Al-Jeelani, H., Goknil, M. K., Shabbaj., I.I., Almehmadi, F.M., Hyvärinen, A., Lihavainen, H., Hämeri, K., 2014. Particulate matter and number concentrations of particles larger than 0.25 μm in the urban atmosphere of Jeddah, Saudi Arabia. Aerosol. Air. Qual. Res. 14(5), 1383-1391.

Hussein, T., Saleh, S. S. A., dos Santos, V. N., Abdullah, H., Boor, B. E., 2019. Black Carbon and Particulate Matter Concentrations in Eastern Mediterranean Urban Conditions: An Assessment Based on Integrated Stationary and Mobile Observations. Atmosphere 10(6), 323.

Hossain, A.M.M., Park, S., Kim, J.S., Park, K., 2012. Volatility and mixing states of ultrafine particles from biomass burning. J. Hazard. Mater. 205, 189–197.

Hosseini, S., Li, Q., Cocker, D., Weise, D., Miller, A., Shrivastava, M., Miller, J.W., Mahalingam, S., Princevac, M., Jung, H., 2010. Particle size distributions from laboratory-scale biomass fires using fast response instruments. Atmos. chem. phys. 10, 8065–8076.

Horvath, H., 2008. Conference on visibility, aerosols, and atmospheric optics, Vienna, September 3–6, 2006. Atmos. Environ. 42 (11), 2569-2570, ISSN 1352-2310.

Ibald-Mulli, A., Wichmann, H.E., Kreyling, W., Peters, A., 2002. Epidemiological evidence on health effects of ultrafine particles. Journal of Aerosol Medicine: Deposition, Clearance, and Effects in the Lung 15 (2), 189–201, ISSN 0894-2684.

Imhof, D., Weingartner, E., Ordóñez, C., Gehrig, R., Hill, M., Buchmann, B., Baltensperger, U., 2005. Real-world emission factors of fine and ultrafine aerosol particles for different traffic situations in Switzerland. Environ. Sci. Technol. 39(21), 8341-8350.

Imhof, D., Weingartner, E., Vogt, U., Dreiseidler, A., Rosenbohm, E., Scheer, V., Vogt, R., Nielsen, O.J., Kurtenbach, R., Corsmeier, U., Kohler, M., Baltensperger, U., 2005.

Vertical distribution of aerosol particles and NOx close to a motorway. Atmos. Environ39, 5710-5721.

Institut National de la statistique et des études statistiques – Insee, 2018. Population légales 2016-Commune de Bron (69029). Available at:https://www.insee.fr/fr/statistiques/3681328?geo=COM-69029.

INRS, 2012. Mesure de concentrations dans les conduits de transport de pollutionsparticulaires. HST, ND 2363 – 228-12.

Jamson, S.L., Brouwer, R., Seewald, P., 2015. Supporting eco-driving. Transp. Res. Part C. Emerg. Technol. 58,629–630.

Janssen, N., Fischer, P., Marra, M., Ameling, C., Cassee, F.R., 2013. Short-term effects of PM2.5, PM10 and PM2.5–10 on daily mortality in the Netherlands. *Science of the Total Environment*, *463–464*, 20–26.

Jekel, M., 2019. Scientific Report on Tyre and Road Wear Particles, TRWP, in the aquatic environment**.** European TRWP Platform.

Ježek, I., Drinovec, L., Ferrero, L., Carriero, M., Moènik, G., 2015. Determination of car on-road black carbon and particle number emission factors and comparison between mobile and stationary measurements. Atmos. Meas. Tech. 8, 43–55.

Jiang, R., Bell, M.L., 2008. A Comparison of Particulate Matter from Biomass-Burning Rural and Non-Biomass-Burning Urban Households in Northeastern China. Environ. Health. Perspect. 116, 907–914.

Jiang, P., Dong, Q., Li, P., 2017. A novel hybrid strategy for PM2.5 concentration analysisand prediction. J. Environ. Manag. 196, 443–457.

Jickells, T. D., An, Z. S., Andersen, K. K., Baker, A. R., Bergametti, C., Brooks, N., Cao, J.J., Boyd, P. W., Duce, R. A., Hunter, K. A., Kawahata, H., Kubilay, N., LaRoche, J., Liss, P.S., Mahowald, N., Prospero, J. M., Ridgwell, A. J., Tegen, I., Torres, R., 2005. Global ironconnections between desert dust, ocean biogeochemistry, and climate. Science 308 (5718),67-71.

Johnson, K., Durbin, T., Jung, H., Cocker, D., Bishnu, D., Giannelli, R., 2011. Quantifying in-use PM measurements for heavy-duty diesel vehicles. Environ. Sci. Technol. 45, 6073–6079.

Jonathan, O.A., Josef, G.T., Andrew, S., 2012. Clearing the air: a review of the effects of particulate matter air pollution on human health. J. Med. Toxicol. 8 (2), 166-175.

Joodatnia, P., Kumar, P., Robins, A., 2013. The behavior of traffic produced nanoparticles in a car cabin and resulting exposure rates. Atmos. Environ. 65, 40-51.

Juneng, L., Latif, M.T., Tangang, F., 2011. Factors influencing the variations of PM10 aerosol dust in KlangValley,Malaysia during the summer. Atmos. Environ. 45, 4370–4378.

Karjalainen, P., Pirjola, L., Heikkilä, J., Lähde, T., Tzamkiozis, T., Ntziachristos, L.,Keskinen, J., Rönkkö, T., 2014. Exhaust particles of modern gasoline vehicles: A laboratory and an on-road study. Atmos. Environ. 97, 262-270.

Kangasluoma, J., Cai, R., Jiang, J., Deng, C., Stolzenburg, D., Ahonen, L. R., Chan, T., Fu, Y., Kim, C., Laurila, TM., Zhou, Y., Dada, L., Sulo, J., Flagan, RC., Kulmala, M., Petaja, T., Lehtipalo, K., 2020. Overview of measurements and current instrumentation for 1–10 nm aerosol particle number size distributions. J. Aerosol. Sci. 148, 105584.

Kettunen, J., Lanki, T., Tiittanen, P., Aalto, P.P., Koskentalo, T., Kulmala, M., Salomaa, V., Pekkanen, J., 2007. Associations of fine and ultrafine particulate air pollution with stroke mortality in an area of low air pollution levels. Stroke 38, 918–922.

Keuken, M. P., Moerman, M., Voogt, M., Zandveld, P., Verhagen, H., Stelwagen, U., 2016. Particle number concentration near road traffic in Amsterdam (the Netherlands): comparison of standard and real-world emission factors. Atmos. Environ. 132, 345-355.

Kesarkar, A.P., Biswal, A., Kesarkar, A.P., Mor, S., Ravindra, K., 2020. High resolutionvehicular PM10 emissions over megacity Delhi: Relative contributions of exhaust and non-exhaust sources. Sci. Total Environ. 699, 134273.

Keyvanfar, A., Shafaghat, A., Muhammad, N. Z., Ferwati, M. S., 2018. Driving behavior and sustainable mobility: policies and approaches revisited. Sustainability 10(4), 1152.

Khan, Y., Johnson, K., Durbin, T., Jung, H., Cocker, D., Bishnu, D., Giannelli, R., 2012.Characterization of PM–PEMS for in-use measurements conducted during validation testing for the PM–PEMS measurement allowance program. Atmos. Environ. 55, 311–318.

Khayatian F, Sarto L, Dall'O' G (2016) Application of neural networks for evaluating energy performance certificates of residential buildings. J. Energy Build, 125, 45–54 (2016).

Kheirbek, I., Haney, J., Douglas, S., Ito, K., Matte, T., 2016. The contribution of motor vehicle emissions to ambient fine particulate matter public health impacts in New York City: a health burden assessment. J. Environ. Health.15(1), 1-14.

Khoshnevisan B, Rafiee S et al (2014) Prediction of potato yield based on energy inputs using multi-layer adaptive neuro-fuzzy inference system. Elsevier MEASUREMENT.47, 521–530.

Kim, K.H., Lee, S.B., Woo, D., Bae, G.N., 2015. Influence of wind direction and speed on the transport of particle-bound PAHs in a roadway environment. Atmospheric Pollution Research 6, 1024-1034.

Kim, Y.J., Kim, K.W., Kim., S.D., Lee, B.K., Han, J.S., 2006. Fine particulate matter characteristics and its impact on visibility impairment at two urban sites in Korea: Seoul and Incheon. Atmos. Environ.40 (2), 593-605.

Kim, S.Y., Peel, J.L., Hannigan, M.P., Dutton, S.J., Sheppard, L., Clark, M.L., Vedal, S., 2012. The temporal lag structure of short-term associations of fine particulate matter chemical constituents and cardiovascular and respiratory hospitalizations. Environmental Health Perspectives, *120*, 1094–1099.

Kim, G., Lee, S., 2018. Characteristics of tire wear particles generated by a tire simulator under various driving conditions. Environ. Sci. Technol. 52 (21), 12153-12161.21.

Kingston, G.B., Lambert, M.F., Maier, H.R., 2005a. Bayesian training of artificial neuralnetworks used for water resources modeling. Water Resour. Res. 41 (12), 1–11.

Kingston, G.B., Maier, H.R., Lambert, M.F., 2005b. Calibration and validation of neuralnetworks to ensure physically plausible hydrological modeling. J. Hydrol. 314 (1–4),

158–176.

Kittelson, D.B., 1998. Engines and nano-particles: a review. J. Aerosol. Sci. 29, 575-588.

Kittelson, D. B., Watts, W. F., Johnson, J. P., 2004. Nanoparticle emissions on Minnesota highways. Atmos. Environ.38 (1), 9-19.

Kittelson, DB., Watts, WF, Johnson, JP., 2003. Nanoparticle emissions on Minnesota highway. Atmos. Environ. 38, 9-19.

Kontses, A., Triantafyllopoulos, G., Ntziachristos, L., Samaras, Z., 2020. Particle number (PN) emissions from gasoline, diesel, LPG, CNG and hybrid-electric light-duty vehicles under real-world driving conditions. Atmospheric Environment, *222*, 117126.

Kozawa, K., Winer, A.M., Fruin, S.A., 2012. Ultrafine particle size distributions near freeways: Effects of differing wind directions on exposure. Atmospheric Environment 63, 250–260.

Kumar, P., Ketzel, M., Vardoulakis, S., Pirjola, L., Britter, R., 2011. Dynamics and dispersion modelling of nanoparticles from road traffic in the urban atmospheric environment‐A review. Journal of Aerosol Science 42, 580–603.

Kumar, P., Fennell, P., Britter, R., 2008b. Measurements of particles in the 5–1000 nm range close to road level in an urban street canyon. Science of the Total Environment 390, 437–447.

Kumar, P., Pirjola, L., Ketzel, M., Harrison, R. M., 2013. Nanoparticle Emissions From 11 Non-Vehicle Exhaust Sources–A Review. Atmospheric Environment 6, 252–277.

Kumar, P., Robins, A., ApSimon, H., 2010. Nanoparticle emissions from biofuelled vehicles—their characteristics and impact on the number-based regulation of atmospheric particles. Atmospheric Science Letters 11(4), 327-331.

Kumar, P., Fennell, P., Britter, R., 2008. Effect of wind direction and speed on the dispersion of nucleation and accumulation mode particles in an urban street canyon. Sci. Total. Environ. 402, 82-94.

Kumar, G., Malik, H., 2016. Generalized regression neural network-based wind speed prediction model for Western Region of India. Procedia Comput. Sci. 93, 26–32.

Kumar, P., Fennell, P., Hayhurst, A., Britter, R., 2009. Street versus rooftop level concentrations of fine particles in a Cambridge Street canyon. Boundary. Layer. Meteorol. 131, 3–18.

Kumar, P.S., Pavithra, K.G., Naushad, M., 2019. Characterization techniques for nanomaterials. In Nanomaterials for Solar Cell Applications, 97-124. Elsevier.

Kumar, P., Morawska, L., Birmili, W., Paasonen, P., Min, H., Kulmala, M., Harrison, R.M., Norford, L., Britter, R., 2014. Ultrafine particles in cities. Environ. Int. 66, 1–10.

Kumar, P., Robins, A., Vardoulakis, S., Britter, R., 2010. A review of the characteristics of nanoparticles in the urban atmosphere and the prospects for developing regulatory controls. Atmos. Environ. 44, 5035-5052.

Kundu, S., Pal, A.K., 2015. The evaluation of airborne respirable particulates in opencast mining area of Jharia coal field using grimm 1.109 real-time portable aerosol spectrometer. *Journal of Biodiversity and Environmental Sciences (JBES), 6*, 276-287.

Kulmala, M., Kontkanen, J., Junninen, H., Lehtipalo, K., Manninen, H. E., Nieminen, T., Franchin, A., 2013. Direct observations of atmospheric aerosol nucleation. Science 339(6122), 943-946.

Krecl, P., Johansson, C., Targino, A. C., Ström, J., Burman, L., 2017. Trends in black carbon and size-resolved particle number concentrations and vehicle emission factors under real-world conditions. Atmos. Environ. 165, 155-168.

Kreider, M. L., Panko, J. M., McAtee, B. L., Sweet, L. I., Finley, 466 B. L., 2010.Physical and chemical characterization of tire-related particles: Comparison of particles generated using different methodologies. Sci. Total Environ. 408, (3), 652-659.

Kwak, J., Kim, H., Lee, J., Lee, S., 2013. Characterization of non-exhaust coarse and fineparticles from on-road driving and laboratory measurements. Sci. Total Environ. 458-460, 273-282.

Kwak, J., Lee, S., Lee, S., 2014. On-road and laboratory investigations on non-exhaust ultrafine particles from the interaction between the tire and road pavement under braking conditions. Atmos. Environ. 97, 195-205.

Lack, D.A., Lovejoy, E.R., Baynard, T., Pettersson, A., Ravishankara, A.R., 2006. Aerosol Absorption Measurement Using Photoacoustic Spectroscopy: Sensitivity, Calibration, and Uncertainty Developments. Aerosol. Sci. Tech.40, 697–708.

Levinson, D., 2010. Equity effects of road pricing: A review. Transp. Rev. 30, 33–57.

Legates, D.R., McCabe, G.J., 1999. Evaluating the use of "Goodness-of-fit" Measuresin hydrologic and hydroclimatic model validation. Water. Res. 35, 233e241.

Lightstone, S.D., Moshary, F., Gross, B., 2017. Comparing CMAQ forecasts with a neuralnetwork forecast model for PM2.5 in New York. Atmosphere 8 (9).

Li, W., Wang, C., Wang, H., Chen, J., Yuan, C., Li, T., Wang, B., 2014. Distribution of atmospheric particulate matter (PM) in rural field, rural village and urban areas of northern China. *Environmental Pollution, 185,* 134-140.

Liu, Z., Hu, B., Zhang, J., Xin, J., Wu, F., Gao, W., Wang, M., Wang, Y., 2017. Characterization of fine particles during the 2014 Asia-Pacific economic cooperation summit: number concentration, size distribution and sources. Tellus, Series B: Chemical and Physical Meteorology 69 (1), 1303228.

Lippman.M., Yeates, D.B., Albert, R.E.,1980. Deposition, retention, and clearance of inhaled particles. The British Journal of Industrial Medicine, *37,* 337–362.

Luhana, L., Sokhi, R., Warner, L., Mao, H., Boulter, P., McCrae, I., Wright, J., Reeves, N.,Osborn, D., 2004. Non-exhaust particulate measurements: results. In: Deliverable 8 of theEuropean Commission DG TREN 5th Framework Particulates Project.

Lu F, Chen Z, Liu W Q, Shao H B (2016) Modeling chlorophyll-a concentrations using an artificial neural network for precisely eco-restoring lake basin. Ecol. Eng. 95, 422–429.

Mac Kinnon, M., Shaffer, B., Carreras-Sospedra, M., Dabdub, D., Samuelsen, G. S., Brouwer, J., 2016. Air quality impacts of fuel cell electric hydrogen vehicles with high levels of renewable power generation. Int. J. Hydrog. Energy 41(38), 16592-16603.

Mahowald, N.M., Ballantine, J.A., Feddema, J., Ramankutty, N., 2007. Global trends invisibility: implications for dust sources. Atmos. chem. phys. 7, 3309-3339.

Maier, H.R., Dandy, G.C., 2000. Neural networks for the prediction and forecasting ofwater resources variables: a review of modelling issues and applications. Environ.Model. Softw 15 (1), 101–124.

Maier, H.R., Jain, A., Dandy, G.C., Sudheer, K.P., 2010. Methods used for the developmentof neural networks for the prediction of water resource variables in river systems: current status and future directions. Environ. Model. Softw 25 (8), 891–909.

Mainka, A., Zajusz-Zubek, E., 2019. PM1 in Ambient and Indoor Air—Urban and Rural Areas in the Upper Silesian Region, Poland. *Atmosphere, 10,* 662.

Mamakos, A., Arndt, M., Hesse, D., Augsburg, K., 2019. Physical Characterization of Brake-Wear Particles in a PM10 Dilution Tunnel. Atmosphere 10 (11), 639.

Mathissen, M., Scheer, V., Vogt, R., Benter, T., 2011. Investigation on the potential generation of ultrafine particles from the tire-road interface. Atmos. Environ. 45, 6172-6179.

Maricq, M. M., Podsiadlik, D. H., Chase, R. E., 1999. Gasoline vehicle particle size distributions: Comparison of steady state, FTP, and US06 measurements. *Environmental Science & Technology, 33,* 2007-2015.

Martinello, K., Hower, J. C., Pinto, D., Schnorr, C. E., Dotto, G. L., Oliveira, M. L. S., Ramos, C. G., 2021. Artisanal ceramic factories using wood combustion: A nanoparticles and human health study. Geosci. Front. 101151.

Mayer, A., Czerwinski, J., Kasper, M., Ulrich, A., Mooney, J.J., 2012. Metal Oxide Particle Emissions from Diesel and Petrol Engines. SAE technical Paper 2012-01-0841, SAE: Warrendale, PA, USE.

Maynard, A.D., Maynard, R.L., 2002. A derived association between ambient aerosol surface area and excess mortality using historic time series data. Atmos. Environ. 36, 5561-5567.

McEntee, J.C., Ogneva-Himmelberger, Y., 2008. Himmelberger Diesel particulate matter, lung cancer, and asthma incidences a long major traffic corridors in MA, USA: a GIS analysis. *Health and Place, 14,* 817-828.

Mehel, A., Murzyn, F., 2015. Effect of air velocity on nanoparticles dispersion in the wake of a vehicle model: Wind tunnel experiments. Atmos. Pollut. Res. 6, 612-617.

Meister, K., Johansson, C., Forsberg, B., 2012. Estimated short-term effects of coarse particles on daily mortality in Stockholm, Sweden. Environ. Health. Perspect. 120, 3431 436.

Mei, M., Song, H., Chen, L., Hu, B., Bai, R., Xu, D., Liu, Y., Zhao, Y., Chen, C., 2018. Early-life exposure to three size- fractionated ultrafine and fine atmospheric particulates in Beijing exacerbates asthma development in mature mice. Part. *Particle and Fibre Toxicology, 15,* 1–16.

Mendoza-Villafuerte, P., Suarez-Bertoa, R., Giechaskiel, B., Riccobono, F., Bulgheroni, C., Astorga, C., Perujo, A., 2017. NOx, NH3, N2O and PN real driving emissions from a Euro VI heavy-duty vehicle. Impact of regulatory on-road test conditions on emissions. *Science of The Total Environment, 609,* 546-555.

Milojevic, A., Wilkinson, P., Armstrong, B., Bhaskaran, K., Smeeth, L and Hajat, S., 2014. Short-term effects of air pollution on a range of cardiovascular events in England and Wales: case-crossover analysis of the MINAP database, hospital admissions and mortality. Heart 100, 1093-1098.

Mordukhovich, I., Coull, B., Kloog, I., Koutrakis, P., Vokonas, P., Schwartz, J., 2015. Exposure to sub-chronic and long-term particulate air pollution and heart rate variability in an elderly cohort: The Normative Aging Study. Environmental Health 14 (1), 87.

Mroz, R. M., Schins, R. P., Li, H., Jimenez, L. A., Drost, E. M., Holownia, A., MacNee, W., Donaldson, K., 2008. Nanoparticle-driven DNA damage mimics irradiation related carcinogenesis pathways. Eur. Respir. J. 31, 241–251.

Murr, L.E., Garza, K.M., 2009. Natural and anthropogenic environmental nanoparticulates: their microstructural characterization and respiratory health implications. Atmos. Environ.43, 2683-2692.

Mueller, S.F., Mallard, J.W., 2011. Contributions of natural emissions to ozone and PM2.5as simulated by the community multiscale air quality (CMAQ) model. Environ. Sci. Technol. 45 (11), 4817–4823.

Namgung, H. G., Kim, J. B., Woo, S. H., Park, S., Kim, M., Kim, M. S., Bae, G.N., Park, D., Kwon, S. B., 2016. Generation of nanoparticles from friction between railway brake disks and pads. Environ. Sci. Technol. 50 (7), 3453-3461.

Natusch, D. F. S., Wallace, J. R., 1974. Urban aerosol toxicity: 489 The influence of particle size.Science 186, 695-699.

Nel, A., Xia, T., Madler, L., Li, N., 2006. Toxic potential of materials at the nanolevel. Science, 311 (5761), 622–627, ISSN 0036-8075.

Nielsen, M. A., 2015). Neural Networks and Deep Learning; Determination Press: USA, 2015. Available online: http://neuralnetworksanddeeplearning.com/ (accessed on 29 December 2017).

Niu, X., Chuang, H. C., Wang, X., Ho, S. S. H., Li, L., Qu, L., Chow, J.C., Watson, J.G., Sun, J., Lee, S., Cao, J., Ho, K. F., 2020. Cytotoxicity of PM2. 5 vehicular emissions in the Shing Mun tunnel, Hong Kong. Environ. Pollut. 263, 114386.

Nussbaumer, T., Czasch, C., Klippel, N., Johansson, L., Tullin, C., 2008. Particulate emissions from biomass combustion in IEA countries. In Proceeding of the 16th European Biomass Conference and Exhibition, Zurich, Switzerland, 2–6 June. p. 40.

Nowak, D. J., Crane, D. E., Stevens, J. C., 2006. Air pollution removal by urban trees and shrubs in the United States. Urban. For. Urban. Green. 4 (3-4), 115-123.

Nowak, D.J., Heisler M.G., 2010. Air Quality Effects of Urban Trees and Parks, 6 – 34, Available at: from https://www.nrpa.org/globalassets/research/nowak-heisler-summary.pdf

Olivares, G., Johansson, C., Strom, J., Hansson, H.C., 2007. The role of ambient temperaturefor particle number concentrations in a street canyon. Atmos. Environ. 41 (10), 2145–2155.

Oberdörster, G., Maynard, A., Donaldson, K., Vincent Castranova, V., Fitzpatrick, J., Ausman, K., Carter, J., Karn, B., Kreyling, W., Lai, D., Olin, S., Monteiro-Riviere, N., Warheit, D., Yang, H., 2005a. Principles for characterizing the potential human health effects from exposure to nanomaterials: elements of a screening strategy. Part. Fibre. Toxicol. 2 (8), 1-35.

Oberdörster, G., Oberdörster, E., Oberdörster, J., 2005b. Nanotoxicology: an emerging discipline evolving from studies of ultrafine particles. Environ. Health. Perspect. 113, 823-839.

Omidvarborna, H., Kumar, P., Tiwari, A., 2020. 'Envilution™'chamber for performance evaluation of low-cost sensors. *Atmospheric Environment, 223*, 117264.

Orfila, O., Saint Pierre, G., Messias, M., 2015. An android based eco driving assistance system to improve safety and efficiency of internal combustion engine passenger cars. Transp. Res. Part C. Emerg. Technol. 58, 772–782.

Organization for Economic Co-operation and Development (OECD), 2020. Working Party onIntegrating Environmental and Economic Policies Non-exhaust emissions from road

Causes, consequences and policy responses. JT03463487. Available at: www.oecd.org

Ostro, B., Tobias, A., Querol, X., Alastuey, A., Amato, F., Pey, J., Perez, N., Sunyer, J., 2011.

The effects of particulate matter sources on daily mortality: a case-crossover study of Barcelona, Spain. Environmental Health Perspectives119, 21781–1787.

Oviedo, D., Sabogal, O., 2020. Unpacking the connections between transport and well-being in socially disadvantaged communities: Structural equations approach to low-income neighbourhoods in Nigeria. *Journal of Transport & Health, 19,* 100966.

Padró-Martínez, L. T., Patton, A. P., Trull, J. B., Zamore, W., Brugge, D., Durant, J. L., 2012. Mobile monitoring of particle number concentration and other traffic-related air pollutants in a near-highway neighborhood over the course of a year. *Atmospheric Environment, 61*, 253-264.

Panko, J.M., Hitchcock, K.M., Fuller, G.W., Green, D., 2019. Evaluation of tire wearcontribution to PM2.5 in urban environments. Atmosphere 10, 99

Pant, P., Baker, S.J., Shukla, A., Maikawa, C., Godri Pollitt, K.J., Harrison, R.M., 2015. The PM10 fraction of road dust in the UK and India: characterization, source profiles and oxidative potential. *Science of the Total Environment, 530–531,* 445–452.

Pant, P., Harrison, R., 2013. Estimation of the contribution of road traffic emissions to particulate matter concentrations from field measurements: a review. *Atmospheric Environment, 77,* 78–97.

Park, I., Kim, H., Lee, S., 2018. Characteristics of tire wear particles generated in a laboratorysimulation of tire/road contact conditions. J. Aerosol Sci. 124, 30–40.

Pasquier, A., André, M., 2017. Considering criteria related to spatial variabilities for the assessment of air pollution from traffic.

Pateraki, S., Asimakopoulos, D.N., Flocas, H.A., Maggos, T., Vasilakos, C., 2012. The role of meteorology on different sized aerosol fractions (PM10, PM2.5, PM 2.5–10). Science of the Total Environment 419, 124-135.

Pekkanen, J., Timonen, K.L., Ruuskanen, J., Reponen, A., Mirme, A., 1997. Effects ofultrafine and fine particles in urban air on peak flow respiratory flow among children with asthmatic symptoms. Environ. Res. 74, 24-33.

Pelkmans, L., Debal, P., 2006. Comparison of on-road emissions with emissions measured onchassis dynamometer test cycles. Transp. Res. D Transp. Environ. 11(4), 233-241.

Perrone, M.R., Becagli, S., Garcia Orza, J.A., Vecchi, R., Dinoi, A., Udisti, R., Cabello, M., 2013. The impact of long-range-transport on PM1 and PM2.5 at a Central Mediterranean site. *Atmospheric Environment, 71,* 176–186.

Peters, T.M., Ott, D., O'Shaughnessy, P.T., 2006. Comparison of the Grimm 1.108 and 1.109 Portable Aerosol Spectrometer to the TSI 3321 Aerodynamic Particle Sizer for Dry Particles. *Annals of Occupational Hygiene, 50,* 843–850.

Pereira, G. M., Teinilä, K., Custódio, D., Gomes Santos, A., Xian, H., Hillamo, R., ..., Castro Vasconcellos, P. D., 2017. Particulate pollutants in the Brazilian city of São Paulo: 1-year investigation for the chemical composition and source apportionment. Atmos. chem. phys. 17(19), 11943-11969.

Pillarisetti, A., Allen, T., Ruiz-Mercado, I., Edwards, R., Chowdhury, Z., Garland, C., Pennise, D., 2017. Small, smart, fast, and cheap: microchip-based sensors to estimate air pollution exposures in rural households. Sensors 17(8), 1879.

Pirjola, L., Paasonen, P., Pfeiffer, D., Hussein, T, Hameri, K., Koskentalo, T, Virtanen, A, Rankko, T., Keskinen, J., Pakkanen, T., 2006. Dispersion of particles and trace gases nearby a city highway: Mobile laboratory measurements in Finland. Atmos. Environ. 40, 867-879.

Plaia, A.Ã., Bondı, A.L., 2006. Single imputation method of missing values in environmentalpollution data sets. Atmos. Environ. 40, 7316–7330.

Projected Emissions (March 2020 Submission). Updated 2020. Available online:http://cdr.eionet.europa.eu/gb/un/clrtap/projected/envxmo40w/overview (accessed on 12October 2020).

Quang, T. N., He, C., Morawska, L., Knibbs, L. D., Falk, M., 2012. Vertical particle concentration profiles around urban office buildings. Atmos. chem. phys. 12(11), 5017-5030.

Qiu, Z., Liu, W., Gao, H. O., Li, J., 2019. Variations in exposure to in-vehicle particle mass and number concentrations in different road environments. Journal of the Air & Waste Management Association, 69 (8), 988-1002.

Rahimi, A., 2017. Short-term prediction of NO2 and NO x concentrations using multilayerperceptron neural network: a case study of Tabriz, Iran. Ecol. Process. 6 (1), 4.

Seigneur, C., 2009.Current understanding of ultrafine particulate matter emitted from mobile sources. The Journal of the Air & Waste Management Association 59, 3− 17.

Report of the GRPE Particle measurement Programme (PMP): Government Sponsored Work Programmes 2003.

Shah, AS., Langrish, JP., Nair, H., McAllister, D.A., Hunter, A.L., Donaldson, K., Newby, D.E., Mills, N.L., 2013. Global association of air pollution and heart failure: a systematic review and meta-analysis. Lancet 382, 1039-1048.

Ruskanen, J., Tuch, T., Ten Brink, H., Peters, A., Khlystov, A., Mirme, A., Kos, G.P.A., Brunekreef, B., Wichmann, H.E., Buzorius, G., Vallius, M., Kreyling, W.G., Pekkanen, J., 2001. Concentrations of ultrafine, fine and PM2.5 particles in three European cities. AtmosphericEnvironment 35, 3729–3738.

Rovelli, S., Cattaneo, A., Borghi, F., Spinazzè, A., Campagnolo, D., Limbeck, A., Cavallo, D. M., 2017. Mass concentration and size-distribution of atmospheric particulate matter in an urban environment. Aerosol. Air. Qual. Res. 17 (5), 1142-1155.

Rymaniak, L., Ziolkowski, A., Gallas, D., 2017. Particle number and particulate mass emissions of heavy-duty vehicles in real operating conditions. MATEC Web of Conferences 118, 00025, VII International Congress on Combustion Engines. DOI: 10.1051/matecconf/201711800025.

Rönkkö, T., Virtanen, A., Vaaraslahti, K., Keskinen, J., Pirjola, L., Lappi, M., 2006.Effect of dilution conditions and driving parameters on nucleation mode particles in diesel exhaust: laboratory and on-road study. Atmos. Environ. 40, 2893–2901.

Rönkkö, T., Kuuluvainen, H., Karjalainen, P., Keskinen, J., Hillamo, R., Niemi, JV., Pirjola, L., Timonen, HJ., Saarikoski, S., Saukko, E., Jarvinen, A., Silvennoinen, H., Rostedt, A., Olin, M., Yli-Ojanpera, J., Nousiainen, P., Kousa, A., Dal Maso, M., 2017. Traffic is a major source of atmospheric nanocluster aerosol. Proc. Natl. Acad. Sci. U S A. 114, 7549-7554.

Rönkkö, T., Timonen, H., 2019. Overview of sources and characteristics of nanoparticles in urban traffic-influenced areas. J. Alzheimer's Dis. 72 (1), 15-28.

Saha, PK., Khlystov, A., Snyder, MG., Grieshop, AP., 2018. Characterization of air pollutant concentrations, fleet emission factors, and dispersion near a North Carolina interstate freeway across two seasons. Atmos. Environ. 177, 143-153.

Samarasinghe, S., 2006. Neural Networks for Applied Sciences and Engineering. Taylor &Francis.

Safari M J S, Aksoy H, Mohammadi M (2016) Artificial neural network and regression models for flow velocity at sediment incipient deposition. J. Hydrol. 541, 1420–1429.

Seo, J., Shim, S., Kwon, S. H., Boo, K. O., Kim, Y. H., O'Connor, F., ..., Morgenstern, O., 2020. The Impacts of Aerosol Emissions on Historical Climate in UKESM1. Atmosphere 11(10), 1095.

Shahraiyni, H.T., Sodoudi, S., 2016. Statistical modeling approaches for PM10 predictionin urban areas; A review of 21st-century studies. Atmosphere 7 (2), 10–13.

Shao, L., Hu, Y., Shen, R., Schäfer, K., Wang, J., Wang, J., Schnelle- Kreis, J., Zimmermann, R., BéruBé, K., Suppan, P., 2017. Seasonal variation of particle-induced oxidative potential of airborne particulate matter in Beijing. Sci. Total. Environ. 579, 1152–1160.

Schauer, J.J., Lough, G.C., Shafer, M.M., Christensen, W.F., Arndt, M.F., DeMinter, J.T., Park, J.S., 2006. Characterization of metals emitted from motor vehicles. Health. Eff. Inst..133, 1-76.

Schneide, I.L., Teixeira, E.C., Silva Oliveira, L.F., Wiegand, F., 2015. Atmospheric particle number concentration and size distribution in a traffic–impacted area. Atmospheric Pollution Research 6, 877-885.

Schneider, I. L., Teixeira, E. C., Dotto, G. L., Yang, C. X., Silva, L. F., 2020. Geochemical study of submicron particulate matter (PM1) in a metropolitan area. Geosci. Front. 101130.

Shao, L., Hu, Y., Shen, R., Schäfer, K., Wang, J., Wang, J., Schnelle- Kreis, J., Zimmermann, R., BéruBé, K., Suppan, P., 2017. Seasonal variation of particle-induced oxidative potential of airborne particulate matter in Beijing. Sci. Total. Environ. 579, 1152–1160.

Simonen, P., Kalliokoski, J., Karjalainen, P., Rönkkö, T., Timonen, H., Saarikoski, S et al., 2019. Characterization of laboratory and real driving emissions of individual Euro 6 light-duty vehicles–Fresh particles and secondary aerosol formation. *Environmental Pollution, 255,* 113175.

Silva, L.F., Schneider, I. L., Artaxo, P., Núñez-Blanco, Y., Pinto, D., Flores, É. M., Gómez-Plata. L., Ramirez, O., Dotto, G. L., 2020a. Particulate matter geochemistry of a highly industrialized region in the Caribbean: Basis for future toxicological studies. Geosci. Front. 101115.

Silva, L. F., Pinto, D., Neckel, A., Oliveira, M. L., 2020b. An analysis of vehicular exhaust derived nanoparticles and historical Belgium fortress building interfaces. Geosci. Front. 11(6), 2053-2060.

Silva, L.F., Pinto, D., Neckel, A., Oliveira, M.L.S., Sampaio, C., 2020c. Atmospheric nanocompounds on Lanzarote Island: Vehicular exhaust and igneous geologic formation interactions. Chemosphere 254, 126822.

Simon, M.C., Hudda, N., Naumova, E.N., Levy, J.I., Brugge, D., Durant, J.L., 2017. Comparisons of traffic-related ultrafine particle number concentrations measured in two urban areas by central, residential, and mobile monitoring. Atmos. Environ. 169, 113-127.

Skrzypek, M., Zejda, J.E., Kowalska, M., Czech, E.M., 2013. Effect of residential proximity to traffic on respiratory disorders in school children in Upper Silesian Industrial Zone, Poland. International Journal of Occupational Medicine and Environmental Health *26,* 83–91.

Slezakova, K., Morais, S., do Carmo Pereira, M., 2013. Atmospheric nanoparticles and their impacts on public health. In Current topics in public health. IntechOpen.

Speranza, A., Caggiano, R., Margiotta, S., Trippetta, S., 2014. A novel approach to comparing simultaneous size-segregated particulate matter (PM) concentration ratios by means of a dedicated triangular diagram using the agri valley pm measurements as an example. *Natural Hazards and Earth System Sciences, 14,* 2727–2733.

Srimuruganandam, B., Nagendra, S. M. S., 2010. Analysis and interpretation of particulate matter–PM10, PM2. 5 and PM1 emissions from the heterogeneous traffic near an urban roadway. Atmos. Pollut. Res. 1(3), 184-194.

Stone, V., Miller, M.R., Clift, M.J.D., Elder, A., Mills, N.L., Møller, P., Schins, R.P.F., Vogel, U., Kreyling, W.G., Alstrup Jensen, K., Kuhlbusch, T.A.J., Schwarze, P.E., Hoet, P., Pietroiusti, A., De Vizcaya-Ruiz, A., Baeza-Squiban, A., Teixeira, J.P., Tran, C.L., Cassee, F.R., 2017. Nanomaterials versus ambient ultrafine particles: an opportunity to exchange toxicology knowledge. *Environmental Health Perspective, 125* (10), 106002.

Stölzel, M., Breitner, S., Cyrys, J., Pitz, M., Wölke, G., Kreyling, W., Heinrich, J., Wichmann, H.E., Peters, A., 2007. Daily mortality and particulate matter in different size classes in Erfurt, Germany. J. Expo. Sci. Environ. Epidemiol. 17 (5), 458-467.

Strawa, A.W., Kirchstetter, T.W., Hallar, A.G., Ban-Weiss, G.A., McLaughlin, J.P., Harley, R.A., Lunden, M.M., 2010. Optical and physical properties of primary on road vehicle particle emissions and their implications for climate change. J. Aerosol. Sci. 41(1), 36-50.

Sugimoto, N., Shimizu, A., Matsui, I., & Nishikawa, M., 2016. A method for estimating the fraction of mineral dust in particulate matter using PM2.5-to- PM10 ratios. *Particuology, 28*, 114–120.

Sun, W., Zhang, H., Palazoglu, A., Singh, A., Zhang, W., Liu, S., 2013. Prediction of 24-hour-average PM2.5 concentrations using a hidden Markov model with differentemission distributions in Northern California. Sci. Total Environ. 443, 93–103.

Sun, Q., Hong, X., &Wold, L.E., 2010. Cardiovascular effects of ambient particulate air pollution exposure. *Circulation, 121*, 2755–2765. https://doi.org/10.1161/

Sun, G., Hoff, S.J., Zelle, B.C., Nelson, M.A., 2008. Development and comparison backpropagation and generalized regression neural network models to predict diurnal and seasonal gas and PM10 concentrations and emissions from swine buildings. Am. Soc. Agric. Biol. Eng. 51, 685–694.

Tan, K.T., Lepp, N.W., 1977. Roadside vegetation: an efficient barrier to the lateral spread of atmospheric lead? Arboricultural Journal 3 (2), 79–85.

Tang G, Zhao P, Wang Y., 2017.Mortality and air pollution in Beijing: the long-term relationship. Atmos. Environ. 150, 238–243.

Thiyagarajan, V., Kalaichelvan, K., Vijay, R., Singaravelu, D.L., 2015. Influence of thermal conductivity and thermal stability on the fade and recovery characteristics of non-asbestos semi-metallic disc brake pad. J. Braz. Soc. Mech. Sci. Eng. 38, 1207–1219.

Thorpe, A., Harrison, R.M., 2008. Sources and properties of non-exhaust particulate matter from road traffic: A review. Sci. Total. Environ. 400, 270–282.

Titos, G., Lyamani, H., Pandolfi, M., Alastuey, A., Alados-Arboledas, L., 2014. Identification of fine (PM1) and coarse (PM10-1) sources of particulate matter in an urban environment. *Atmospheric Environment, 89*, 593–602.

Timmers, V. R., Achten, P. A., 2016. Non-exhaust PM emissions from electric vehicles. Atmos. Environ. 134, 10-17.

Tittarelli, A., Borgini, A., Bertoldi, M., De Saeger, E., Ruprecht, A., Stefanoni, R., ..., Crosignani, P., 2008. Estimation of particle mass concentration in ambient air using a particle counter. Atmos. Environ. 42 (36), 8543-8548.

Terzano, C., Di Stefano, F., Conti, V., Graziani, E., Petroianni, A., 2010. Air pollution ultrafine particles: Toxicity beyond the lung. Eur. Rev. Med. Pharmacol. Sci. 14 (10), 809-821.

Thorpe, A.J., Harrison, R.M., 2008. Sources and properties of non-exhaust particulate matter from road traffic: a review. Sci. Total. Environ. 400, 270–282.

Trejos, E. M., Silva, L. F., Hower, J. C., Flores, E. M., González, C. M., Pachón, J. E., Aristizábal, B. H., 2021. Volcanic emissions and atmospheric pollution: A study of nanoparticles. Geosci. Front. 12(2), 746-755.

Tsai, Y.I., 2005. Atmospheric visibility trends in an urban area in Taiwan 1961-2003. Atmospheric Environment 39, 5555-5567. TSI, 2008. Model 3936 Scanning Mobility Particle Sizer TSI Incorporated, USA. P/N 1933796.

Valavanidis, A., Fiotakis, K., Vlachogianni, T., 2008. Airborne particulate matter and human health: toxicological assessment and importance of size and composition of particles for oxidative damage and carcinogenic mechanisms. Journal of Environmental Science and Health, Part C, 26(4), 339-362.

Vakili M, Sabbagh-Yazdi S R, Khosrojerdi S, Kalhor K (2017) Evaluating the effect of particulate matter pollution on estimation of daily global solar radiation using artificial neural network modeling based on meteorological data. J. Clean. Prod 141, 1275–1285.

Veerabhadra Swamy, K.T., Lokesh, K.S., 1993. Lead dispersion studies along highways. Indian Journal of Environmental Health 35 (33), 205–209.

Vehkamaki, H., Kulmala, M., Lehtinen, K.E.J., 2003. Modelling binary homogeneousnucleation of water-sulfuric acid vapors: parameterization for high temperatureemissions. Environ. Sci. Technol. 37, 3392–3398.

Venkataraman, C., Rao, G.U.M., 2001. Emission Factors of Carbon Monoxide and Size-ResolvedAerosols from Biofuel Combustion. Environ. Sci. Technol. *35*, 2100–2107.

Verheggen, B., Weijers, E. P., 2010. Climate change and the impact of aerosol. A literature review.

Virtanen, A., Rönkkö, T., Kannosto, J., Ristimaki, J., Makela, J., Keskinen, J., Pakkanen, T., Hillamo, R., Pirjola, L., H., Ameri., K., 2006.Winter and summer time size distributions and densities of traffic related aerosol particles at a busy highway in Helsinki. Atmos. chem. phys.6, 2411-2421.

Vincent, J.H., 2007. Science, Standards, Instrumentation and Applications. John Wiley & Sons: Hoboken, NJ, USA. 636.

Vogt, R., Scheer, V., Casati, R., Bender, T., 2003.On road measurement of Particle emission in the exhaust plume of a diesel passenger car. Environ. Sci. Technol. 37, 4070 4076.

Voukantsis, D., Karatzas, K., Kukkonen, J., Rasanen, T., Karppinen, A., Kolehmainen, M., 2011. Intercomparison of air quality data using principal component analysis, and forecasting of PM10 and PM2.5 concentrations using artificial neural networks, in Thessalloniki and Helsinki. Sci. Total Environ. 409, 1266–1276.

Wang, C. F., Chang, C. Y., Tsai, S. F., Chiang, H. L., 2005. Characteristics of road dust fromdifferent sampling sites in northern Taiwan. J. Air. Waste. Manag. Assoc. 55(8), 1236-1244.

Wang, W., Shao, L., Li, J., Chang, L., Zhang, D., Zhang, C., Jiang, J., 2019. Characteristics of individual particles emitted from an experimental burning chamber with coal from the lung cancer area of Xuanwei, China. Aerosol. Air. Qual. Res. 19, 355–363.

Wichmann, H.E., Spix, C., Tuch, T., Wolke, G., Peters, A., Heinrich, J., Kreyling, W.G., Heyder, J., 2000. Daily mortality and fine and ultrafine particles in Erfurt, Germany. Part e I: role of particle number and mass. Research Report (Health Effect Institute) 98, 5-86.

Wilson, M. R., Lightbody, J. H., Donaldson, K., Sales, J., Stone, V., 2002. Interactions between ultrafine particles and transition metals in vivo and in vitro. Toxicol. Appl. Pharmacol. 184, 172 –179.

World Health Organization., 2006. *WHO Air quality guidelines for particulate matter,* ozone, nitrogen dioxide and sulfur dioxide: global update 2005: summary of risk assessment (No. WHO/SDE/PHE/OEH/06.02). Geneva: World Health Organization.

World Health Organization (WHO), 2018. Ambient (outdoor) air pollution. https://www.who.int/es/news-room/fact-sheets/detail/ambient-(outdoor)-air-quality-and-health.

World Health Organization (WHO). 2013. Review of evidence on health aspects of air pollution- REVIHAAP Project; WHO Regional Office FOR Europe: Copenhagen, Denmark.

World Health Organization, (WHO). 2016. Ambient (Outdoor) Air Quality and Health.Retrieved. http://www.who.int/mediacentre/factsheets/fs313/en, Accessed date: 14 September 2017.

Wu, W., Dandy, G.C., Maier, H.R., 2014. Protocol for developing ANN models and itsapplication to the assessment of the quality of the ANN model development process indrinking water quality modelling. Environ. Model. Softw 54, 108–127.

Xing, J., Shao, L., Zheng, R., Peng, J., Wang, W., Guo, Q., Wang, Y., Qin, Y., Shuai, S., Hu, M., 2017. Individual particles emitted from gasoline engines: Impact of engine types, engine loads and fuel components. J. Clean. Prod. 149, 461–471,

Xing, J., Shao, L., Zhang, W., Peng, J., Wang, W., Hou, C., Shuai, S., Hu, M., Zhang, D., 2019. Morphology and composition of particles emitted from a port fuel injection gasoline vehicle under real-world driving test cycles. J. Environ. Sci. (China). 76, 339– 348.

Xing, J., Shao, L., Zhang, W., Peng, J., Wang, W., Shuai, S., Hu, M., Zhang, D., 2020. Morphology and size of the particles emitted from a gasoline-direct-injection-engine vehicle and their ageing in an environmental chamber. Atmos. chem. phys. 20 (5), 2781-2794.

Xu, X.H., Brook, J.R., Guo, Y.S., 2007. A statistical assessment of saturation and mobile sampling strategies to estimate long–term average concentrations across urban areas. The Journal of the Air & Waste Management Association 57, 1396–1406.

Young, L. H.,Wang, Y.T.,Hsu, H.C., Lin, C.H., Liou, Y.J., Lai, Y.C., Lin, Y.H.,Chang,W.L., Chiang, H.L., Cheng, M.T., 2012. Spatio-temporal variability of sub micrometer particle number size distributions in an air quality Management district. SCI. Total Environment 425, 135–145.

Yu, H., Kaufman, Y. J., Chin, M., Feingold, G., Remer, L. A., Anderson, T. L., ..., Zhou, M., 2006. A review of measurement-based assessments of the aerosol direct radiative effect and forcing. Atmos. chem. phys.*6*(3), 613-666.

Zajusz-Zubek, E., Radko, T., Mainka, A., 2017. Fractionation of trace elements and human health risk of submicron particulate matter (PM1) collected in the surroundings of coking plants. Environmental Monitoring and Assessment, 189(8), 389.

Zhang, L., Cheng, Y., Zhang, Y., He, Y., Gu, Z., Yu, C., 2017. Impact of air humidity fluctuation on the rise of PM mass concentration based on the high-resolution monitoring data. Aerosol. Air. Qual. Res. 17(2), 543-552.

Zhang, J., Chen, Z., Lu, Y., Gui, H., Liu, J., Liu, W., Wang, J., Yu, T., Cheng, Y., Chen., Y., 2017.Characteristics of aerosol size distribution and vertical backscattering coefficient profile during 2014 APEC in Beijing. Atmospheric Environment 148, 30-41.

Zhu, Y., Hinds, W.C., 2005. Predicting particle number concentrations near a highway based on vertical concentration profile. Atmospheric Environment 39, 1557-1566.

Zhu, Y., Hinds, W. C., Shen, S., Sioutas, C., 2004. Seasonal trends of concentration and size distribution of ultrafine particles near major highways in Los Angeles. Aerosol Science and Technology38, 5–13.

Zhu, Y., Hinds, W.C., Kim, S., Sioutas, C., 2002a. Concentration and size distribution of ultrafine particles near a major highway. The Journal of the Air & Waste Management Association 52, 1032-1042.

Zhu, Y., Hinds, W.C., Kim, S., Shen, S., Sioutas C., 2002 b. Study of ultrafine particles near a major highway with heavy-duty diesel traffic. Atmospheric Environment 36, 4323–433.

Zhu, Y., Hinds, W.C., 2005. Predicting particle number concentrations near a highway based on vertical concentration profile. Atmos. Environ. 39, 1557-1566.

Zhu, J., Penner, J. E., Lin, G., Zhou, C., Xu, L., Zhuang, B., 2017. Mechanism of SOA formation determines magnitude of radiative effects. Proc. Natl. Acad. Sci. USA. 114, 12685–12690.

Zhu, R., Hu, J., Bao, X., He, L., Lai, Y., Zu, L., Li, Y., Su, S., 2016. Tailpipe emissions fromgasoline direct injection (GDI) and port fuel injection (PFI) vehicles at both low and high ambient temperatures. *Environnemental Pollution. 216*, 223–234.

Zwozdziak, A., Sówka, I., Willak-Janc, E., Zwozdziak, J., Kwiecińska, K., Balińska-Miśkiewicz, W., 2016. Influence of PM1 and PM2.5 on lung function parameters in healthyschoolchildren—a panel study. Environ. Sci. Pollut. Res. Int. 23, 23892–2390

Appendix

Table 1

Sampling measurement Methods	Authors	Instruments	Size range	Advantages	Disadvantages	$PNCs(p/cm^3)$ /PMCs $(\mu g/m^3)$
Real world measurements	Béji et al., 2020	ELPI and FMPS	10 nm-10 µm	ELPI: Robust and large size range	ELPI: Wide channels plates may affect the result	1.0×10^5 Brakewear particles in motorway
				FMPS: Fast indicates well process changes	Less accurate than the SMPS	
	Carpentieri and Kumar, 2011	DMS50	5-560nm	Very small particles	Not suitable for larger particles	(Min-Max) 6.5. 10^4 -7.388 10^6. Vehicle

						exhaust emissions (30km/h)
	Gouriou et al., 2004	SMPS	SMPS :30nm-10µm	SMPS: Very small particles	SMPS: not suitable for larger particles and not used friendly and questionable cost	(Min-Max) 8.5×10^{4}-1.1×10^{6}
	Imhof et al., 2005	ELPI	ELPI: 10 nm-10 µm	ELPI: Robust and large size range	ELPI: Wide channels plates may affect the result	(At high traffic – At low traffic) 9.5×10^{4} - 1.95×10^{4}
	Karjalainen et al., 2014	ELPI, CPC	30 nm -10µm; 5.6-560 nm	ELPI: Robust and large size range	ELPI: Wide channels plates may affect the result	(Min-Max) 4.0×10^{4}-5.0×10^{4}

				CPC: flow control feedback loop for greater concentration accuracy	CPC:Not compatible with SMPS	
	Keuken et al., 2016	CPC 3775, CPC3783	7-310nm 0.03-10μm	Flow control feedback loop for greater concentration accuracy	No compatible with SMPS	(Workingdays-weekend) 3.16×10^4-2.88×10^4
	Krecl et al., 2017	CPC	28-410 nm	CPC: Has a flow control feedback loop for greater concentration accuracy	No compatible with SMPS	Max –exhaust emissions 6.4×10^3
	Bukowiecki et al., 2003	SMPS, GRIMM1108	7-10 nm	SMPS: Very small particles	SMPS: not suitable for larger particles and not used friendly and	total particle background number concentration

					relatively high cost	- Rural road 1.5×10^4 - Urban road 3.5×10^4 -Motorway 8×10^4
				GRIMM: Minimum of maintenance is needed and automatically check system	Not suitable for smaller particles	
	Belkacem et al., 2020	FMPS	5-560nm	FMPS: Fast indicates well changes in process	Less accurate than the SMPS	(Min-Max) $1.04\ 10^4$ - $2.70\ 10^4$.
	Alam et al., 2011;	GRIMM 1109	0.3-20µm	Minimum of maintenance is needed and automatically check system	Not suitable for smaller particles	(Min-Max) -At 0.27µm: 12.9×10^9 - 2.9×10^9 -At 2.5 µm 10.5×10^6-

						6.0×10^{6}
In situ measurements	Srimuruganandam, and Nagendra, 2010	GRIMM 1107	0.25-32µm PM10 PM2.5 PM1	Minimum of maintenance is needed and automatically check system	Not suitable for smaller particles	(Min-Max), PM10, PM2.5, PM1 Weekdays: 148–292,81–122, 64–100 µg/m^3 Weekend 150–290, 85–134, 68–110µg/m^3.
	Bilal et al., 2019;	TEOM	PM2.5	Agrees will with filter samples	With high concentration the filter has to be changed; Not suitable for smaller particles	(Min-Max) Spring period 34.55- 45.77 Summer period 17.92-31.48 Autumn period 43.37-51.32

						Winter period 47.48-54.77
	Filonchyk et al., 2016;	TEOM1400	PM2.5-PM10	Agrees well with filter samples	With high concentration the filter has to be changed; Not suitable for smaller particles	Average mass concentrations PM2.5: 26 PM10 :66
	Tittarelli et al., 2008;	Particle Counter	0.3-10μm	Fluids with high viscosity or extreme contamination can be conveniently diluted prior to counting	Not suitable for smaller particles	Average mass concentrations - At rainy time >0 PM10: 46.20 PM2.5: 31.43 - At temperature >13.5 °C PM10:28.39 PM2.5: 21.04

	Choi and Paulson, 2016	MMP, FMPS3091 CPC3007	5.6-560 nm 0,01 à 1,0 µm	FMPS: Fast indicates well changes in process	Less accurate than the SMPS	Max 8.5×10^{3}
				CPC: has a flow control feedback loop for greater concentration accuracy	With high concentration the filter has to be changed; Not suitable for smaller particles	
	Geller et al., 2005	CPC SMPS	7-270nm	CPC: Has a flow control feedback loop for greater concentration accuracy	No compatible with SMPS	(Min- Max) - Gasoline 1.4×10^{5}- 6.9×10^{5} -Diesel + gasoline 3.9×10^{5}- 7.8×10^{5}

	Giugliano et al., 2005	GRIMM1107	PM1, PM2.5	GRIMM: Minimum of maintenance is needed and automatically check system	Not suitable for smaller particles	(Min-Max) Spring period PM2.5:9.3-39.7, PM1: 8.5-35.8 - Summer period PM2.5:3.4-40.3 PM1:2-36.3 - Autumn period PM2.5 :13.9-70.1 PM1:11.7-63.6 - Winter period PM2.5:12-128.1 PM1: 9.1-79.8

	Gomišček et al., 2004	TEOM	PM1, PM2.5, PM10.	Agrees will with filter samples	With high concentration the filter has to be changed; Not suitable for smaller particles	(Min-Max), in Urban area) - Winter period PM1: 4.4-75.1 PM2.5:4.7-96.4 PM10:5.7-104.6 NC[11]: 1.34×10^4 - 6.28×10^4 - Summer period PM1: 3.0-32.6 PM2.5: 4.1-42.7 PM10 : 7.2-58.3 NC :8.75×10^3-4.17×10^4

[11] NC: Number concentration

	Hussein et al., 2014	EDM-180D, GRIMM	0.25-32 µm PM1 PM2.5 PM10	GRIMM: Minimum of maintenance is needed and automatically check system	Not suitable for smaller particles	Annual average PM; PM1: 13.34 PM2.5:35.54 PM10:107.02
	Hussein et al., 2019	CPC 3007-2-TSI	10nm-1µm	Has a flow control feedback loop for greater concentration accuracy	No compatible with SMPS	(Min –Max), PNCs 2.7 - 1.1× 10^5
	Namgung et al., 2016	FMPS, GRIMM 1109	5.6-560nm 0.3-	GRIMM: Minimum of maintenance is needed and automatically check	GRIMM: Not suitable for smaller particles	Total number concentration, Railway Brake Disks and Pads wear

			20µm	system		1.5×10^{3}-10^{7}
				FMPS: Detects well changes in process	FMPS: Less accurate than SMPS	